Heritability of Behavioral and Brain Measures in a Large Cohort of Healthy Twin and non-Twin Subjects

A DISSERTATION
SUBMITTED TO THE FACULTY OF
UNIVERSITY OF MINNESOTA
BY

Jasmine Elizabeth Joseph

IN PARTIAL FULFILLMENT OF THE REQUIREMENTS
FOR THE DEGREE OF
DOCTOR OF PHILOSOPHY

Apostolos P. Georgopoulos, MD, Ph.D., Thesis Advisor
Peka Christova Savayan, Ph.D., Thesis Co- Advisor

January 2020

Acknowledgements

My heartfelt gratitude to my advisors, Dr. Apostolos P. Georgopoulos and Peka Christova Savayan, for their leadership and mentorship, and whose guidance shaped me as a both as a person and as a scientist. They pushed me to stay on top of the literature, and always made sure I understood both the big-overall concepts and the nitty-gritty details of the dissertation. They were extremely supportive and patient when I was a new parent in the middle of my dissertation. I feel incredibly grateful to them for encouraging me very step of the way.

I am thankful to my committee members, Dr. Armando Manduca and Dr. Mohamed F. Mokbel, for being part of my committee, and making time in their extremely busy schedule. I am grateful to the BICB graduate advisors, Dr. Chad Myers and Dr. Yuk Sham, for their amazing support and sponsorship.

I'd like to thank the members in the Brain Science Center, past and present, for their support and encouragement; especially Rachel Johnson, for always brightening up my day, being a wonderful friend, and sharing her strong communication skills, and Matthew Sanders, for always helping out with all the technical details.

I thank my Twin Cities family for their warmth, community, humor and love; if it were not for them, I am not sure how I would have made it through a new location and harsh climate. Katya, Rebecca, Maureen, Maggie, Taylor, Johnson Family, and the Nehotte Family- I thank you all for your friendship, encouraging me, the many meals, discussions and laughter. To Arin's wonderful teachers at Bright Horizons for providing the best care to my son so I could continue to work on my dissertation. Last, but not least, thank you to my in-laws: Ramachanrdra Rao Penke and Bhagya Satee Lakshmi Penke for your unconditional love and support above all else.

Dedication

To my parents, Jay Vadakkelthottathil Joseph and Elsie Thomas Joseph, “Fortune favors the bold” - thank you for the many sacrifices you made so that I could have all the opportunities in the world.

To my sister, Jennifer Mary Joseph and my brother, Jason Thomas Joseph, they have always been there for me and supported me; siblings are and will always be there lifelong friends.

To my son, Arin Joseph Penke, you are the most precious gift and blessing given to me. You have brought so much joy and happiness to our families, thank you for being my son.

To Nalinichandra Penke, my husband, thank you for believing in me, trusting me, supporting me and sticking by me through it all

Abstract

This research investigated comprehensively the effects of genetics on behavioral traits, brain structure and function, and their associations in a large cohort of monozygotic (MZ) twins, dizygotic (DZ) twins, non-twin siblings (SIB) and non-related (NR) individuals (N = 1206, total) provided by the Human Connectome Project (HCP). All primary measures available are of the highest quality and quantitatively assessed. They include the following for each individual: (a) Measures of behavioral traits in 5 domains (motor, sensory, cognitive, emotion, and personality); (b) volumes of 70 cortical brain areas extracted from high-resolution (0.7 mm isotropic) structural magnetic resonance imaging (sMRI) data; (c) resting-state blood oxygenation level dependent (BOLD) activity of the same areas extracted from long-duration (1200 volumes), fast-acquisition (every 0.72 s), high-resolution (2 mm isotropic) functional MRI (fMRI) data; and (d) white matter integrity measures (fractional anisotropy [FA] and mean diffusivity [MD] for 7 brain regions regions) derived from high angular resolution diffusion imaging (HARDI) MRI (dMRI) data at 1.25 mm spatial resolution and very strong magnetic field gradients at (100 mT/m). Data extraction and preprocessing was performed using a dedicated 704-processor high-performance computer cluster at the Brain Sciences Center using Matlab. Univariate and multivariate statistical analyses were carried out in personal computers using Matlab and IBM-SPSS (version 24). These analyses include the following. (a) Computation of common univariate statistics (mean, variance, etc.); (b) computation of intra class correlation (ICC) for each of the 4 genetic groups (MZ, DZ, SIB, NR) and its z-transform [zICC = atanh(ICC)] for each primary measure above; (c)

analysis of variance (ANOVA) of zICC across genetic groups for each measure; (d) computation of heritability using Falconer's formula; (e) multidimensional scaling (MDS) and hierarchical tree clustering (HTC) of this heritability for the different data sets (behavioral, sMRI, fMRI, dMRI). These analyses yielded substantial new information on the effects of genetics on brain and behavior, and partially elucidated underlying associations among the various diverse measures above. To our knowledge, this is the first such comprehensive study carried out.

Table of Contents

List of tables

Page

List of figures

Page

Chapter 2: Behavior

Chapter 3: Diffusion MRI

Chapter 1 Overview

Magnetic Resonance Imaging (MRI) is a medical diagnostic technique that creates images of the human body using the principle of nuclear magnetic resonance. MRI allows for a multifaceted, noninvasive study of the brain structure and function. Neuroimaging and genetics are an intersection of two areas of research, aimed at improving the understanding of the genetic underpinnings of brain structure, function, and connectivity for both the healthy and diseased brain. The advances and availability of the high-quality data from the Human Connectome Project (HCP), provides a unique and unprecedented opportunity to evaluate genetic effects on a multitude of neural and behavioral measures, making it feasible to systematically explore the human connectome. This research analyzes three neuroimaging modalities, structural magnetic resonance imaging (sMRI), functional magnetic resonance imaging (fMRI), and diffusion magnetic resonance imaging (dMRI). In addition to the neuroimaging data, there are large amount of behavioral data across 5 domains: motor, sensory, cognition, emotion and personality. The HCP participants were grouped into four distinct genetic groups: monozygotic (MZ) twins, dizygotic (DZ) twins, siblings (SB) and unrelated participants (NR) in order to analyze their neuroimaging and behavioral data. Heritability calculations are conducted using Falconer's formula to estimate the genetic contribution of various behavioral measures, structural and functional brain measures, and their association, in order to obtain a quantitative estimate of the contribution of heritability.

1.1 Organization of dissertation:

Chapter 1 provides the background information on the concepts used throughout the chapters: heritability, twin studies, statistical methods, and neuroimaging techniques.

Chapter 2 presents Behavior. The measures were collected using reliable and validated measures to assess a wide array of functions and behaviors from 5 domains: motor, cognition, emotion, personality, and sensory. The 5 domains were used to calculate heritability estimates.

Chapter 3 analyzes dMRI, the images are micro-architectural detail of white matter tracts and provides information about white matter integrity. Fractional anisotropy (FA) and mean diffusivity (MD) of 7 representative white matter regions will be extracted from high-resolution diffusion weighted imaging acquisitions and heritability analysis were performed using the 4 genetic groups.

Chapter 4 is sMRI and is used to study the anatomy and the volume of the brain. Volumes of 70 cortical brain areas (35 per hemisphere) were extracted from high resolution (0.7 mm isotropic) T1 and T2 weighted scans using the FreeSurfer (FS) software package. Participants were grouped into four distinct genetic groups and brain volume and heritability analysis was conducted.

Chapter 5 is fMRI which is used to study connectivity in the brain while the participant is lying “at rest” in the scanner. The ARMIA (15,1,1) model is used to pre-whiten the BOLD signal and the innovations are used quantify the heritability of the BOLD signal innovations using the 4 genetic groups.

Chapter 6 summarizes the result of this multimodal study.

1.2 Heritability

Heritability is a term that can cause confusion because it is both used in common everyday speech and also as a technical term in genetics (Visscher et al., 2008). In common speech heritability loosely means 'being heritable', but as a technical term in genetics heritability is a population parameter with exact definitions. Specifically, heritability is the proportion of variance in a particular trait or phenotype in a population that is due to genetic variation, as opposed to environmental influences (Visscher et al., 2008). Heritability can range from 0 (no genetic contribution) to 1 (all differences on a trait reflect genetic variation). There are two important points of the definition. (1) Heritability does not apply to individuals but to variations within a group (or population). And (2) the estimate of heritability is not fixed but can change. Differences among groups in a range of genetic variation and/or environmental variation will result in different estimates of heritability. Thus, heritability of a trait depends critically on the environment. Even if two genetically identical populations were considered, if the environment were different, then heritability could differ, depending on the magnitude of the effect of the environment on the trait. "Although calculating heritability can be complex, one fact that can be exploited to calculate heritability is the fact that identical twins are on average exactly twice as similar genetically as non-identical twins. Thus, allowing a straightforward statistical procedure to estimate the proportion of variability in complex outcomes that is associated with causally distant genes (Turkheimer, 2000)."

1.2.1 Approaches to calculate heritability - Studies on Twins

Twin studies are the most powerful approach for investigating the influence of genetics and environment on human phenotypes (Jansen, 2015). The classical twin study compares phenotypic resemblances of MZ and DZ twins. MZ twins are derived from a single fertilized egg, and therefore inherit identical genetic material, while DZ twins which are derived from two different fertilized eggs. MZ twins are expected to have the greatest similarity since they are genetically identical. DZ twins share on average 50 percent of their genes (similar to ordinary full siblings) and share childhood environment, including in utero environment, to a greater degree than ordinary siblings.

By comparing the phenotypic expression between MZ twins and DZ twins, the extent of genetic and environmental contributions to a phenotype can be established. Twin studies divide the genetic and environmental factors into four variances: additive genetic (A), non-additive genetic (D), common environmental (C), and unique environmental (E) (Jansen, 2015). Therefore, if additive genetic effects are influencing a trait, then MZ twins will resemble each other more on that trait than the DZ twins. Similarly, the distribution of certain phenotypes in families with known biological relationships (parents, siblings) can help segregate genetic and environmental influences (Jansen, 2015) (See ACE model below).

1.2.2 Calculation of Heritability

Observed phenotypes (P) of a trait of interest can be partitioned using biologically plausible nature–nurture models into a statistical model representing the contribution of the unobserved genotype (G) and unobserved environmental factors (E):

$$\text{Phenotype (P)} = \text{Genotype (G)} + \text{Environment (E)} \quad (1)$$

The variance of the observable phenotypes (σ_{P^2}) can be stated as a sum of unobserved variances (σ_{G^2} and σ_{E^2}):

$$\sigma_{P^2} = \sigma_{G^2} + \sigma_{E^2} \quad (2)$$

Heritability is defined as a ratio of variances, by expressing the proportion of the phenotypic variance that can be attributed to variance of genotypic values: broad sense heritability (H^2) is defined as the proportion of trait variance that is due to all genetic factors including dominance and gene interactions

$$\text{Heritability (broad sense)} = H^2 = \sigma_{G^2} / \sigma_{P^2} \quad (3)$$

The genetic variance (σ_{G^2}) can be partitioned into the variance of additive genetic effects of breeding values (σ_{A^2}), dominance (interactions between alleles at the same locus) (σ_{D^2}), and epistatic (interactions between alleles at different loci) (σ_{I^2}):

$$\sigma_{G^2} = \sigma_{A^2} + \sigma_{D^2} + \sigma_{I^2} \quad (4)$$

Narrow sense heritability or strict sense heritability, h^2 is defined as the proportion of trait variance that is due to additive genetic factors:

$$\text{Heritability (narrow or strict sense)} = h^2 = \sigma_{A^2} / \sigma_{P^2} \quad (5)$$

1.2.2.1 Heritability ACE Model

The ACE model is a statistical model widely used in genetics epidemiology and behavioral genetics to analyze the results of twin studies. It aims to decompose sources of phenotypic variation into three categories: additive genetic variance (A), common environmental factors (C), and non-shared environmental factors plus measurement error (E). Some assumptions of the ACE model are: that there is no genetic dominance or

epistasis, that all genetic effects are additive, and the absence of gene-environment interactions.

MZ Twins

Twin 1	Twin 2
$A + C + E$	$A + C$
$A + C$	$A + C + E$

DZ Twins

Twin 1	Twin 2
$A + C + E$	$1/2A$
$1/2A$	$A + C + E$

MZ Twins

Twin 1	Twin 2
1	$A + C$
$A + C$	1

DZ Twins

Twin 1	Twin 2
1	$1/2A$
$1/2A$	1

r_{MZ} = A + C r_{DZ} = ½A + C

Therefore: $r_{MZ} - r_{DZ}$ = ½ A and $2(r_{MZ} - r_{DZ}$ = ½ A)

Since heritability is being classified as narrow sense or additive heritability this leads to: Falconer's formula A = $h^2 = 2(r_{MZ} - r_{DZ})$.

1.2.2.2 Heritability Falconer Formula

Falconer's Formula (Falconer, 1965) is used in twin studies (see section 2.1.1) to determine the genetic heritability of a trait based on the difference between intraclass correlations (ICC) in MZ twins and DZ twins. Heritability is a statistic that summarizes how much of the phenotypic variation in a trait is due to variation in genetic factors. Falconer's formula h^2 defines heritability as twice the difference in the intraclass correlation of a trait between MZ and DZ twins:

$$h^2 = 2(ICC_{MZ} - ICC_{DZ}) \quad (6)$$

The rationale is that any difference between MZ twins must be environmental (non-genetic), while the difference between DZ twins is both genetic and environmental, so the difference between the two is half-genetic. Falconer's formula will be used to calculate heritability in brain structure and function, and behavioral domains.

1.2.3 Heritability in the Brain

Twin studies can give insight into heritability of brain development, aging, morphology and function. The heritability estimates for most brain structures slightly increase from to childhood to adulthood (Jansen et al., 2015).

In a meta-analysis of twin studies published over the past 50 years (1958 – 2012), Polderman et al. (2015) researched the heritability of a wide range of human traits on more than 14 million twin pairs across 39 different countries. The study reported that not one trait had a weighted heritability estimate of zero and thus providing evidence that all human traits are heritable (Polderman et al., 2015). The study also found that, for 69% of the traits, the twin correlations were consistent with the additive genetic variation model. This suggests for many of the complex traits, genetic variants can be distinguished using a simple additive (narrow sense) genetic model (equation 5 above).

Evidence for genetic influence has been found for behavioral disorders such as alcoholism, schizophrenia, Alzheimer’s, autism, attention deficit hyperactivity disorder (ADHD) and reading disability (Plomin, 1994).

1.3 Data Human Connectome Project (HCP)

The HCP is an NIH-funded project led by Washington University, University of Minnesota, and University of Oxford aiming to provide state-of-the-art neuroimaging and

non-imaging data. The data provided will enable detailed analysis of genetic influences and characterizations of the human brain connectivity and function. The HCP dataset provides a unique and unprecedented opportunity to evaluate rigorously and comprehensively genetic effects on a multitude of brain, behavioral and cognitive measures the data consists of twins and non-twin siblings.

1.3.1 Population

The participant population consists of 1206 healthy adults, including twins and non-twin siblings, ranging in age of 22 - 37. This allows for an in-depth evaluation of the effects of genetics on brain measures and behavior.

Out of 1206 HCP participants, only the participants had genetically confirmed data were selected. This is especially important to have genetically confirmed data for the zygosity of the MZ and DZ twins. The exact number used for each modality varies depending on the available neuroimaging and behavioral data present for each participant. The exact number used for each modality is specified in each chapter. The siblings of twins and half siblings are excluded.

In the SB group there are, within the same family sometimes, 2, 3, 4 or 5 siblings. For families with a sibling count of more than 2, a pair is randomly selected for the SB group. In the NR group individuals were randomly paired. For each measurement, for the SB and NR groups, the ICC was calculated for randomly paired individuals. After repeating this process 1001 times, the median ICC was found.

Analyses of MZ and DZ pairs will allow estimation of the extent to which genotype, shared environment, and non-shared influences contribute to variation in traits and brain measures.

1.3.2 Behavior Data

A large amount of data, across many behavioral domains, especially for measures that have the potential to co-vary in interesting ways (across subjects) with brain connectivity and function, were collected for each subject. Standardized behavioral tests were used as much as possible to increase the prospects that findings based on the HCP data can in the future be related to other large- scale projects comparing brain and behavior.

1.3.3 MRI Data

Data will be analyzed from 3 MRI acquisitions: sMRI, fMRI, and dMRI. Participants were scanned on a customized 3T scanner at Washington University. Papers have been published that explicate in detail the instrumentation and image acquisition methods (Uğurbil et al., 2013), preprocessing pipelines (Glasser et al., 2013), diffusion imaging (Sotiropoulos et al., 2013), resting-state fMRI (Smith et al., 2013), and informatics and quality control processes (Marcus et al., 2014). An overall report of HCP's neuroimaging approaches was published in 2016 (Glasser et al., 2016).

1.4 Methodology

Throughout this dissertation there are commonly used statistical methods throughout each chapter. If a statistical method is used only for a specific chapter it is discussed in

that chapter (example: ARIMA (15,1,1) in Chapter 5 fMRI). Below are the commonly used statistical methods across all chapters:

Intraclass Correlation (ICC). ICC quantifies the agreement between pairs of measurements, when the assignment of the pairs is not fixed. It was originally proposed by Fisher (1958) and introduced in genetics to quantify the agreement between measurements for siblings (Pederson, 1971; Ponzoni & James, 1978; Sedgwick, 2013). ICC will be estimated for each one of the 4 genetic groups for each measure and data kind using the IBM-SPSS package (one-way random model).

Falconer's Formula. Falconer's Formula (equation 6 above) will be applied to determine the narrow-sense, strict genetic heritability of a measure based on the difference between ICCs in MZ twins and DZ twins.

3.1 Statistical analyses of ICC and heritability

General. ICC and its z-transform zICC will be computed for each measure. Negative ICC values will be rejected (Giraudeau,1996). The effects of group on zICC across measures and domains will be evaluated using an ANOVA and independent samples t-test, as needed. Falconer's heritability estimates will be calculated for each measure. The effects of group and gender will be assessed for positive heritability estimates using an ANOVA.

Multidimensional Scaling (MDS). MDS is a powerful tool to identify relations among items in a multidimensional space. It is a dimensionality reduction method used to reduce the number of dimensions in a multidimensional data set, typically to two or three dimensions. The input to MDS is a proximity (square) matrix, which typically consists of

pairwise dissimilarities between items. MDS places the items in a low-dimensional space such that the distances between items in this space are as close as possible to their corresponding distances in the original space. The derived plot captures arrangements of items that share common attributes in the reduced space and thus may reveal associations hitherto unsuspected. In this analysis, the nonmetric MDS implemented in the IBM-SPSS package will be used.

Hierarchical Tree Clustering (HTC). HTC is a multivariate method that places items in hierarchically organized clusters, forming a tree (dendrogram). HTC assumes the presence of a root, which, in this proposal, is the heritability, i.e. that items to be clustered are all heritabilities. HTC organizes objects into a dendrogram and clusters are defined by removing branches from the dendrogram (Langfelder, Zhang, & Horvath, 2008). The hierarchical clustering process looks for pairs of samples that are the most similar. The input is a dissimilarity matrix, therefore, the pair that has the lowest dissimilarity is the most similar. The point at which the pairs are joined is called a node. This step keeps repeating and the dissimilarity is recalculated between each merged pair and other samples. The analysis will use between-groups linkage and squared Euclidean distance to compute a dendrogram using the IBM-SPSS package.

Chapter 2 Behavior

2.1 Introduction

The powerful and influential role of genetics in human development is undeniable. The imprint of genetics starts at fertilization when the sperm and oocyte fuse together to form a new single cell which grows and develops into a unique individual. Genetics has a direct role in the heritability of physical traits, diseases and disorders. However, when it comes to the heritability of behavioral traits, although genes do not have a direct role, they do influence heritability of behavioral traits. A question that is commonly asked in the behavioral genetics field is: How much influence does genetics have on human behavior? One way the field attempts to answer this question is to separate out an individual's variation into genetic and environmental components by using family, twin and adoption studies. Behavioral testing is also used to determine genetic influence. Behavioral testing provides valuable data that helps elucidate the brain mechanisms underlying a specific behavior and also assesses a participant's abilities such as intelligence (verbal, nonverbal) and cognitive skills (language, reading, memory). By using the data collected from behavioral testing, heritability studies can be conducted to quantify the effects of genetics.

The literature shows that all human behavioral traits are heritable to some degree (W. Johnson, 2011; Turkheimer, 2000). However, there has not been a comprehensive study of a single population across many different behavior domains. Chapter 2 of this dissertation uses known genetic relationships and behavioral testing in a young, healthy

population to determine the influence of genetics and heritability across five different behavioral domains: motor, emotion, personality, sensory and cognition.

2.1.1 Motor

Although motor skills such as walking, dexterity, strength and endurance can be learned by practicing, some individuals can improve quicker than others, which suggests a genetic component. A study conducted by Missitzi et al. in 2013 used the twin model (see Chapter 1) to compare differences in MZ and DZ twins to elucidate the relative contribution of genes and environment on individual differences in motor control and learning. The study found that for motor control, the correlation for MZ and DZ twins were 0.77 and 0.39 respectively. Heritability was estimated to be 0.68. For motor learning, the study found correlations to be 0.58 and 0.19 for MZ and DZ twins respectively and heritability to be 0.70. These findings by Missitzi et al. (2013) suggest that heredity plays a major part in individual differences in motor control and motor learning, making them strongly genetically dependent.

2.1.2 Emotion

Emotion is essential to human behavior and central to the everyday human experience because emotional traits measure qualities such as psychological well-being, social relationships, stress and efficacy responses (Bevilacqua & Goldman, 2011; Dolan, 2002). One topic of interest is to how different domains interact with and influence each other. For example, emotion exerts a powerful influence on cognition, which is an area of interest because it encompasses qualities such as attention, memory, and reasoning (Dolan, 2002). Another area of interest is mental disorders where emotional

disequilibrium is a common denominator (Bevilacqua & Goldman, 2011). In terms of heritability, emotion is moderately heritable (40-60%) (Bouchard & Loehlin, 2001; Bouchard & McGue, 1990) but is also influenced by environment.

2.1.3 Personality

Human personality is characterized as inborn traits that influence behavior across many situations. Personality can be measured by many factors, and one way of scientifically determining personality is the Big Five Factor Model described as follows: 1. Openness: appreciation for a variety of experiences. 2. Conscientiousness: planning rather than being spontaneous. 3. Extraversion: being sociable, energetic and talkative. 4. Agreeableness: being kind, sympathetic and happy to help. 5. Neuroticism: inclined to worry or be vulnerable or temperamental.

Jang, Livesley, & Vemon, (1996) studied 123 pairs of MZ twins and 127 pairs of DZ twins and determined personality using the Big Five Model. Their results showed genetic influence on the five dimensions: neuroticism (0.41), extraversion (0.53), openness (0.61), agreeableness (0.41), and conscientiousness (0.44). Another study using twins by Power & Pluess (2015) found that the Big Five personality traits have substantially heritable components explaining 40–60% of the variance, although identification of associated genetic variants has remained unclear.

2.1.4 Sensory

Sensory systems such as vision, hearing, touch, taste, and smell help the brain perceive and interpret the physical world around us. In children, difficulty in processing and integrating information can overwhelm them and create confusing behavior.

Research has shown that sensory traits are heritable, but it is not definite how much. One example of a sensory system is pain. A study conducted by Trost et al. (2015), used MZ and DZ twins to examine the genetic, environmental and observed contributions to pain. The heritability estimate for pain was found to be 37% (Trost et al., 2015).

2.1.5 Cognition

Cognitive functions such as thinking, reading, learning, memory, reason, and attention are core brain-based skills that are used to carry out simple and complex tasks. Cognitive skills take incoming information and convert it into useful knowledge on a daily basis. For example, answering the telephone involves recognition (knowing what a telephone is and what it is used for), perception (hearing the ring tone), decision making (answering or not to answer), motor skill (lifting the phone and pushing buttons), language skills (talking and understanding language), social skills (interacting with another human being) (Michelon, 2006). Cognition traits are important in research because they are one of the most reliable behavioral traits (Haworth et al., 2010). Another reason that cognition traits are important is because they can be used to predict important social outcomes such as educational and occupational levels better than other behavioral traits (Haworth, 2010). The heritability of cognitive skills increases from childhood to adulthood (Briley & Tucker-Drob, 2013; Haworth et al., 2010). Haworth et al. (2010) looked at data from six studies containing information from 11,000 twin pairs from four countries and found that heritability increased from 41% at adolescence to 66% at young adulthood.

2.2 Heritability Calculations

Human behavior traits emerge out of a complex and nonlinear developmental process. To understand some of these multifaceted processes, behavior measures are included in this study (see Table 2.1) in order to assess a wide range of human functions and abilities. The literature review shows that different behavioral traits are heritable across many different domains. In a meta-analysis of twin studies published over the past 50 years (1958 – 2012), the heritability of a wide range of human traits on more than 14 million twin pairs across 39 different countries was studied. The study reported that not one trait had a weighted heritability estimate of zero, thus providing evidence that all human traits are heritable (Polderman et al., 2015). The report also found that twin correlations were consistent with the additive genetic variation model for the majority of the traits (69%). This pattern of twin correlation was consistent for traits in the neurological; ear, nose and throat; cardiovascular and ophthalmological domains. When the traits were grouped into 28 general domains, three of the 28 general trait domains (activities, reproduction, and dermatological) were inconsistent with the additive model, while 25 of the 28 general domains were consistent. This suggests that for many of the complex behavioral traits used in this chapter of the dissertation, genetic variants can be distinguished using an additive (narrow sense) genetic model (See Chapter 1).

2.3 Methods

2.3.1 Participants

HCP participants are young healthy adults, age 22 to 37 years, who are free of major psychiatric or neurological diseases (Marcus et al., 2014). The full set of inclusion and exclusion criteria is detailed in a manuscript published by Van Essen et al. (2013). The

final release included 1206 participants; however, since heritability is heavily dependent on known genetic relationships (twins, siblings, non-related) (See Chapter 1), only participants that were genetically verified were selected for analysis. Participants that were not genetically verified were removed from analysis. Participants that are half siblings or siblings of twins are also excluded.

From the 1206 subjects, 1142 (genetically and zygosity verified) subjects were selected. In order to determine the heritability, behavioral data of 1142 participants were grouped into the following 4 genetic groups and analyzed: (1) MZ twins (N = 298; 149 pairs), (2) DZ twins (N = 188; 94 pairs), (3) non-twin SBS (N = 298; 149 pairs; if sibling count is more than 2 the pair is randomly selected from the siblings), and (4) NR (N = 76 (not members of any other group); 38 pairs (randomly paired)).

2.3.2 Behavioral Measures

Behavioral measures that were collected (Van Essen et al., 2013) used reliable and validated measures to assess a wide array of functions and behaviors within a reasonable amount of time (3-4 hours). Quantitative data from the following five domains were used. (Non-quantifiable data have been excluded. See Table 2.1 for detailed information on individual behavioral traits contained in each domain.)

1. Motor (M): These measures quantify the participant's motor strength and skills (N = 4).
2. Cognition (C): These measures cover a wide range of cognitive functions, including episodic memory, working memory, executive function, language, and speed of cognitive processing (N = 18). The last two measures Self-

regulation/Impulsivity (Delay Discounting) and Sustained Attention (Short Penn Continuous Performance Test: Percentage) were calculated by averaging the measures listed in description in Table 2.1

3. Emotion (E): These are self-reported measures pertaining to the emotional state and outlook of each participant, namely social relationships, psychological well-being, emotional recognition and stress (N = 24).
4. Personality (P): These measures come from the 60-item version of the Costa and McRae Neuroticism/Extroversion/Openness Five Factor Inventory (NEO-FFI) (N = 5).
5. Sensory (S): These measures cover the following sensory modalities: visual activity, contrast, and color, audition, olfaction, pain and taste (N = 5).

2.3.3 Statistical methods

See Chapter 1 for details on the statistical methods used in this chapter.

2.4 Results

Test scores were analyzed from 56 traits in 5 domains (motor, sensory, cognition, emotion, and personality). Specifically, 4 analyses were carried out, as follows. First, the ICC and zICC were computed for each genetic group and trait. An ANOVA was performed on the zICC with the genetic group as a fixed factor to evaluate differences between groups. Second, h^2 was computed for each domain to compare heritabilities across domains. Third, an MDS analysis was done using median h^2 domain values to evaluate possible groupings of domain heritabilities. Finally, an HTC analysis was

performed on the same heritability data to explore their clustering more explicitly. The results found are the following.

First, the mean zICC differed significantly among groups ($P < 10^{-16}$, F-test in ANOVA) and varied systematically, such that MZ>DZ>SB>NR (Fig. 2.1); all pairwise comparisons were statistically significant ($P < 0.05$).

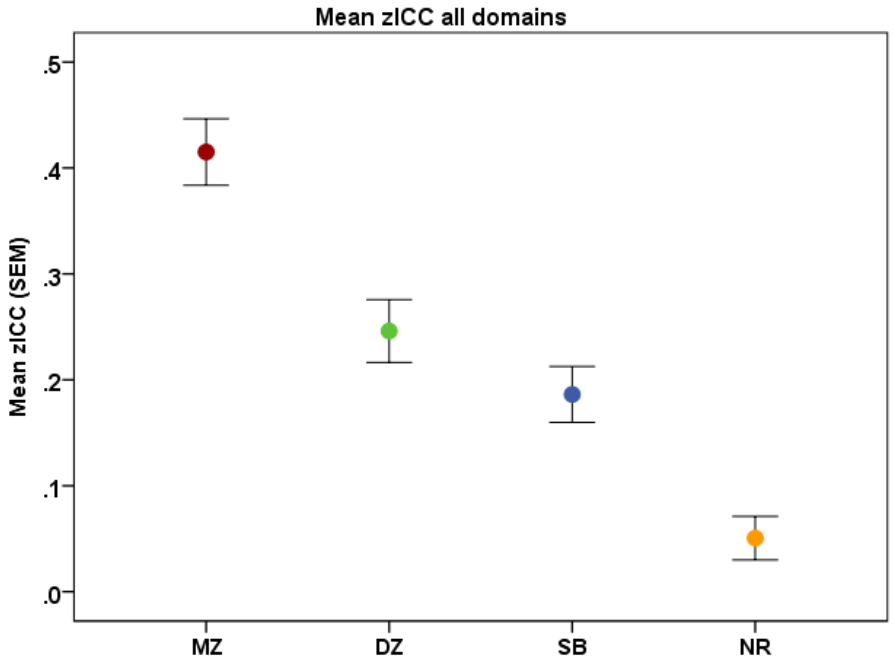

Fig. 2.1 Mean zICC ± SEM per genetic group

Participants were also split by gender and the same systematic variation was observed (Fig 2.2, 2.3). A specific comparison of the zICC between DZ and SB groups, since those pairs share the same amount (50%) of genetic material. The zICC of these groups did not differed significantly ($P = .123$, ANOVA). MZ twins were split by gender and by domain groups but they did not differ significantly (Fig 2.4, 2.5).

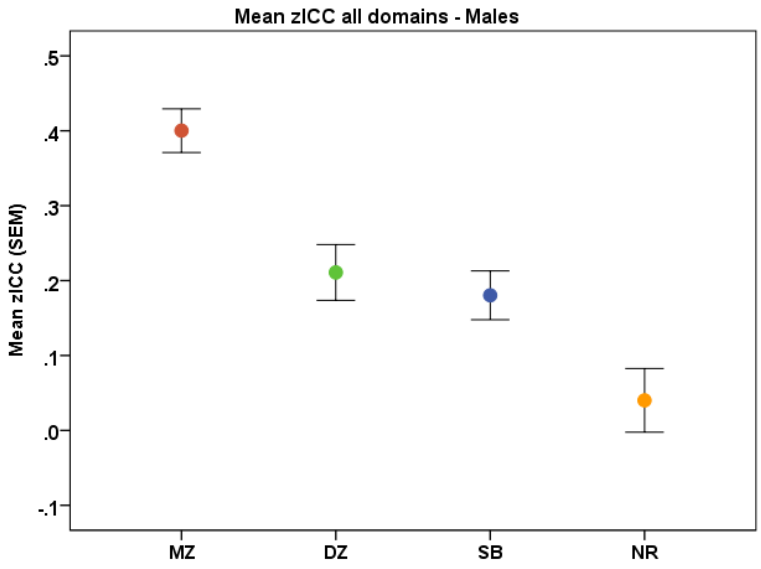

Fig. 2.2 Mean zICC ± SEM per genetic group for males.

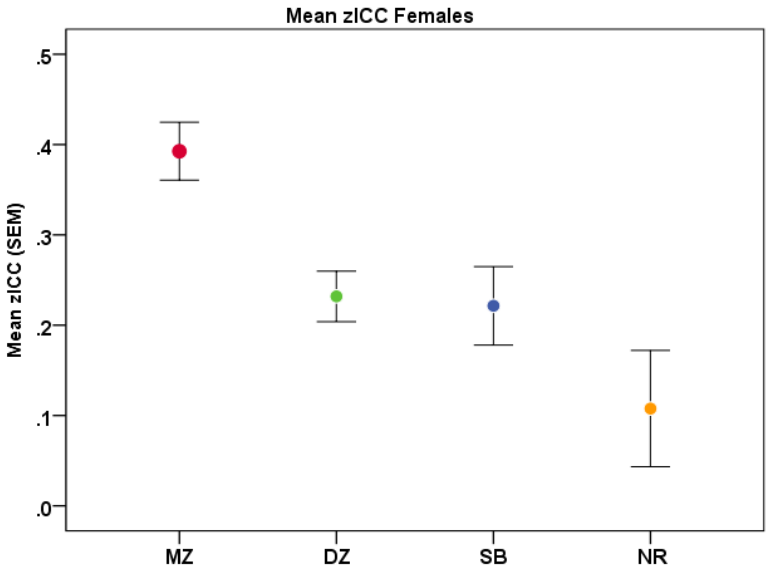

Fig. 2.3 Mean zICC ± SEM per genetic group for females

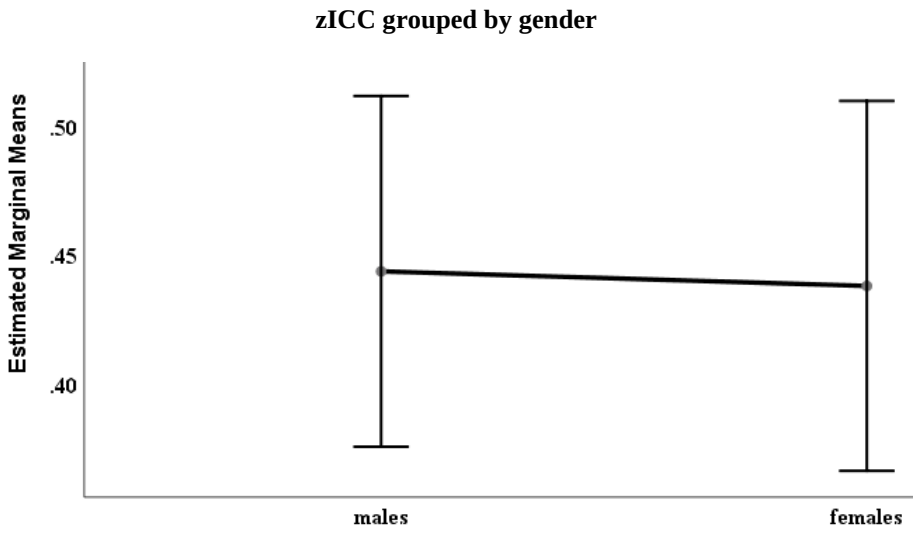

Fig. 2.4 Mean zICC ± SEM for MZ males and females.

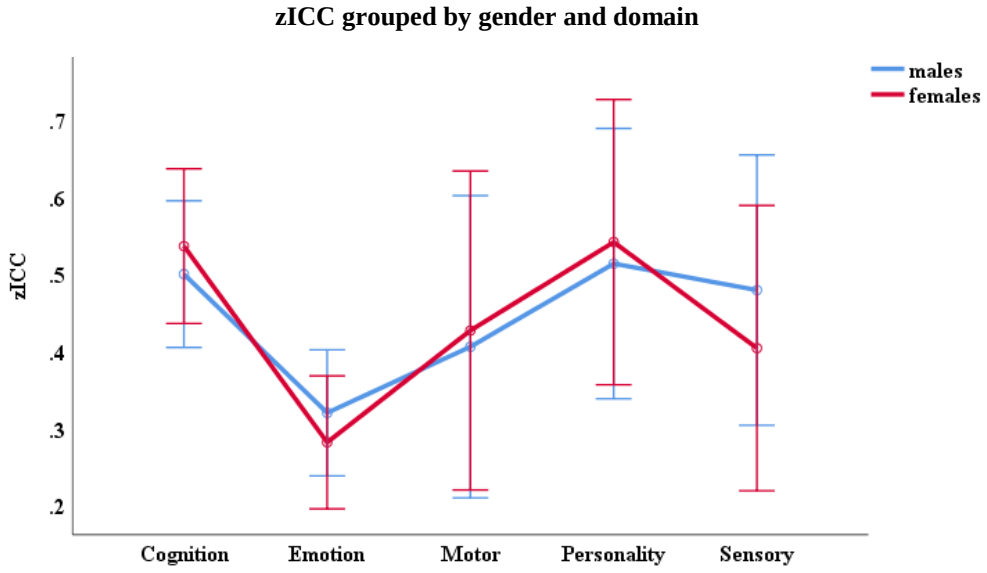

Fig. 2.5 Mean zICC ± SEM MZ by gender and domain.

Second, h^2 was computed for each domain to compare heritabilities across domains; negative heritabilities were removed. The heritabilities did not differ significantly among domains (Fig. 2.6, 2.7, 2.8; P = 0.076, F-test in ANOVA). Overall the heritability values for the 5 domains were: Cognition h^2 = .405, Emotion h^2 = .316, Motor h^2 = .138, Personality h^2 = .444, and Sensory h^2= .193. For males the heritability values were: Cognition h^2 = .483, Emotion h^2 = .360, Motor h^2 = .294, Personality h^2 = .364 and Sensory h^2= .669. For females the heritability values were: Cognition h^2 = .364, Emotion h^2 = .301, Motor h^2 = .132, Personality h^2 = .561 and Sensory = .237. When the participants were split by gender, the overall pattern was followed by all domains for males and females, except in males which had a lower heritability value for personality and had a higher heritability value for sensory. One hypothesis could be that that this finding reflects the shared neural substrates among the 5 domains.

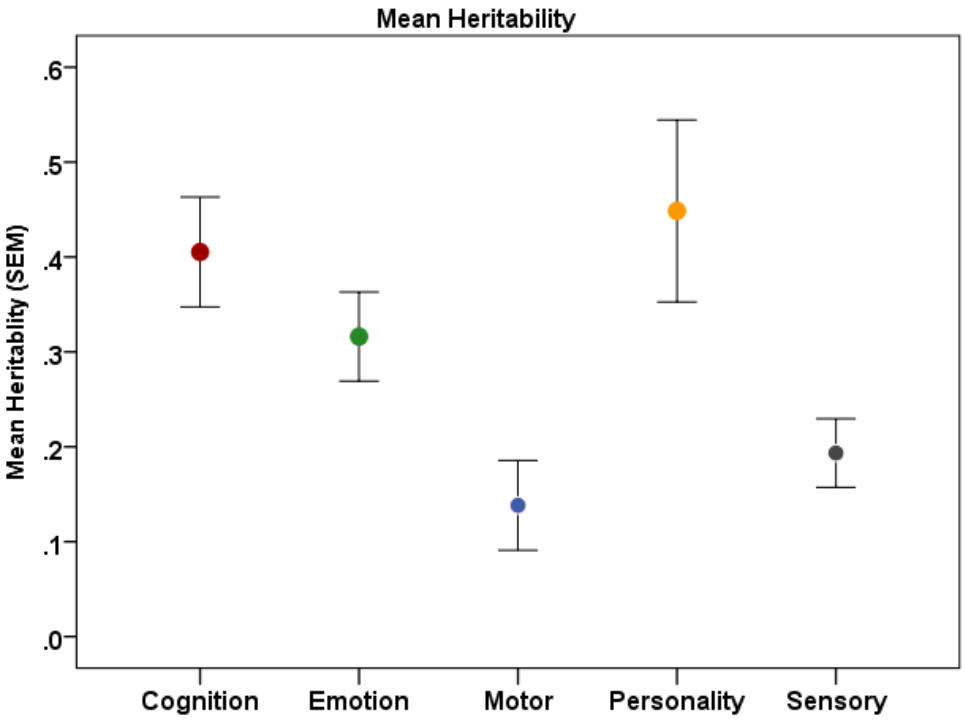

Fig. 2.6 Mean h^2 ± SEM per behavioral domain.

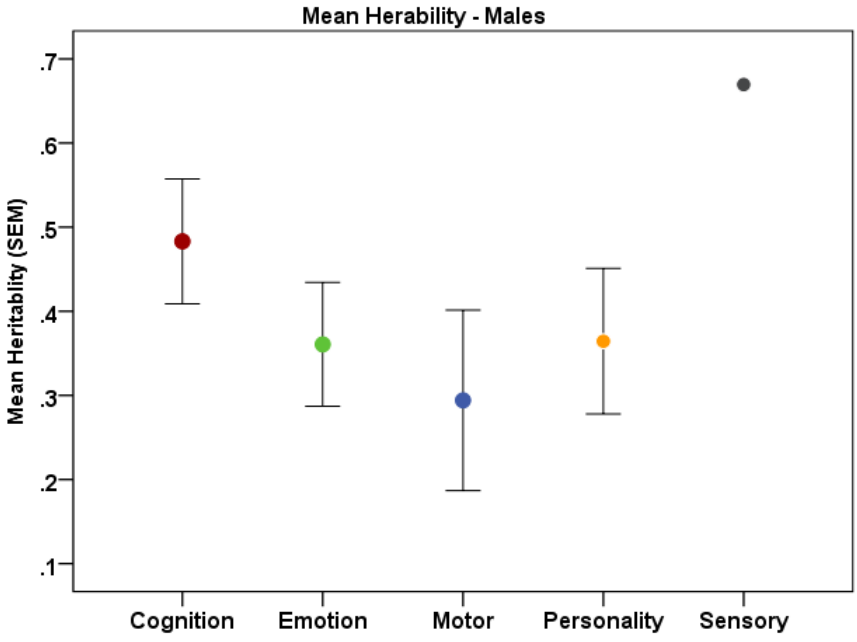

Fig. 2.7 Mean h^2 ± SEM per behavioral domain for males

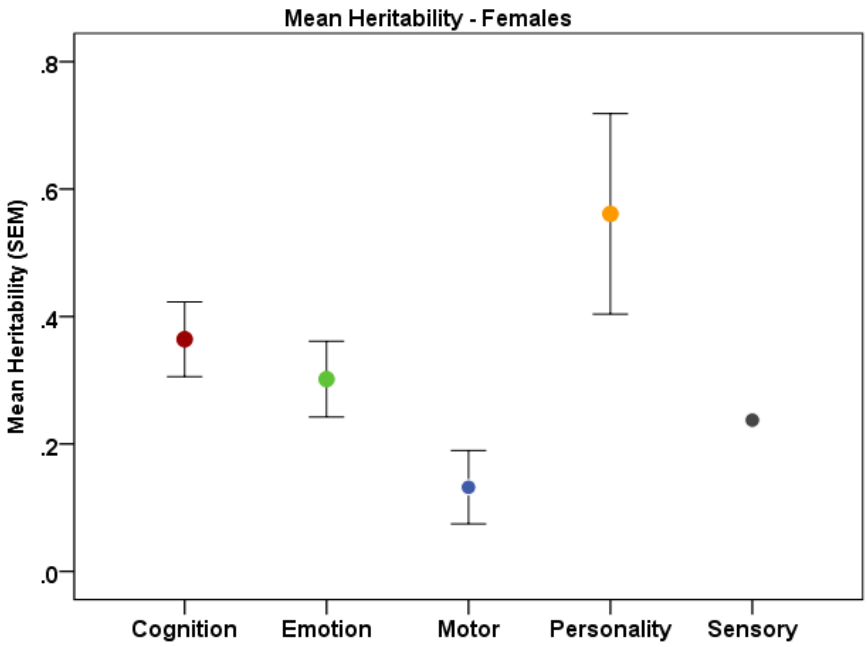

Fig. 2.8 Mean h^2 ± SEM per behavioral domain for females

Third, the MDS analysis of the behavioral domain heritabilities (Fig. 2.9) revealed a separation of the 5 domains in 4 quadrants comprising motor and sensory domains in the (upper and lower right quadrant), emotion and cognition (lower left), and personality (upper left). The fit of the nonmetric (ordinal) model was excellent (normalized raw stress = 0.00004, Dispersion Accounted For = 0.99).

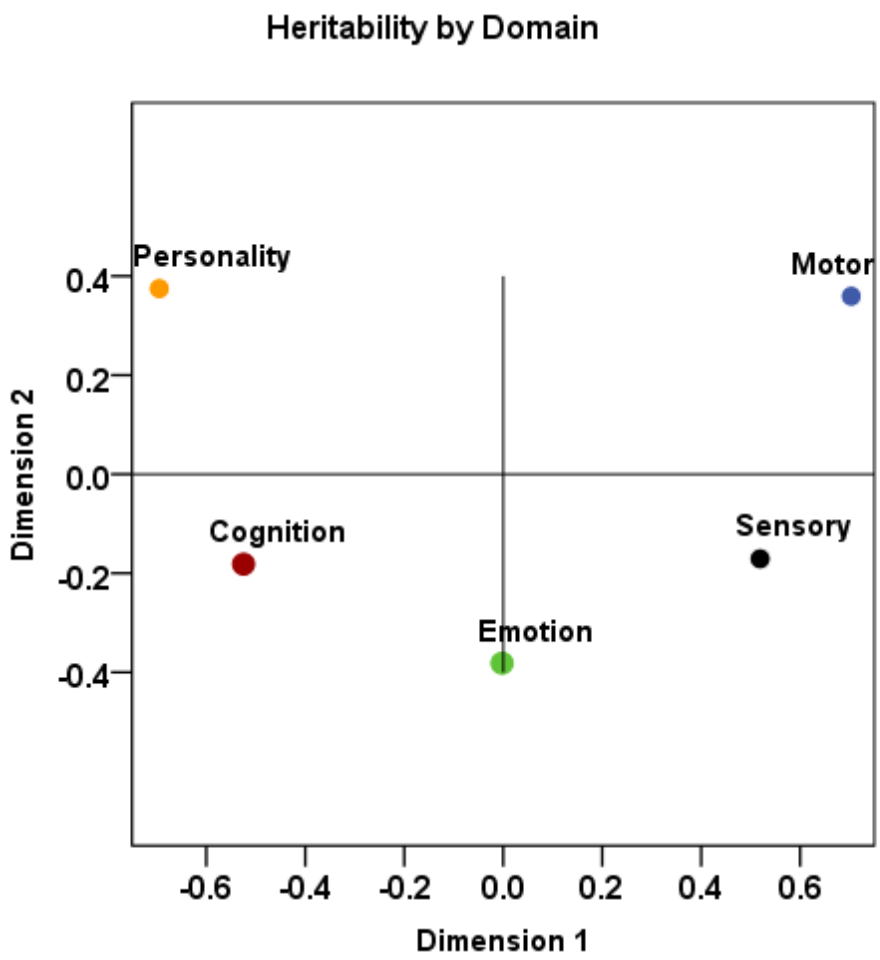

Fig. 2.9 MDS of median h^2 of the 5 behavioral domains.

Finally, the grouping and gradient above was confirmed in the HTC dendrogram (Fig. 2.10), which comprises 2 branches, one containing (motor, sensory) in one branch and in 2 separate sub-branches, (emotion) in one branch and the other containing (cognition, personality) in a single branch.

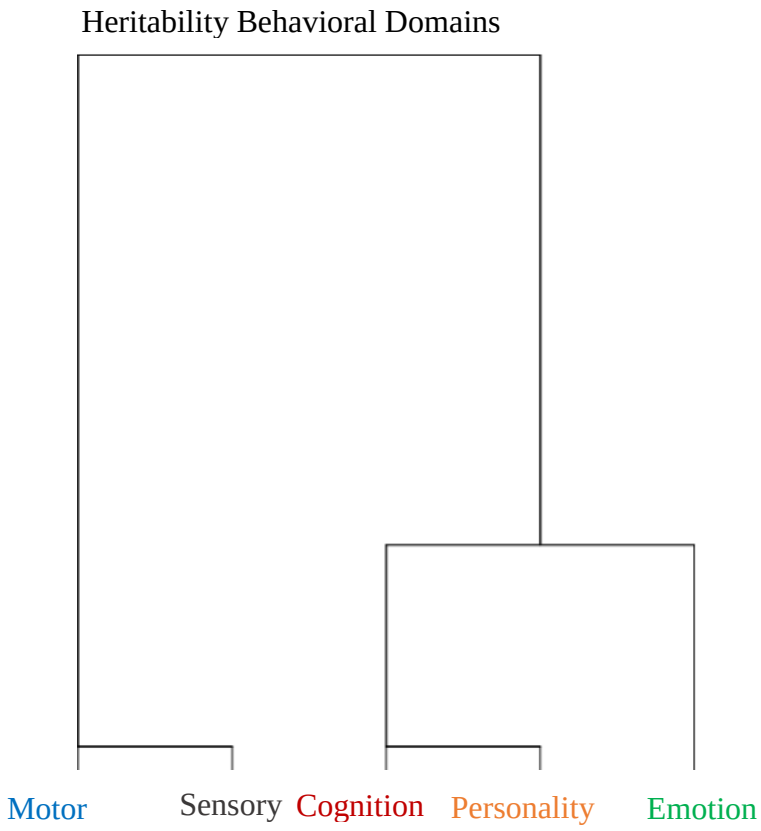

Fig. 2.10 HTC of median h^2 of the 5 domains.

2.5 Discussion

The relationship between genetics, behavior and heritability is a topic of research across many different disciplines such as sociology, education, neuroscience, and politics (Toga & Thompson, 2005). The goal of Chapter 2 is to determine the heritability of behavioral traits in five domains in a young, healthy population using known genetic relationships (twins, siblings).

The grouping of participants into genetic groups resulted in the zICC differing significantly and varying systematically among the groups, such that MZ>DZ>SIB>NR for behavioral measurements. This result is expected and consistent with the literature

since MZ twins share all genetic effects, while DZ twins share on average 50 % of their genetic effects. Siblings also share, on average, 50% of their genetics; however, it is expected that they would have lower zICC (and heritability values) because their environmental variation is higher compared to twins. The non-related participants are expected to be last in terms of similarity since they are not expected to have any genetic effects.

The heritability results are in agreement with the literature: most human behavioral traits have some degree of heritability across different domains (W. Johnson, 2011; Turkheimer, 2000). The heritabilities did not differ significantly among domains (Fig 2.6-8). The hypothesis for this result is that heritability relates to brain biology/function which is overlapping among the various behavioral domains, all of which share converging brain networks. Across the genders there is a pattern of heritability (from largest to smallest): cognition, emotion and motor.

MDS and HTC were used to decipher grouping of the heritabilities based on domain. Since the dimensions are not fixed, a reasonable interpretation of the MDS findings (Fig. 2.9) can be elucidated by splitting the graph by the 2nd dimension. This would position motor-sensory on the right side of the graph and cognition-personality on the left side of the graph with emotion in the middle. This shows that the relevant gradient extends from simple, sensory-motor domains to complex, cognitive-affective domains. This grouping of the MDS is further confirmed in the HTC results (Fig. 2.10). For example, a genetic interpretation could be that the motor and sensory areas of the brain were influenced by the same genetic factor, whereas the cognition, personality and emotion areas were influenced by a different genetic factor. Hence, there is an overlap in genes regulating

processes of cognition, personality and emotion, while other genes play a role in the sensory-motor functioning area (Polderman et al., 2015).

2.6 Conclusion

One could argue that it is not possible to detangle the factors involved because of the hundreds of genes, circuits and environmental exposures involved in human behavioral traits. However, the fact that behavior is genetically driven—i.e., heritable—enables genetic approaches to be applied to the variance in behavior even though there are differences (Bevilacqua & Goldman, 2011). Advances in brain imaging and genetics have enabled research of genetic and environmental influences on the human brain. It empowers researchers to visualize different aspects of brain structure and function. This enables researchers to determine which aspects of brain structure and function are heritable and to link those features to behavioral and phenotypical traits.

Domain	Subdomain (Measure Name)
Cognition	Episodic Memory (Picture Sequence Memory) Executive
	Executive Function/Cognitive Flexibility (Dimensional Change Card Sort)
	Executive Function/Inhibition (Flanker Inhibitory Control and Attention Task)
	Fluid Intelligence (Penn Progressive Matrices: Number Correct)
	Fluid Intelligence (Penn Progressive Matrices: Response Time)
	Language/Reading Decoding (Oral Reading Recognition)
	Language/Vocabulary Comprehension (Picture Vocabulary)
	Processing Speed (Pattern Comparison Processing Speed)
	Spatial Orientation (Penn Line Orientation: Total Number Correct)
	Spatial Orientation (Penn Line Orientation: Total Positions Off for All Trials)
	Spatial Orientation (Penn Line Orientation: Median Reaction Time)
	Sustained Attention (Short Penn Continuous Performance Test: True Positive)
	Sustained Attention (Short Penn Continuous Performance Test: Longest Run of Non-Responses)
	Verbal Episodic Memory (Penn Word Memory Test: Total Number Correct)
	Verbal Episodic Memory (Penn Word Memory Test: Response Time)
	Working Memory (List Sorting)
	Mean Self-regulation/Impulsivity (Delay Discounting) ((DDisc_AUC_200 + DDisc_AUC_40K) / 2)
	Sustained Attention (Short Penn Continuous Performance Test: Percentage) ((SCPT_TP + SCPT_TN) / (SCPT_TP + SCPT_TN + SCPT_FP + SCPT_FN) * 100)
	Emotion Recognition (Penn Emotion Recognition Test: Number of Correct Responses)
	Emotion Recognition (Penn Emotion Recognition Test: Correct Responses Median Response Time
	Emotion Recognition (Penn Emotion Recognition Test: Correct Anger Identifications)
	Emotion Recognition (Penn Emotion Recognition Test: Correct Fear Identifications)
	Emotion Recognition (Penn Emotion Recognition Test: Correct Happy Identifications)
	Emotion Recognition (Penn Emotion Recognition Test: Correct Neutral Identifications)

Emotion	Emotion Recognition (Penn Emotion Recognition Test: Correct Sad Identifications)
	Negative Affect (NIH Toolbox Anger-Affect Survey)
	Negative Affect (NIH Toolbox Anger-Hostility Survey)
	Negative Affect (NIH Toolbox Anger-Physical Aggression Survey)
	Negative Affect (NIH Toolbox Fear-Affect Survey)
	Negative Affect (NIH Toolbox Fear-Somatic Arousal Survey)
	Negative Affect (NIH Toolbox Sadness Survey)
	Psychological Well-being (NIH Toolbox General Life Satisfaction Survey)
	Psychological Well-being (NIH Toolbox Meaning and Purpose Survey)
	Psychological Well-being (NIH Toolbox Positive Affect Survey)
	Social Relationships (NIH Toolbox Friendship Survey)
	Social Relationships (NIH Toolbox Loneliness Survey)
	Social Relationships (NIH Toolbox Perceived Hostility Survey)
	Social Relationships (NIH Toolbox Perceived Rejection Survey)
	Social Relationships (NIH Toolbox Emotional Support Survey)
	Social Relationships (NIH Toolbox Instrumental Support Survey)
	Stress and Self Efficacy (NIH Toolbox Perceived Stress Survey)
	Stress and Self Efficacy (NIH Toolbox Self-Efficacy Survey)
Motor	Endurance (2-minute walk test)
	Locomotion (4-meter walk test)
	Dexterity (9-hole Pegboard)
	Strength (Grip Strength Dynamometry)
Personality	Five Factor Model NEO-FFI (Agreeableness)
	Five Factor Model NEO-FFI (Openness)
	Five Factor Model NEO-FFI (Conscientiousness)
	Five Factor Model NEO-FFI (Neuroticism)
	Five Factor Model NEO-FFI (Extroversion)
Sensory	Audition (Words in Noise)
	Olfaction (Odor Identification Test)
	Pain (Pain Intensity and Interference Surveys) (self-report)
	Taste (Regional Taste Intensity Test)
	Contrast Sensitivity (Mars Contrast Sensitivity)

Table 2.1 of Behavior Measures

Chapter 3 Diffusion MRI (dMRI)

3.1 Introduction

dMRI is a non-invasive neuroimaging technique, that uses existing MRI technology and equipment to capture the diffusion of water molecules in images called diffusion weighted images (DWI) (Soares et al., 2013). dMRI exhibits extremely high sensitivity to water movements in the human body and records the diffusion of water in tissues; this is especially useful for brain tissue (Le Bihan and Breton, 1986). The self-diffusion coefficient of free water is around $3.0 \times 10^{-9} m^2 s^{-1}$ at 37°C (Le Bihan and Iima, 2015). In a healthy brain, water diffuses at a slower rate as compared to free water, while

malignant brain tissue has an even slower rate of diffusion. dMRI has the capability to detect the decrease of water diffusion in ailing brains compared to healthy brain. Thus, by measuring the diffusion of water in the brain, researchers can determine the characteristics of healthy brain tissue and malignant brain tissue.

3.2 dMRI for brain studies

dMRI has been applied to better understand neurodevelopment in several studies from neonates through to the 8th decade of life (Moseley, 2002; Neil et al., 2002). The literature reveals that the most established clinical application of dMRI is for detection and evaluation of ischemic infracts stroke. The increase in DWI signal in areas of acute stroke, relative to unaffected brain, is typically so striking that this finding has been referred to as the "lightbulb sign" of acute stroke (Maas and Mukherjee, 2005). Previous work on dMRI has studied neurodevelopmental disorders (e.g. autism), neuropsychiatric disorders (e.g. schizophrenia, depression) or neurologic disorders (e.g. Parkinson's disease) (Snook, et al., 2005), but has limited studies for healthy human brains.

The limited dMRI studies of healthy brains “have been performed with a variable number of subjects and differing age ranges” (Gazes et al., 2016; Snook et al., 2005). It is important to have a narrow age range for neuroimaging studies as age can dramatically affect the results. For example, in a study of neonates and children, researchers found opposite trends in mean diffusivity and anisotropy with age (McKinstry et al., 2002). However, even within a narrow age range, brain developmental stages also affect the research findings. For example, after 40 years of age, the brain starts to age and decline, and this affects research results. Neuroimaging studies demonstrate that the human brain

is actively changing and developing (in size, vasculature, and cognition) roughly until mid-twenties to mid- thirties (Johnson et al., 2009). Brains that have reached that age range are particularly useful for understanding healthy human brains; but, there are limited studies of young participants who are free of complicated diseases, making it difficult to study the aging process of the normal brain (Sowell, 2004). The 22-to-37-year-old brains of the HCP population are particularly important to study since at that age, the brain is considered a fully developed brain but not an aging brain.

The HCP dataset is also valuable for its dramatic advances in dMRI imaging techniques. The imaging data that results in with improved spatial, temporal and angular resolutions. This makes the HCP dataset to date the most comprehensive dataset of numbers of young participants whose brains are fully developed and are free of complicating diseases to study healthy brain (Shi and Toga, 2017).

dMRI Principles and Concepts

dMRI principles and basic concepts have been described and reviewed in the literature at length (Le Bihan et al., 2001; Mukherjee, et al., 2008). Diffusion refers to the random Brownian motion of molecules in a liquid or gas (Kingsley, 2010). dMRI takes advantage of the fact that water molecules have different rates of diffusion in different substances (Le Bihan and Breton, 1985).

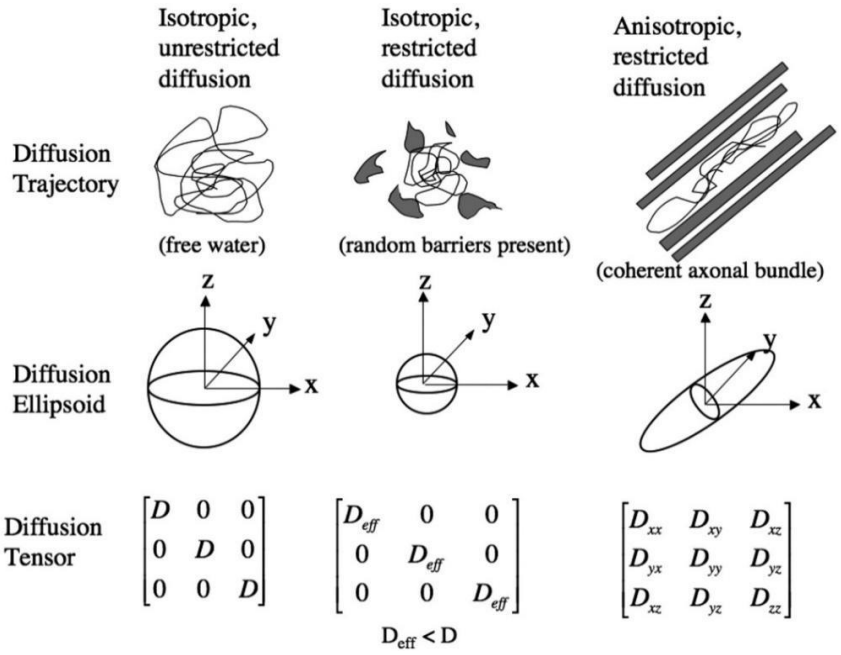

Figure 3.1 Mukherjee, et al., 2008 Diffusion Tensor MR Imaging and Fiber Tractography: Theoretic Underpinnings

For example, in a liquid that is relatively homogenous such as water, the diffusion rate of molecules is the same in every direction (unrestricted) or isotropic (Fig. 3.1). However, in biological tissues, the diffusion of water molecules is restricted by tissue boundaries and membranes causing diffusion to be restricted or is anisotropic (Fig. 3.1). In the brain, water molecules diffuse differently along the tissues depending on its type (GM/WM), integrity (healthy or diseased), architecture (round, elongated), and presence of barriers (membranes, tumors). Diffusion in WM tends to be more anisotropic compared to GM which is usually more isotropic (Pierpaoli et al., 2006). The aim of dMRI and specifically diffusion tensor imaging (DTI) is to detect the diffusion of water molecules in WM in order to evaluate the microstructural integrity of the WM (Tromp, 2015).

Based on the assumption that water is always moving (due to Brownian motion) and leads to a natural diffusion of water at all times, Basser et al. (1994) modeled the movement of water by an ellipsoid. An ellipsoid is mathematically represented by a 3×3 symmetric tensor (Soares et al., 2013)(Fig. 3.1). "The three diagonal elements, Dxx, Dyy, Dzz, represent diffusion as measured along each of the principal (x, y and z) axes. The six off-diagonal terms (Dxy, Dxz, Dyz, etc.) (Fig 3.1) return the correlation of random motions between each pair of principal directions (Elster, 2017).

The diffusion ellipsoid (Fig 3.2) has three-unit vectors and their corresponding lengths (λ1, λ2, and λ3), the eigenvalues (Elster, 2017). The eigenvalues of the diffusion tensor are either parallel (λ1) or perpendicular (λ2, λ3) to the white matter tracts. λ2, λ3 are not often reported but can yield insight into the microstructural changes of the tissue.

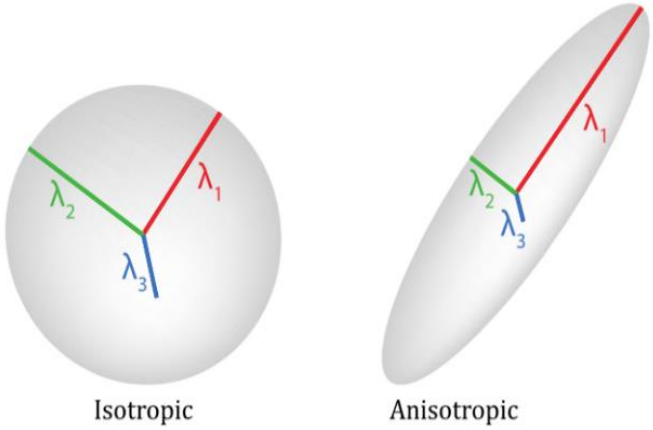

Figure 3.2 Do Tromp 2016

The diameter of the ellipsoid approximates the diffusivity of water in that particular direction and the major principle axis is oriented in the direction of maximum diffusivity (Jellison et al., 2002). For perfect isotropic diffusion, the ellipsoid becomes a sphere with λ1 = λ2 = λ3 (Elster, 2017) (Fig 3.2). As diffusion becomes more anisotropic, the ellipsoid becomes elongated: λ1 > λ2 > λ3 (Fig 3.2). The DTI enables the indirect measurement of water movements within each voxel of the brain (Basser et al., 1994) providing a unique opportunity for studying WM architecture (Jellison et al., 2002)

3.3 WM Measurements

Analysis of dMRI data allows scientists to acquire key measurements to quantify the microstructural integrity of the WM. One key measure is fractional anisotropy (FA), which describes the preferred direction of diffusion in a given voxel. FA values ranges between zero and one. A value of zero means that the diffusion of water molecules is unrestricted (isotropic) and free to diffuse in all directions. A value of one means that diffusion occurs only along one axis and is fully restricted (anisotropic).

$$FA = \frac{\sqrt{(\lambda_1 - \lambda_2)^2 + (\lambda_2 - \lambda_3)^2 + (\lambda_3 - \lambda_1)^2}}{\sqrt{2}\sqrt{\lambda_1^2 + \lambda_2^2 + \lambda_3^2}}$$

Another key measurement is mean diffusivity (MD), which is the average of the three eigenvalues and correspond to the molecular diffusion rate (lower values mean low diffusivity) (Soares et al., 2013)

$$MD = \frac{\lambda 1 + \lambda 2 + \lambda 3}{3}$$

Together FA and MD help researchers determine the flow of water and infer the shape of the brain's WM. Thus, allowing researchers to study the different connections of the brain and approximate the microstructural integrity of WM. Figure 3.3 is an example of a brain image with the DTI fit. The colors show the direction of water diffusion; red means that the diffusion direction is in the left-right direction, green indicates anterior-posterior direction, and blue superior-inferior direction (Do Tromp, 2016).

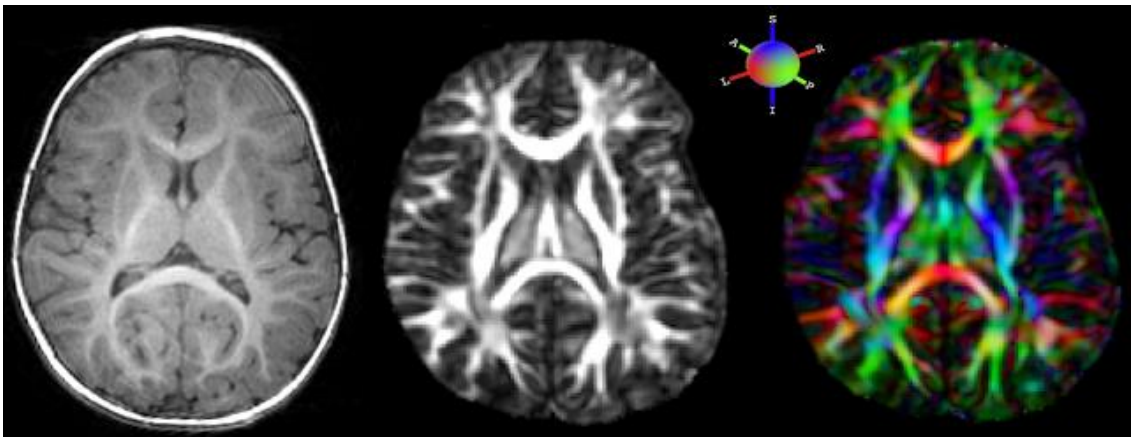

Figure 3.3 Examples of a T1 anatomical, fractional anisotropy (FA), and red-green-blue (RGB) colored FA image source: http://www.diffusion-imaging.com

3.4 Heritability of WM integrity

WM integrity is highly heritable (Shen et al., 2014). A study conducted by Chiang et al. (2011), found that WM integrity in the left splenium of the corpus callosum, and the right inferior longitudinal fasciculus (ILF)/inferior fronto-occipital fasciculus (IFO), was significantly more heritable in the adolescents than in adults. They found in adolescents that genetic factors attributed to 70–80% of the variation in FA, while in adults, only 30–40% was attributable. Kochunov et al. (2010) performed heritability and genetic analyses for the 10 major cerebral WM tracts in healthy individuals (182 males/285 females; average age 47.9 ± 13.5 years; age range: 19–85 years). They found significant heritability for FA ($h^2 = 0.52 \pm 0.11$; $p = 10^{-7}$) and radial ($h^2 = 0.37 \pm 0.14$; $p = 0.001$) measures, while axial measurements were not significantly heritable ($h^2 = 0.09 \pm 0.12$; $p = 0.20$). Kochunov et al. (2016) conducted another study using an Amish population, with large family pedigrees and high environmental homogeneity, to study heritability measures from the corpus callosum (CC). They found high heritability of FA (h^2=0.67)

and radial diffusivity (h^2=0.72). The same group did another study of heritability of FA using a subset of 481 HCP participants and found high heritability (h^2=0.53-0.90) of eleven major WM tracts (Kochunov et al., 2015). By comparing the heritability values of different populations, the group found similarities in regional heritability which suggests that the additive genetic contribution to WM structure is consistent across populations.

3.5 Methods

3.5.1 Subjects

A total of 819 participants were used to make the following 4 different genetic groups to determine the heritability and associations of the WM data: (1) MZ twins (N = 268; 134 pairs), (2) DZ twins (N = 144;72 pairs), (3) non-twin SB (N = 315; 144 pairs), and (4) NR (N = 92, not members of any other group) 46 randomly paired). See Chapter 1 more details for the inclusion and exclusion criteria.

3.5.2 Diffusion data collection and preprocessing

Diffusion data was collected at Washington University St Louis using a customized Siemens 3 T scanner with a 100mT/m maximum gradient strength and a 32-channel head coil (Uğurbil et al., 2013). Diffusion data were collected using a Stejskal-Tanner (monopolar) diffusion-encoding scheme a single-shot, single refocusing spin-echo, echo-planar imaging sequence with very high resolution 1.25 mm isotropic spatial resolution (TE/TR=89.5/5520ms, FOV=210×180mm). The WU-Minn consortium, decided to use the high-angular resolution diffusion imaging (HARDI) approach (Tuch et al., 2005) and modified to incorporate multiple shells of b values (Sotiropoulos et al., 2013). Three gradient tables of 90 diffusion-weighted directions and six b=0 images each

were collected with right-to-left and left-to-right phase encoding polarities for each of the three diffusion weightings (b=1000, 2000, and 3000 s/mm^2). The total imaging time for collection of diffusion data was about 1 hour (6 runs each approximately 9 minutes and 50 seconds).

3.5.3 HCP Diffusion pipeline

The diffusion preprocessing pipeline normalizes the b0 image intensity across runs; corrects for EPI distortions, eddy-current-induced distortions, and subject motion; corrects for gradient-nonlinearities; registers the diffusion data with the structural; brings it into 1.25mm structural space; and masks the data with the final brain mask (Glasser et al., 2013; Sotiropoulos et al., 2013).

3.5.4 Diffusion processing pipeline

1. Basic preprocessing: Intensity normalization across runs, preparation for later modules. 2. ‘TOPUP’ algorithm for EPI distortion correction. 3. ‘EDDY’ algorithm for eddy current and motion correction. 4. Gradient nonlinearity correction, calculation of gradient b-value/b-vector deviation. 5. Registration of mean b0 to native volume T1w with FLIRT BBR +bb register and transformation of diffusion data, gradient deviation, and gradient directions to 1.25mm structural space. Brain mask based on FreeSurfer segmentation. [Source HCP Reference Manual]

3.5.5 DTI processing for extracting FA values

FA maps were obtained by the fitting diffusion tensor model using FSL-FDT toolkit (Behrens et al., 2003). The data were then processed using FSL's tract-based spatial statistics (TBSS; http://fsl.fmrib.ox.ac.uk/ fsl/fslwiki/TBSS) analytic method

(Smith et al., 2006). These co-registered FA maps were averaged to produce a mean FA map. The volume of this mean FA skeleton above threshold FA=0.2 was then used to create a skeleton mask, in order to exclude minor tracts, non-white matter regions, and areas of possible misalignment. The skeletonized white matter was extracted and the region of interest (ROIs) FA values were calculated. The tract-wise ROIs were created using the stereotaxic white matter atlas based on DTI in an ICBM (International Consortium for Brain Mapping) template (Mori et al., 2008). FA values were calculated for 4 major white matter groups (Mori et al., 2008) (ROIs Table 3-1).

Four WM Groups	ROI Name	ROI Short
association fibers	cingulum cingulate gyrus	CCG
	cingulum hippocampus	CH
	external capsule	EC
	Fornix	FB
	sagittal stratum	SS
	superior fronto occipital fasciculus	SFOF
	superior longitudinal fasciculus	SLF
	uncinated fasciculus	UF
commissural fibers	body of corpus callosum	BCC
	genu of corpus callosum	GCC
	splenium of corpus callosum	SCC
	tapetum	TA
projection fibers	anterior corona radiata	ACR

	anterior limb of internal capsule	**ALIC**
	cerebral peduncle	**CP**
	posterior corona radiata	**PCR**
	posterior limb of internal capsule	**PLIC**
	posterior thalamic radiation	**PTR**
	retrolenticular of internal capsule	**RIC**
	superior corona radiata	**SCR**
tracts in brainstem	**corticalspinal tract**	**CT**
	inferior cerebellar	**IC**
	medial lemniscus	**ML**
	middle cerebellar peduncle	**MCP**
	pontine crossing tract part of MCP	**PCMCP**
	superior cerebral peduncle	**SCP**

Table 3.1 (Above) Regions of interest (ROIs) examined as defined by the stereotaxic white matter atlas (Mori et al., 2008).

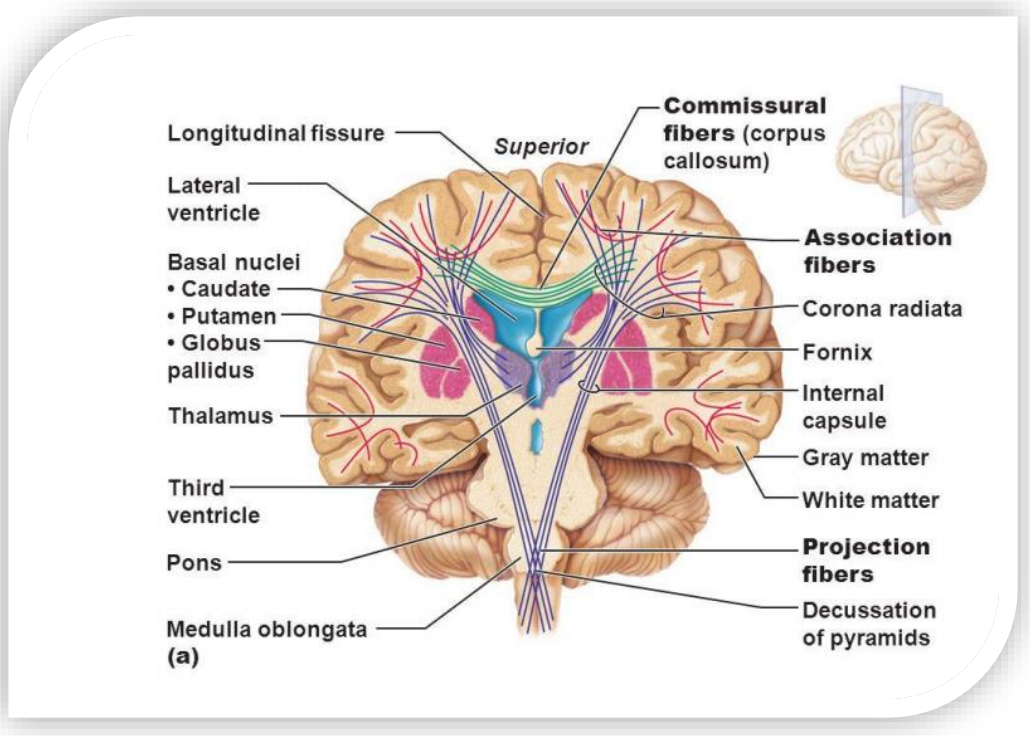

Figure 3.4 White matter areas and fibers (Pearson Education 2010)

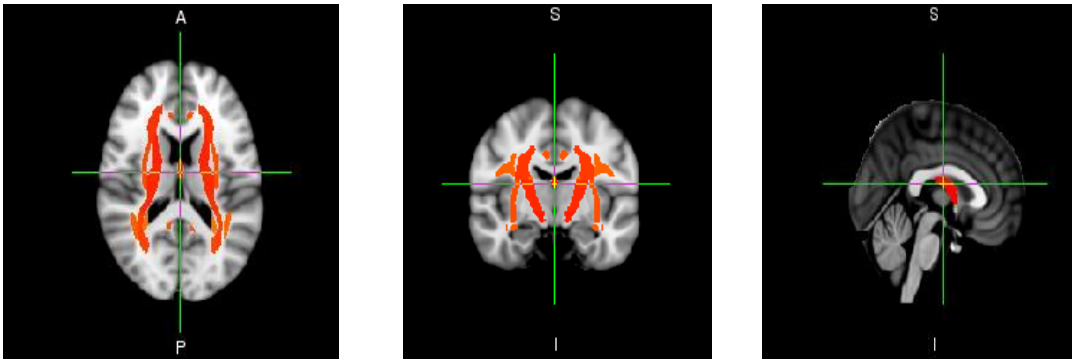

Figure 3.5 WM ROIs ICBM-DTI-81 white-matter labels atlas (Mori et al., 2008)

3.6 Statistical methods

See Chapter 1 for details on the statistical methods used in this chapter.

3.7 Results

Data were analyzed by grouping WM areas into four groups (association fibers, commissural fibers, projection fibers, and tracts in the brain stem based on Mori et al. atlas (2008) (Table 3-1). Four analyses were carried out: first, the ICC and zICC were computed for each genetic group and WM areas. An ANOVA was carried out on zICC with group as a fixed factor to evaluate differences between groups. Second, h^2 was computed for each area to compare heritabilities across areas. Third, MDS analysis was done using h^2 domain values to evaluate possible groupings of WM heritabilities. Finally, the HTC analysis was performed on the same heritability data to explore their clustering more explicitly. The results found are discussed in the following section.

First, zICC differed significantly among groups ($p < .05$, F-test in ANOVA) and varied systematically, such that MZ>DZ>SB>NR for FA (Fig. 3.6) and MD (Fig. 3.7). This general arrangement is as expected and consistent with literature reviews as MZ are the most genetically similar followed by DZ, SB and NR as the least similar group. A specific comparison was carried out for zICC between DZ and SB groups, since those pairs on average share the same amount (50%) of genetic material. The zICC of these groups differed highly significantly for FA measures ($p = 0.029$, ANOVA). This finding indicates a lesser role of genetic factors in the phenotypic variance of SB compared to DZ. The zICC was not significant between DZ and SB for MD ($p = .153$). The MZ zICC were grouped for FA and MD by gender; the zICC of these groups did differed significantly ($p < 0.05$) (Fig 3.8).

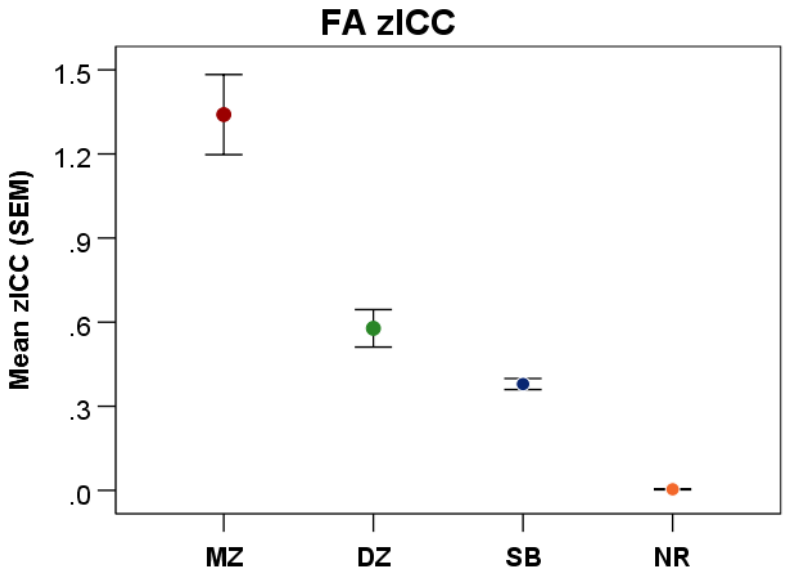

Figure 3.6 FA zICC ± SEM per genetic group.

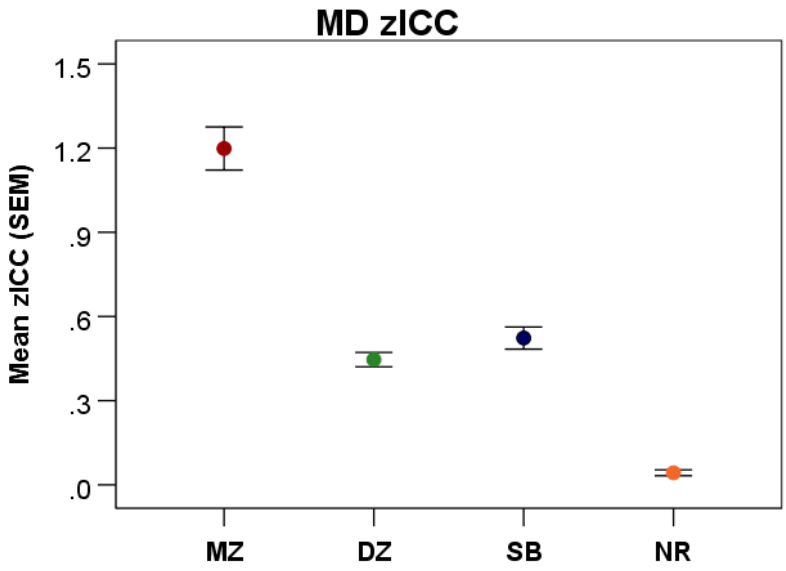

Figure 3.7 MD zICC ± SEM per genetic group.

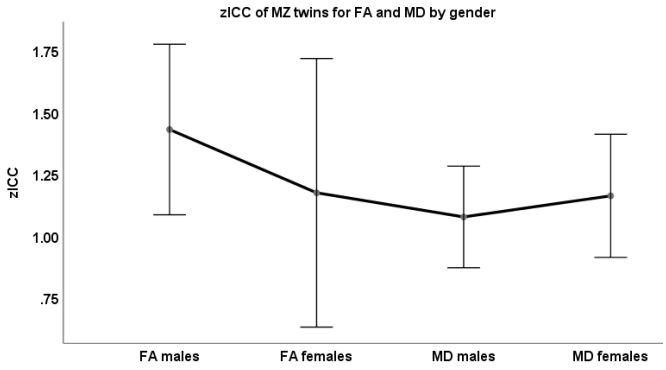

Figure 3.8 zICC of FA and MD of MZ twins by gender

Second, FA and MD heritabilities differed significantly between all areas (Fig. 3 .9-10) ($p < .05$) except for between commissural and projection fibers ($p > .05$). This finding may reflect the shared fibers that among the commissural and projection fibers. In examining the heritability of FA association fibers ($h^2 = .77$) were the most heritable followed by tracts in brain stem fibers ($h^2 = .69$), projection fibers ($h^2 = .64$), and commissural fibers ($h^2 = .62$). In examining the heritability of MD of the groups we have identified that tracts in the brainstem ($h^2 = .84$) had the highest heritability, followed by projections fibers ($h^2 = .82$), association fibers ($h^2 = .81$) and finally commissural fibers ($h^2 = .79$).

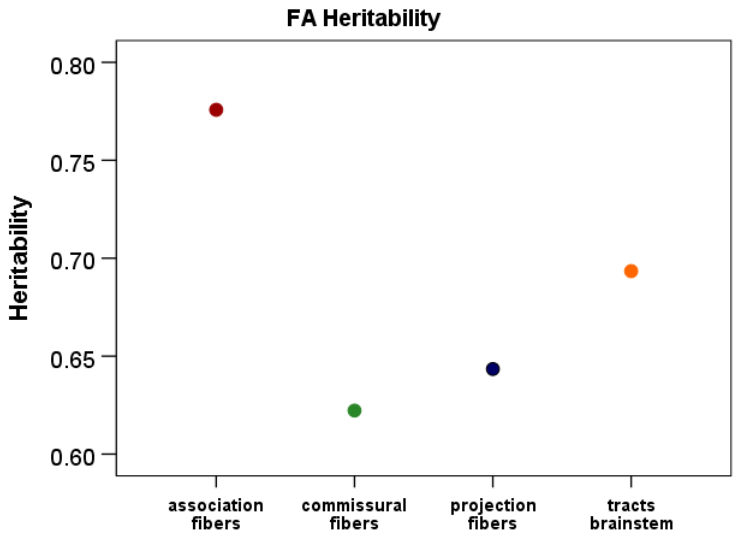

Figure 3.9 FA of h^2 per white matter parcellation map (Mori et al., 2008).

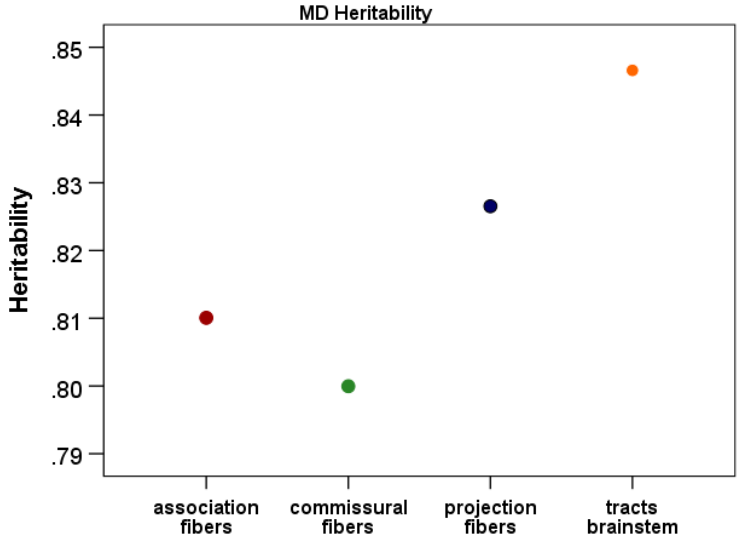

Figure 3.10 MD of h^2 per white matter parcellation map (Mori et al., 2008)

Third, the MDS analysis of FA heritabilities (Fig. 3.11) revealed a separation of the heritabilities into 3 quadrants comprising commissural fibers and projection fibers (upper left quadrant), association fibers (upper right), and tracts in the brain stem (lower left). The MDS analysis of the MD heritabilities (Fig. 3.12) revealed a separation of the 4 areas domains in 4 quadrants comprising commissural fibers (upper left quadrant), tracts in the brain stem (upper right), association fibers (lower left) and projection fibers (lower right).

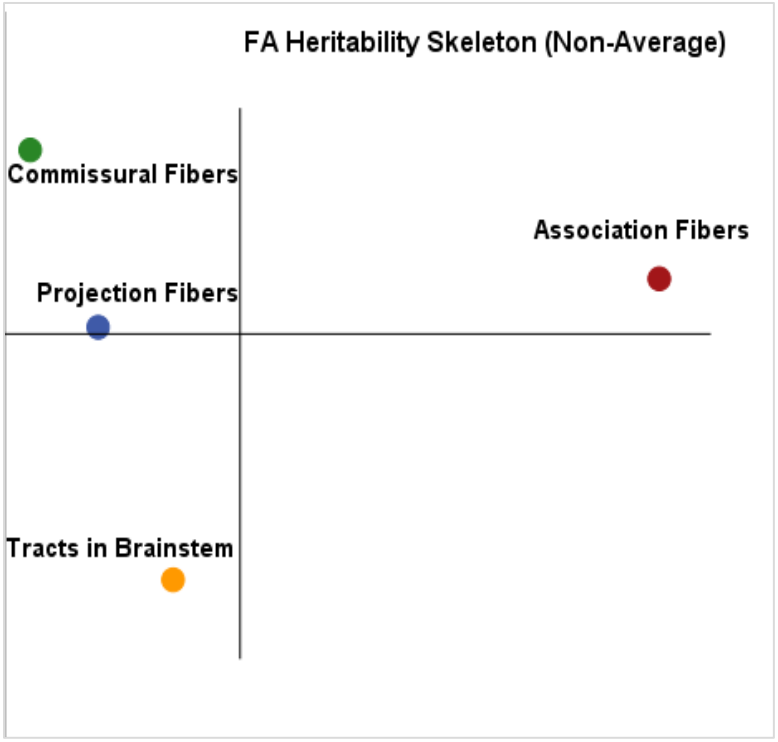

Figure 3.11 FA MDS of h^2 of the four white matter groups.

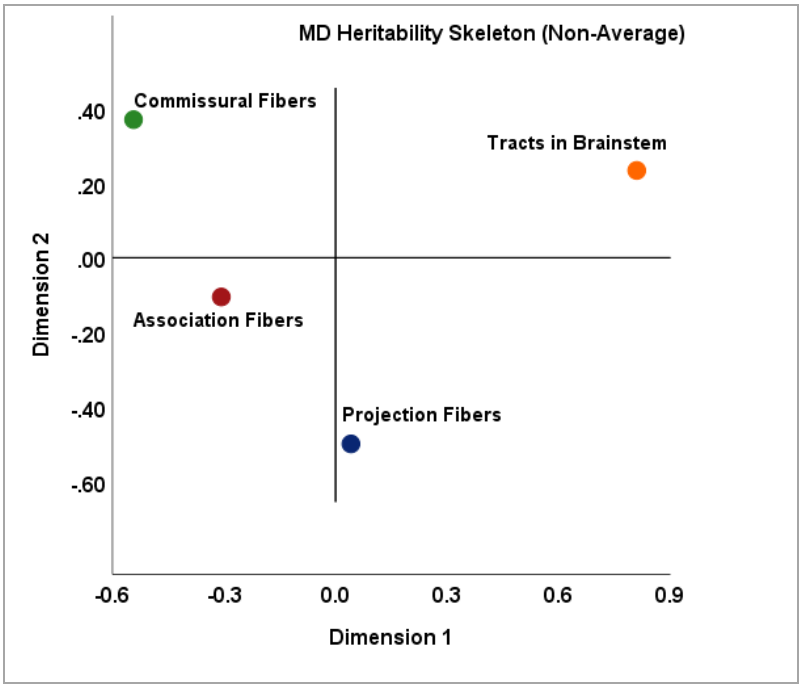

Figure 3.12 MD MDS of h^2 of the four white matter groups.

Finally, the grouping and gradient for FA was confirmed in the HTC dendrogram (Fig. 3.13), which comprises 2 branches, one containing (commissural fibers, projection fibers) and (tracts in the brain stem) in 2 separate sub-branches, and the other containing (association fibers) in a single branch. The grouping and gradient for MD was also confirmed in the HTC dendrogram (Fig. 3.14), which comprises 2 branches, one containing (association fibers, commissural fibers) and the other containing (projection fibers, tracts in the brainstem in 2 separate sub-branches.

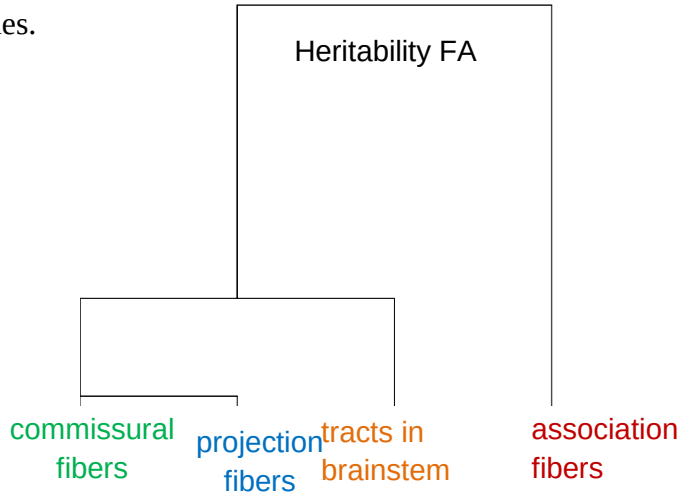

Figure 3.13 FA HTC of h^2 of the four WM areas.

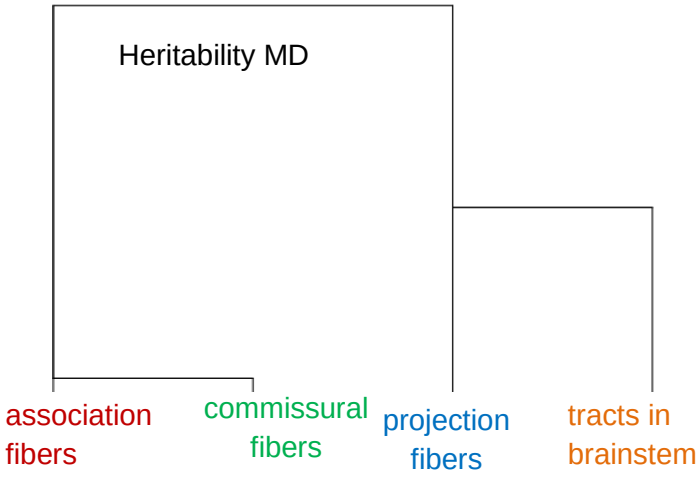

Figure 3.14 MD HTC of h^2 of the four WM areas.

3.8 Discussion

The goal of Chapter 3 is to determine the heritability of WM regions of the healthy brain using known genetic relationships (twins, siblings) and key WM measurements, fractional anisotropy (FA) and mean diffusivity (MD).

The grouping of participants into genetic groups resulted in the zICC differing significantly and systematically among the groups, such that MZ>DZ>SB>NR for both FA and MD measurements. The results found are consistent with the literature since MZ twins share all genetic effects, while DZ twins share on average 50 % genetic effects. Siblings also share on average 50 % of their genetics; however, it is expected that they would have lower zICC (and heritability values) because their environmental variation is higher compared to twins. The non-related participants are last in terms of zICC since they are not expected to have any common genetic effects.

To calculate heritability we used the classical Falconer Formula (Falconer, 1965) and grouped WM areas of the brain into 4 groups based on (Mori et al., 2008) atlas: association fibers, projection fibers, commissural fibers, and tracts of the brain stem.

FA, a measure obtained from DTI data, is highly sensitive to microstructural changes. It can be used to examine differences of brain structural integrity(Alexander et al., 2007a) and to describe heritability. The FA heritability of the regions were identified in the current study as the following (from most heritable to lowest): association fibers, tracts in brain stem, projection fibers, and commissural fibers. Although the commissural fibers had the lowest heritability of the four areas, the heritability value of 0.6 is considered a reasonably high heritability value considering that heritability value of traits usually range from 0.3 to 0.6 (Carey, 2001). This suggests a high consistency of additive genetic

contribution to FA values in WM regions of the brain. HTC and MDS were used to decipher grouping of the heritabilities based on areas. Results showed commissural fibers and projection fibers in the same quadrant, association fibers in another quadrant, and tracts of the brain stem as a separate quadrant. A possible explanation for this result is that commissural fibers and projection fibers connect different parts of the brain. Commissural fibers are axons that connect the two hemispheres of the brain, and projection fibers connect each region to other parts of the brain or to the spinal cord (Standring, 2005). In contrast, the association fibers connect regions within the same hemisphere of the brain (Standring, 2005).

MD is another measure obtained from DTI data that is used to examine differences of brain structural integrity (Clark, 2011) and can also be used to decipher heritability. Examination of the heritabilities of the ROIs, using MD as the measurement, shows that tracts in the brainstem had the highest heritability, followed by projections fibers, association fibers and finally commissural fibers. Similar to the FA results for heritability, the MD results show the commissural fibers had the lowest heritability of the four areas; however, their heritability value of 0.799 is considered a high heritability value considering that heritability values for traits usually range from 0.3 to 0.6 (Carey, 2001). The MDS analysis of the MD heritabilities revealed a separation of the areas into 4 quadrants. However, since the dimensions are not fixed for MDS, HTC can give insight into the grouping of the areas. HTC revealed commissural fibers and association fibers in one branch, and projection fibers and tracts in the brain stem in another branch. A possible explanation for this result is that commissural fibers and association fibers

based on anatomy (Fig 3.4) share considerable areas of fiber crossing, while projection fibers and tracts of the brainstem connect different parts of the brain.

The heritability results do not imply that the same genes are responsible for the similar patterns of heritability found using the measures; instead they provide a reliable phenotype for discovery of genetic factors that affect cerebral WM structure and integrity (Kochunov, 2015). The heritability results of FA and MD show similar patterns of heritability except for association fibers. If association fibers are excluded, then both measures follow the pattern of, tracts of the brain stem having the highest heritability, followed by projection fibers and commissural fibers. Association fibers connect areas within the same hemisphere allowing distinct cortical areas to "associate" with one another. In contrast, tracts in the brain stem, projection fibers and commissural fibers are axons that connect different parts of the brain (Standring, 2005). The MDS results for both measures are open to interpretation; however, the HTC can give some insight into how to interpret the results. The HTC results show different groupings for FA and MD measurements. A key question that is often posed in the field is how to relate and interpret the two measures extracted from diffusion images to their biology. Many research studies primarily focus on FA; however, that may not be enough to characterize the tissue changes (Alexander et al., 2007) or heritability. Using both measurements (FA and MD) may help to better understand how the diffusion tensor is changing; thus, leading to a better understanding of heritability values. For example, Madden et al. (2012), found a pattern of decreased FA values and increased MD values in the CC areas of the ageing brain. The biological interpretation of this pattern is a loss/disruption of

both axons and myelin. By understanding the patterns of FA and MD heritabilities in a young health population gives a blue print of patterns healthy brain measurements and heritability of those measurements.

Chapter 4 Structural MRI (sMRI)

4.1 Introduction

Structural magnetic resonance imaging (sMRI) is a non-invasive neuroimaging technique that has become the standard measure for routine examination of the brain (Symms, 2004). sMRI offers superb anatomical detail, high sensitivity to pathological changes and great border visualization of human brain's GM, WM and cerebral spinal fluid (CSF) (Symms, 2004). sMRI quantifies and evaluates different areas of the brain (size, location) thus determining the overall integrity of the brain. In recent years, sMRI, has been rapidly expanding into a neuroimaging tool to investigation not only brain structure but also to investigate of the genetics of brain structure (Winterer et al., 2005).

4.2 sMRI Principles and Concepts

sMRI provides neuroimaging data to describe the anatomical structure (size, shape, and integrity) of the GM and WM of the brain. GM contains cell bodies (neurons) while WM, is mainly composed of long-range nerve fibers (myelinated axons); the different composition of tissue, causes a different MRI signal in GM and WM. An MRI pulse sequence is a programmed set of changing magnetic gradients and radiofrequency; combinations of these pulse sequence parameters affect tissue contrast and spatial resolution. For example, modifications to common pulse sequence parameters such as repetition time (TR) and echo time (TE) emphasize different aspects of brain tissue resulting in anatomical images that emphasize contrast between GM and WM. T1-weighted and T2-weighted are the most common MR images produced with variation to the pulse sequence parameters. T1-weighted images are produced by using short TE and

short TR times while T2-weighted with long TR and long TE. T1 images contrast between GM (dark gray) and WM (lighter gray) tissues, while CSF is void of signal (black). Fat, such as lipids in the myelinated white matter, appears bright. T1-weighted imaging offers good contrast between GM, WM and CSF, and it is used most frequently used to quantitatively study of brain morphology, especially of individual brain structures (Keller & Roberts, 2009). T2-weighted images show contrast between CSF (bright) and brain tissue (dark). Some T2 sequences demonstrate additional contrast between GM (lighter gray) and WM (darker gray). T2-weighted images are commonly used for quantification of intracranial volume (ICV), due to the signal intensity of CSF in the T2 sequence permits a more straightforward way to quantify CSF (Keller & Roberts, 2009).

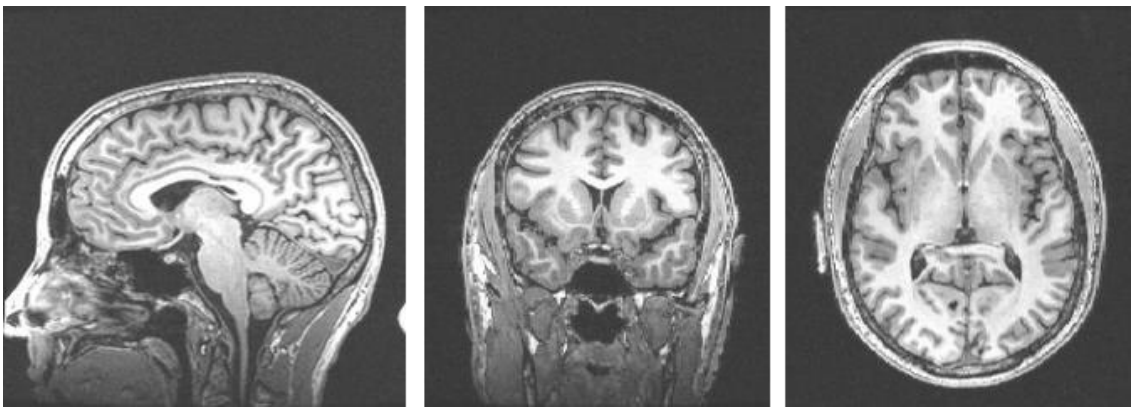

Fig 4.1- T1 weighted image source: http://fmri.ucsd.edu/Howto/3T/structure.

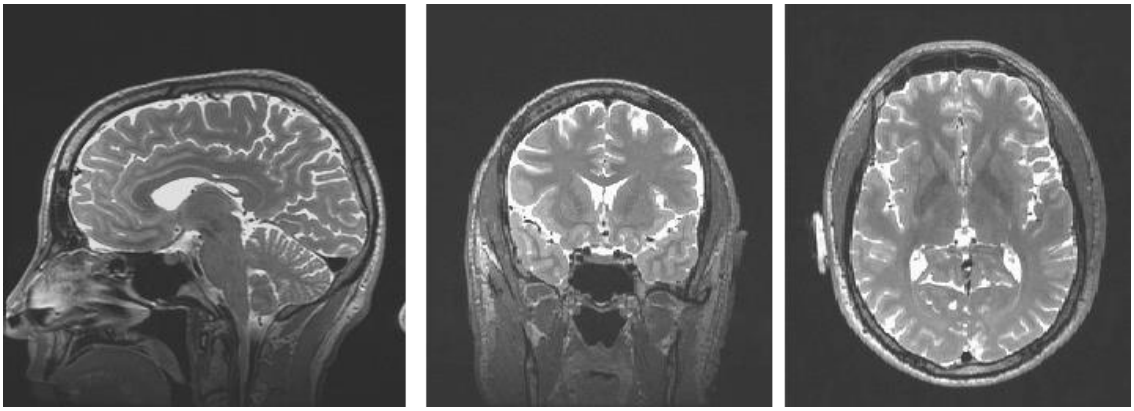

Fig 4.2 - T2 weighted imaged source: http://fmri.ucsd.edu/Howto/3T/structure

4.3 Heritability of sMRI (Brain Volume)

Heritability of human brain volume has a wide range heritability estimates and less studied in young healthy adults compared to middle age to older populations.

The lobes (temporal, frontal, parietal, and occipital) of the brain are related to different brain functions such as, movement, memory, spatial awareness, sensory, visual processing center, perception and emotion (Ribas, 2010). The additive heritability estimates for the lobes are the following: temporal lobe 74.3%, frontal lobe 68.6%, parietal lobe 72.7% and occipital lobe 60.3% (Blokland et al., 2012; Brun et al., 2009). Other studies reported similar additive genetic estimates: 54% for total frontal, 47% for total parietal lobes (Geschwind et al., 2002). Lukies et al. (2017) found that genetic effects strongly determine lobar volumes for the frontal (86.7%), temporal (92.3%), parietal (86.5%) and occipital (64.3%) lobes.

Genetic influence on the human cortical areas was investigated by Wen et al. (2016), who reported a heritability range from approximately 0 (caudal anterior-cingulate cortex) to 0.67 (precentral gyrus, insula cortex).

4.4 Methods

4.4.1 Subjects

Out of 1206 HCP participants, 1113 participants have sMRI acquisitions. Of those participants with imaging data, 1053 participants had genetically confirmed family relations. Siblings of twins are excluded. Additionally, 33 participants are excluded from analysis because the estimated ICV was not accurate. Of those participants that have genetically confirmed, and good quality data consists of the following: 260 (130 pairs)

MZ twins, 148 (74 pairs) DZ twins, 317 participants out of 134 families are siblings, and 101 are unpaired twins or unrelated individuals. The following 4 groups of participants were studied by pairing the individuals of: (1) MZ twins (MZ); (2) DZ twins (DZ); (3) siblings (SB) and (4) unrelated individuals (NR).

In the SB group there are, within the same family sometimes, 2, 3, 4 or 5 siblings. For families with a sibling count of more than 2, a pair is randomly selected making 134 pairs out of 268 selected siblings for SB group. In the NR group 101 individuals were randomly paired in 50 pairs. For each ROI, for SB and NR groups, the ICC was calculated for randomly paired individuals. After repeating this process 1001 times, the median ICC was found.

4.4.2 sMRI data collection

sMRI data were collected at Washington University St. Louis using a customized Siemens 3 T scanner. The structural scans include a pair of T1-weighted and a pair of T2-weighted images, acquired at high resolution of 0.7 mm (compared to the standard 1 mm resolution) (Glasser et al., 2013)

4.4.3 sMRI data preprocessing

sMRI data is processed by three structural pipelines: PreFreeSurfer Pipeline, FreeSurfer Pipeline and PostFreeSurfer Pipeline with the aim to provide high quality volume and surface data. The software used for the sMRI pipelines are freely available from the FSL (Jenkinson et al., 2012) and FreeSurfer (Dale et al., 1999) and Connectome

Workbench (Marcus et al., 2014) image analysis suites. The pipelines are described below.

4.4.3.1 sMRI PreFreeSurfer pipeline

The main goals of the first structural pipeline, PreFreeSurfer, are to produce an undistorted "native" structural volume space for each subject, align the T1w and T2w images, perform a B1 (bias field) correction, and register the subject's native structural volume space to MNI space. Hence, there are two volume spaces in HCP data: 1) The subject's undistorted native volume space which is the best approximation of the subject's physical brain. 2) Standard MNI space that is useful for comparisons across subjects and studies (1200 HCP Release Reference Manual, 2017).

4.4.3.2 sMRI FreeSurfer pipeline

The FreeSurfer pipeline is based on FreeSurfer 5.3.0-HCP and was modified to capitalize on HCP's high-resolution data. The main goals of the second pipeline are to segment the volume into predefined structures, reconstruct cortical surfaces, and perform FreeSurfer's folding-based surface registration to their surface atlas (fsaverage) (1200 HCP Release Reference Manual)

4.4.3.3 sMRI PostFreeSurfer pipeline

The final structural pipeline, PostFreeSurfer, produces all of the GIFTI surface and auxiliary files necessary for viewing the data in Connectome Workbench, performs individual surface registration using cortical folding surface features and the MSM algorithm (MSMSulc), down sampling registered surfaces for connectivity analysis,

creating the final brain mask, and creating myelin maps. (1200 HCP Release Reference Manual, 2017).

4.4.4 FreeSurfer

FreeSurfer is a software package for the analysis and visualization of structural and functional neuroimaging data. FreeSurfer provides a full processing for structural MRI data; technical details of these procedures are described in detail in prior publications (Dale et al., 1999; Fischl & Dale, 2000; Fischl et al., 2004). Briefly, this processing includes:

- Skull stripping, B1 bias field correction, and GM- WM segmentation
- Reconstruction of cortical surface models (GM-WM boundary surface and pial surface)
- Labeling of regions on the cortical surface, as well as subcortical brain structures
- Nonlinear registration of the cortical surface of an individual with a stereotaxic atlas

4.4.5 Desikan Atlas

The Desikan-Killiany atlas (Desikan et al., 2006) parcellation scheme labels cortical sulci and gyri into 68 and 2 hippocampi (35 for each hemisphere) ROIs. In the volume-based stream, the 70 regions are automatically labeled in left and right hemispheres are averaged for a total of 35 ROIs. Volumes were calculated for the major lobes: frontal, occipital, parietal, and temporal, by grouping the 35 ROIs into their respective lobes. A list of the ROIs used to calculate heritability is shown in Table 4.1.

4.4.6 Inter-individual variability

Participants are compared by regional volumes; however, it is likely that the individuals with larger structures have larger brains and individuals with smaller structures have smaller brains. To account this variability among individuals, the regional brain volume is normalized and expressed as the percent of the ICV it occupies (Voevodskaya et al., 2014; Whitwell et al., 2009). Estimated Total Intracranial Volume (eTIV) is generated by FreeSurfer and used to estimate the ICV. Cortical volume measures from the left and right hemisphere were averaged and the mean brain volume was expressed as the percent of the ICV. The calculated percent of cortical areas is a unitless value between 0 and 100.

4.4.7 Removing extreme values from data

Extreme values are excluded from analysis by specifying the numerical criteria that define extremes (Tukey 1977). First, we calculate the interquartile range (IQR=Q3 - Q1=H3-H1) as the difference between 75 percentile, Q3, and 25 percentiles, Q1, called Tukey's Hinges. The values for Q1 – 3×IQR and Q3 + 3×IQR are the "upper and lower fences" that identify the "reasonable" values from the extreme values. The values that lie outside the outer fences are considered extreme values and are removed. All data that were inside the outer fences were included into analysis.

4.4.8 Statistical methods

See Chapter 1 for details on the statistical methods used in this chapter.

4.5 Results

First, zICC differed significantly among groups ($p < .05$, F-test in ANOVA) and varied systematically, such that MZ>DZ>SB>NR for lobe volumes (Fig. 4.3) and Desikan (cortical) (Fig. 4.4) ROI volumes. This general arrangement is as expected and consistent with literature reviews as MZ are the most genetically similar followed by DZ, SBs and NR as the least similar group. A specific comparison was carried out for zICC between DZ and SBs groups, since those pairs on average share the same amount (50%) of genetic material; however, the zICC was not significantly different for lobe volumes and Desikan ROI volumes ($p > .05$) between DZ and SBs groups. However, comparison of brain groups showed that overall mean zICCs were higher for lobar volumes (Fig. 4.3), lower for the ROIs (Fig. 4.4).

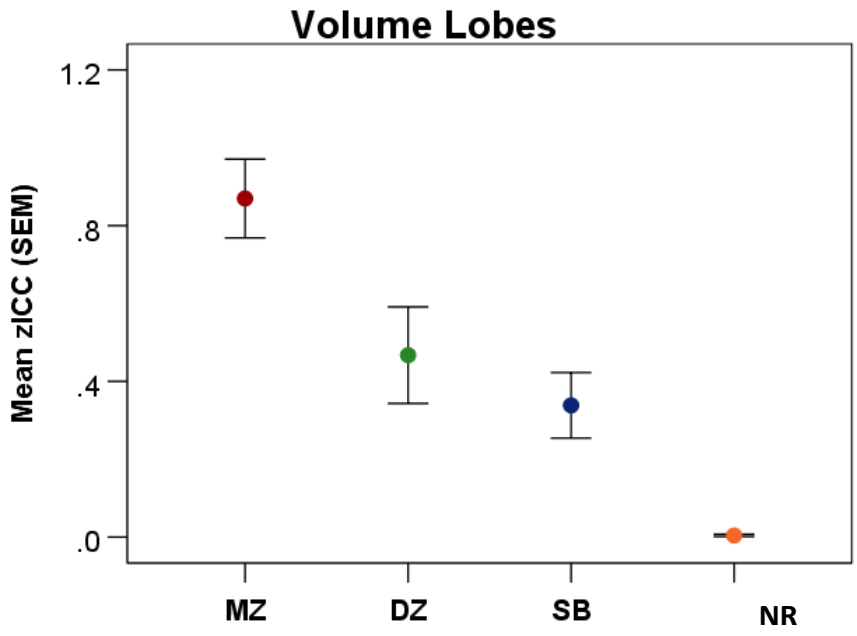

Figure 4.3 Volume Lobes zICC ± SEM per genetic group.

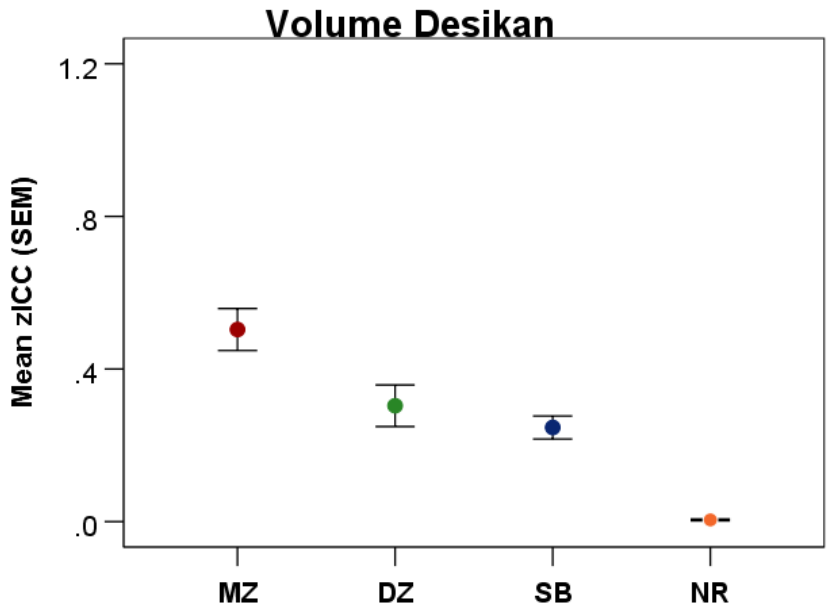

Figure 4.4 Volume Desikan zICC ± SEM per genetic group.

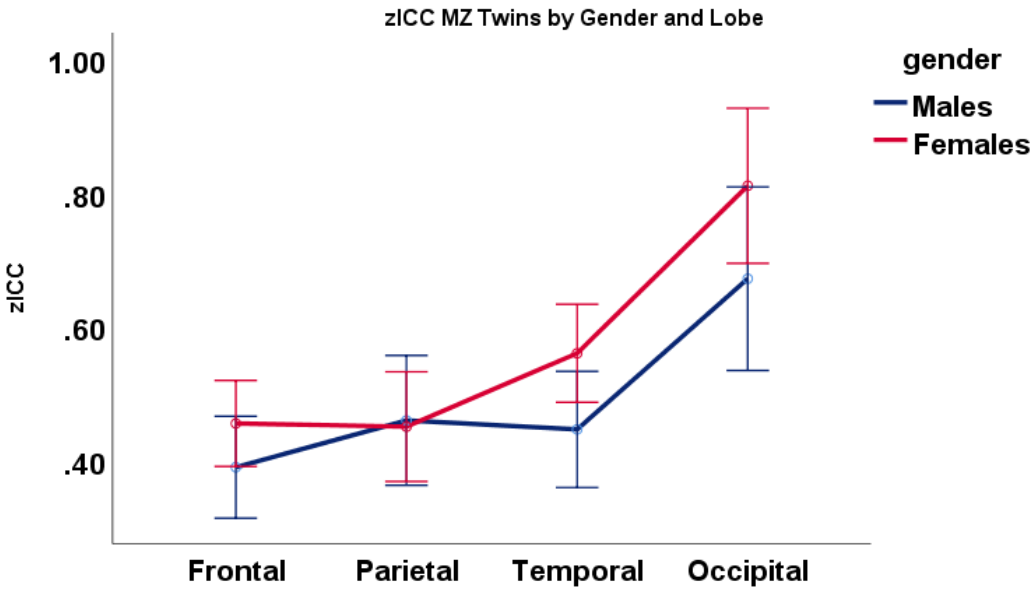

Figure 4.5 zICC of twins grouped by gender and lobes

Frontal Lobe	h_b^2
Rostral middle frontal	0.076
Caudal middle frontal	0.106
Medial orbito frontal	0.112
Superior frontal	0.156
Pars triangularis	0.248
Lateral orbito frontal	0.258
Precentral	0.376
Paracentral	0.436
Rostral anterio rcingulate	0.47
Parsorbitalis	0.566
Parietal Lobe	h_b^2
Precuneus	0.01
Superiorpariet al	0.264
Postcentral	0.288
Inferiorparietal	0.316
Insula	0.332
Posterior cingulate	0.378
Supramarginal	0.392
Isthmus cingulate	0.682
Occiptal Lobe	h_b^2
Pericalcarine	0.152
Lingual	0.308
Cuneus	0.41
Lateral occipital	0.552
Temporal Lobe	h_b^2
Transverse temporal	0.088
Temporal pole	0.226
bankssts	0.282
fusiform	0.288
Para hippo campal	0.296
Superior temporal	0.316
entorhinal	0.524
Inferior temporal	0.616
Hippocampus	0.714
Middle temporal	0.758

Table 4.1 Desikan ROIs and h^2 values

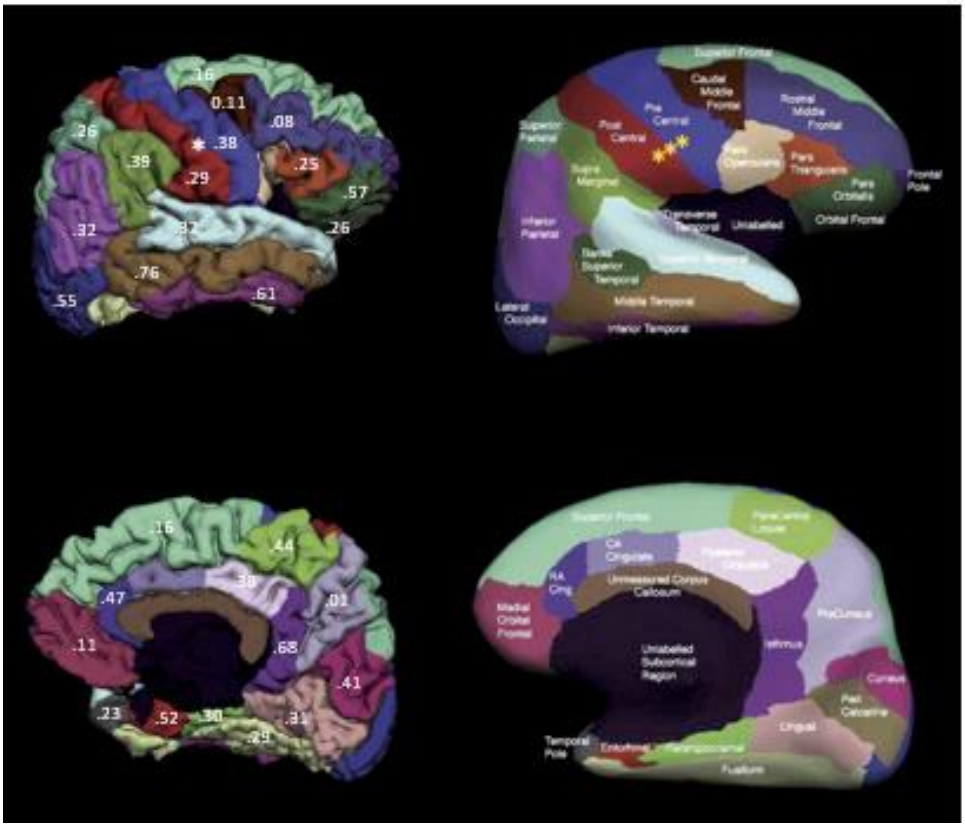

Figure 4.6 Desikan ROIs and h^2 values

Second, a t-test was performed on the Desikan area heritabilities which yielded a significant result (table 4.1, Fig. 4.6) ($p < .05$). In examining the heritability of the Desikan areas, the results show that most Desikan areas have some degree of heritability. The middle temporal ($h^2 = 0.758$) had the highest heritability and the transverse temporal had the lowest heritability ($h^2 = 0.088$) for the temporal lobe. The isthmus cingulate ($h^2 = 0.682$) highest for the heritability while the precuneus had the lowest heritability ($h^2 = 0.01$) for the parietal lobe. The lateral occipital ($h^2 = 0.552$) had the highest heritability while pericalcarine ($h^2 = 0.152$) had lowest heritability for occipital lobe. The pars orbitalis ($h^2 = 0.566$) had the highest heritability while rostral middle frontal ($h^2 = 0.076$) had lowest heritability for frontal lobe.

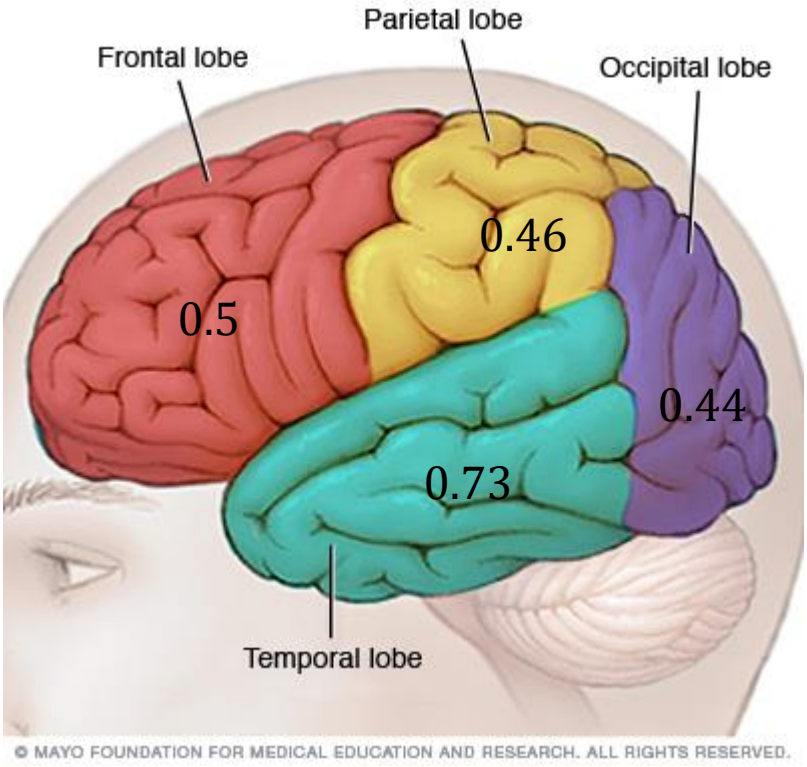

Figure 4.7 Lobes h^2 values

A t-test was also performed on the four lobes area heritabilities which yielded a significant result (Fig. 4.6) ($p < .05$). In examining the heritability of the lobes, the temporal lobe ($h^2 = 0.73$) was the most heritable, followed by frontal lobe ($h^2 = 0.5$), parietal lobe ($h^2 = 0.46$) and occipital lobe ($h^2 = 0.44$) (Fig. 4.7).

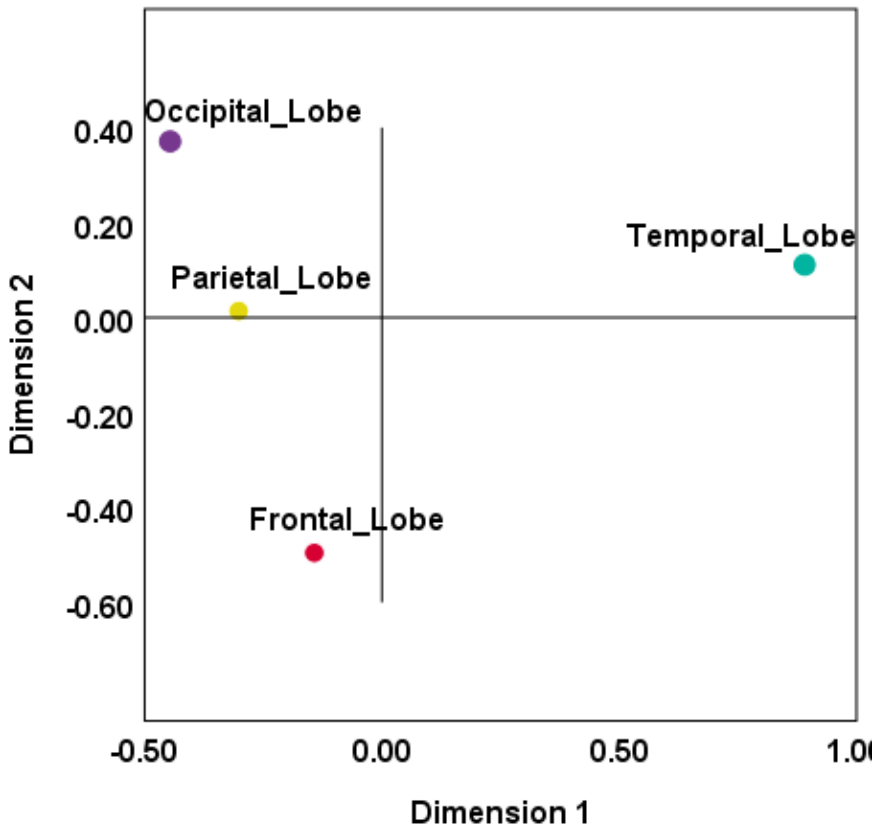

Figure 4.8 MDS of Lobes h^2 values

Third, the MDS analysis of lobular heritabilities (Fig. 4.8) revealed a separation of the heritabilities into 3 quadrants comprising occipital and parietal lobe (upper left quadrant), temporal lobe (upper right), and frontal lobe (lower left).

Finally, the grouping and gradient for lobes was confirmed in the HTC dendrogram (Fig. 4.9), which comprises 2 branches, one containing (parietal, occipital and frontal lobe) and the other branch containing the temporal lobe.

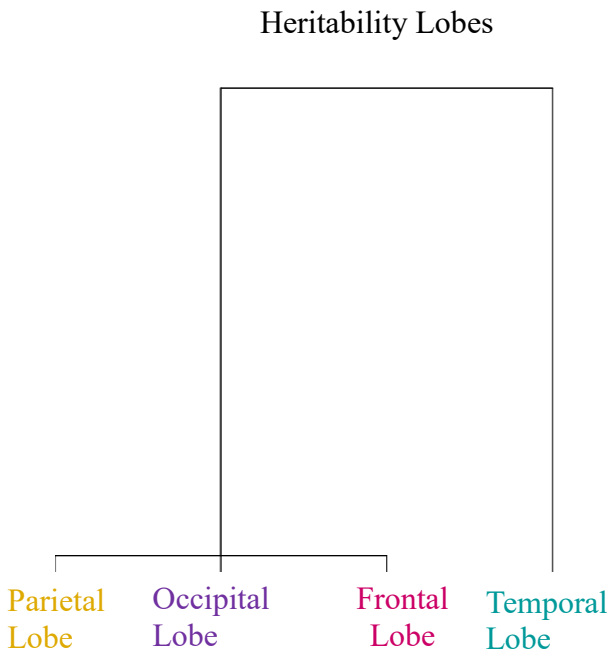

Figure 4.9 HTC of Lobes h^2 values

4.6 Discussion

The goal of Chapter 4 is to determine the heritability of structural brain volumes of the healthy brain using known genetic relationships (twins, siblings) in different regions of the brain using the Desikan atlas.

The grouping of participants into genetic groups resulted in the zICC differing significantly and systematically varying among the groups, such that MZ>DZ>SB>NR for the lobes and Desikan areas. This revealed the expected pattern of genetic influence for a heritable trait, since MZ twins share all genetic effects, while DZ twins share on average 50 % genetic effects. Siblings also share on average 50 % of their genetics; however, it is expected that they would have lower zICC (and heritability values) because

their environmental variation is higher compared to twins. The non-related participants are expected to be last in terms of similarity since they are not expected to have any genetic effects. All participant groups, except for the NR groups, showed a pattern of decreasing ICC with overall decreasing volume of brain regions from the larger lobe volumes to the smaller cortical ROIs.

To calculate the heritability of brain volumes, cortex was parcellated into 35 ROIs based on the Desikan-Killiany atlas (Desikan et al. 2006) parcellation scheme. The results show that most Desikan areas have some degree of heritability (table 4.1). Heritability values were not calculated for the caudal anterior-cingulate cortex, frontal pole and pars opercularis since the ICC value or heritability was negative. The middle temporal area (h^2 = 0.758) in the temporal lobe was the most heritable while by precuneus (h^2 = .01) in the parietal lobe was the lowest (Table 4.1, Fig. 4.5). Genetic influence on the human cortical areas was investigated by Wen et al. (2016), who reported a heritability range from ~0 (caudal anterior-cingulate cortex) to 0.67 (precentral gyrus, insula cortex).

Heritability was also calculated for the four major lobes: frontal, occipital, parietal, and temporal. The heritability findings for the four lobes in this dissertation are the following: frontal lobe (50%), temporal lobe (73%), parietal lobe (46%) and occipital lobe (44%). These results have similar heritability pattern to Lukies et al. (2017) 86.7%, 92.3%, 86.5%, 64.3%; Geschwind et al. (2002) 54%, 46%, 47% 28%; and Panizzon et al. (2009) 85%, 86%, 82%, 48% for the same four lobes respectively. These three studies and the results from this dissertation found that the occipital lobe had the weakest genetic contribution of the four lobes.

Differences in heritability estimates found in this dissertation and previous studies mentioned may be due to a number of factors. There are methodological differences like sample sizes, different ages of participants, or solely twin participants. The previous studies used different ethnicities in their study population and the age trends toward middle to advanced age. Therefore, the differences observed in heritability compared to previous studies may reflect ethnic variation. An immense advantage of this study is that it involved a young healthy population with an age range of 22- 37 (Van Essen et al., 2013). This may explain some of the differences since heritability of brain volume has been observed to vary with age (Batouli et al., 2014; Pfefferbaum et al., 2000). Having a young healthy population with a narrow age range gives an excellent blueprint of heritability values for this particular age range.

Another difference and significant advantage of this dataset compared to others is the high-resolution MRI T1-weighted scans with voxel dimensions of 0.7 x 0.7 x 0.7 mm while standard T1- weighted acquisition dimensions are 1 x 1 x 1 mm. Other notable differences are: (1) the quality of the dataset used, (2) the study design that includes not only twins, but also siblings, and unrelated individuals, and (3) wide range of brain areas.

Since the HTC and MDS analysis were performed on a single dissimilarity matrix, the two dimensions are not fixed, this leaving the grouping of the lobe heritabilities open to interpretation. By splitting the graph by the second-dimension results in the frontal, parietal and occipital lobes to be in a single dimension. One possible explanation for this result is that the heritability of the lobes follows the anatomical and spatial positioning of the lobes (Fig 4.6, 4.7).

The actual extent of genetic influence on brain structures and volumes is likely to vary spatially across the brain. A plausible developmental hypothesis could be that the earliest-maturing brain regions have structural volumes that are more genetically influenced. However, because human brain development is structurally and functionally a nonlinear process, regions within a lobe have different maturation patterns. Therefore, another plausible developmental hypothesis could be that, the brain regions that are developing and maturing slowly are regions under constant genetic influence. For example, the temporal lobe resulted in the highest heritability amongst the four lobes. It is also one of the last lobes to mature fully; however, certain areas of the temporal lobe such as the medial aspects of the inferior temporal lobe mature early and do not change much thereafter (Gogtay et al., 2004). A similar pattern is found for the frontal lobe which had the second highest heritability. The parietal and occipital lobes are the lobes with lower and similar heritability values. This result could be because parts of the brain associated with more basic functions matured early (Gogtay et al., 2004) and the heritability of brain volume changes (lowers) over time (Pfefferbaum et al., 2000).

Chapter 5 Functional MRI (fMRI)

5.1 Introduction

Functional magnetic resonance imaging (fMRI), based on the same technology as MRI (See Chapter 1), has revolutionized neuroscience over the past decade due to its unprecedented capability to non-invasively and safely image the brain with excellent spatial and good temporal resolution (Poldrack et al., 1996). fMRI is one of the more recently developed forms of neuroimaging but the idea underpinning the technique builds on a long history of knowledge about the brain. From the 1890s, it has been known that more active areas of the brain receive more oxygenated blood (Roy CS, 1890). In 1990 Ogawa et al. made a key scientific finding by determining that changes in blood oxygen levels caused the magnetic resonance imaging properties to change i.e., that the fMRI image varied with the level of oxygenation in blood. Since oxygen is used up by active neurons, a pivotal discovery was made that fMRI could distinguish neurons that were functionally active from those that were relatively inactive thus, initiating the remarkable possibility of studying brain function in humans.

Since fMRI gives detailed images of brain activity, it can be used to determine precisely which parts of the brain are handling critical functions such as thought, speech, vision, movement and sensation (Mayfield, 2018). This is a key difference and advantage of fMRI compared to sMRI (Chapter 4) and dMRI (chapter 3) which, although are unique and have their own advantages, are static anatomical structural images of the brain and are not used to study activation and functional changes of the brain.

Brain development is heavily influenced by genetic factors; family or twin studies indicate that brain structure and function are heritable to some extent. Advances in modern neuroimaging, such as fMRI in combination with genetics allow neuroscientists to investigate genetic and environmental factors that influence human brain structure and function (Park et al., 2013). This emerging field (neuroimaging and genetics/genomics) has been made possible by recent technological advances in genetics and neuroimaging methods and have numerous applications in medicine and neuroscience (Fritsch et al., 2015).

5.2 fMRI Heritability

The human brain, formed by a complex network of interconnected brain regions, is influenced by genetics; however, the extent of that influence is not yet known, but can be investigated using twin studies and fMRI (Heuvel et al., 2013). Heritability (See Chapter 1) of several structural and functional aspects of the brain are known to be highly heritable with measures varying between 0.42 and 0.60 (Glahn et al., 2010; Peper et al., 2009; Thompson et al., 2013). Compared to brain structure (Chapter 4), heritability studies of brain function are scarce and reveal a lower heritability estimate (~40 %) (Jansen et al., 2015). Large MRI consortia, such as the HCP, are an important component to explaining heritability due to its statistical powers, which will eventually lead to more information about brain functioning and heritability (Jansen, 2015).

5.2.1 fMRI Heritability in the Literature

A 2013 study conducted by Heuvel et al. used 12-year-old Dutch twins (n = 21 MZ, and 22 DZ twin pairs) to study heritability of whole brain connectivity during early brain development. In contrast to the findings in adult twins (0.60), the heritability estimates in the 12-year-old Dutch twins were lower (0.42). This may suggest an increase in genetic control during aging and the existence of a set of genes shaping the global architecture of functional brain communication during early brain development (Heuvel et al, 2013).

Glahn et al. (2010) published heritability estimates for connectivity using independent component analysis (ICA) a multivariate decomposition method in 333 individuals. The group calculated heritability for the default mode connectivity (DMC), a large-scale brain network of interacting brain regions that are highly correlated and distinct from other networks in the brain (Buckner et al., 2008). The heritability was estimated to be 0.424. The gray matter density from within this brain region was also heritable ($h^2 = 0.327$). However, the genetic correlation between functional connectivity and gray matter density was non-significant ($\rho g = 0.077$, $p = 0.836$), suggesting that different genes may influence structure and function or that there is a lack of power to detect genetic overlap (Thompson, 2013).

Another manuscript balanced different graph theory-based parameters to maximize “communication efficiency” while minimizing “connection cost” (Fornito et al., 2011). They measured spontaneous fluctuations of the BOLD signal using fMRI imaging in healthy twins (16 monozygotic pairs and 13 dizygotic pairs) to characterize

cost-efficient properties of brain network functional connectivity between 1041 distinct cortical regions. At the global network level, 60% of the interindividual variance in cost-efficiency of cortical functional networks was attributable to additive genetic effects, suggesting substantial heritability. De-composing this global network effect in the 0.09–0.18 Hz range indicated that genetic influences were not distributed homogeneously throughout the cortex, and regional heritability estimates (bilateral posterior cingulate and medial prefrontal cortices, dorsolateral prefrontal and superior parietal cortices, and lateral temporal and inferomedial occipital regions) ranged from <0.10 to 0.81 (0.51 median).

One research group, Adhikari et al. (2018), studied two datasets, collected ten years apart to determine if they could detect genetic influences on resting state connectivity. The results showed that between 20–40% of the inter-subject variance in functional connectivity within functional networks was under genetic control. The pattern of heritability was similar between two cohorts, which were collected using very different imaging protocols and sample designs. Together, these findings strongly suggest that resting state connectivity is under a moderate genetic control and this heritability can be detected (Adhikari, 2018).

To quantify neural interactions in local cortical networks, (Christova and Georgopoulos, 2018), quantified the interactions in six cortical areas of 854 individuals from the HCP. Each time series was pre-whitened with an autoregressive integrative moving average (ARIMA) model (Box and Jenkins 1976) of orders (P = 15, d = 1, q = 1) (Christova et al., 2011). They found that the strength of zero-lag correlation between pre-

whitened, BOLD fMRI time series decreased (rate of decrease, b) with distance as a power law. For twins, the rate of decrease was significantly correlated between monozygotic twins, less so between dizygotic twins or nontwin siblings, and not at all in nonrelated individuals. Using Falconer's formula, heritability was calculated as h = 0.188.

5.3 fMRI BOLD Signal Brief History and Background

5.3.1 fMRI BOLD Signal

Ogawa et al. (1990) were the first to report the BOLD contrast in the rat brain. In 1992, three studies were the first to explore the BOLD contrast in humans: Kwong et al., Ogawa et al., and Bandettini et al. (Ugurbil, 2004). The changes in blood flow are repeatedly captured by the MRI scanner at hundreds of thousands of locations, creating a time series of brain images with the ability to deduce oxygenation changes in brain over time. By generating a map of blood flow and consequently functional brain activity, fMRI helps researchers pinpoint areas of the brain that are most active, providing insight into the inner workings of the human brain (Hart et al., 2017).

The BOLD signal measures the ratio of oxygenated to deoxygenated hemoglobin in the blood. Hemoglobin has different magnetic properties and produces different local magnetic fields depending on the state hemoglobin exists in: 1) diamagnetic when oxygenated (oxyhemoglobin) or 2) paramagnetic when deoxygenated (deoxyhemoglobin) (Pauling, 1936). Oxyhemoglobin has no unpaired electrons and is diamagnetic (repelled by a magnetic field), while deoxyhemoglobin is formed when oxygen is released,

exposing its iron core and thus becomes strongly paramagnetic (attracted by a magnetic field). Oxyhemoglobin increases the MR signal and deoxyhemoglobin suppresses the MR signal; as the concentration of deoxyhemoglobin decreases, the fMRI signal increases (Wager & Lindquist, 2015). The BOLD signal detects these small changes in magnetic properties of blood caused by metabolic and vascular responses to neuronal activity (Faro et al., 2010). As neural activity increases so does the metabolic demand for oxygen and nutrients.

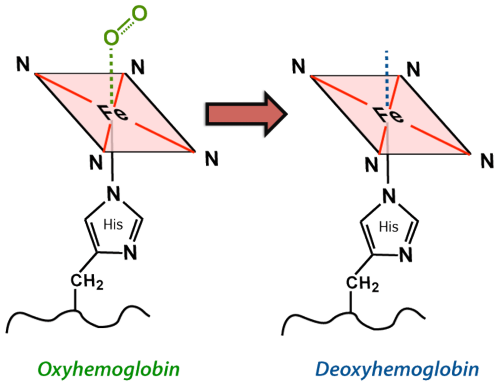

Figure 5-1 Elster, Allen D. 2019 MRIquestions

The changes in the MR signal are triggered by an instantaneous neuronal activity known as the hemodynamic response function (HRF). As oxygen is extracted from the blood, the hemoglobin becomes paramagnetic and can lead to a decrease in BOLD signal ("initial dip"). Following a ~2 sec delay (Ogawa et al., 1990), the BOLD signal will start to gradually increase due to an over compensation in blood flow (oxyhemoglobin) and will reach its peak a in BOLD signal 4-6 seconds following activation. After reaching its peak, the BOLD signal plateaus after 6–12 seconds and returns to the baseline, typically

undershooting slightly. This post-stimulus undershoot is due to a combination of reduced blood flow and increased blood volume.

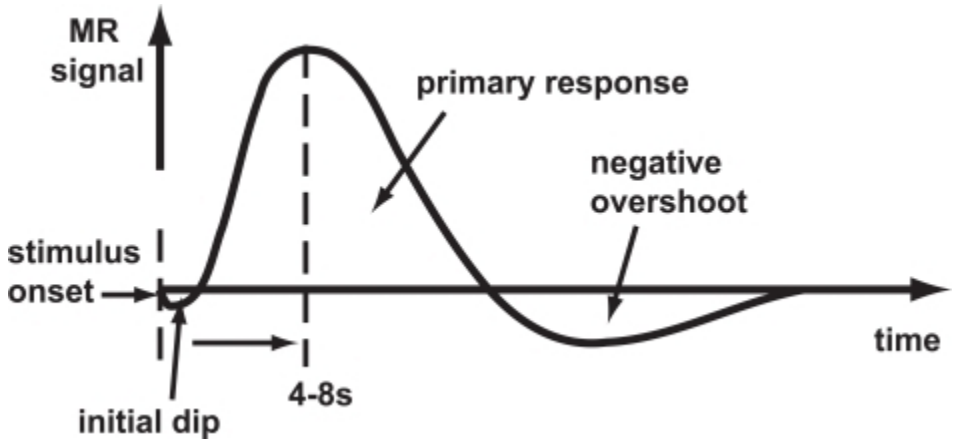

Figure 5-2 Kornak J, 2011 HRF

It is important to note that BOLD signal does not directly measure neuronal activity, rather it measures the metabolic demands (oxygen consumption) of active neurons (Wager & Lindquist, 2015). Since the BOLD signal can indirectly measure neuronal activity, rsfMRI can be used measure the functional connectivity of the brain at resting state (Hart, 2017) and adheres to the principle that 'brain regions that are wired together, fire together.'

There are two general categories of fMRIs acquired by the MRI scanner: 1) task-based fMRI (tfMRI) - participants who are given a particular task to perform while in the scanner and 2) resting state fMRI (rsfMRI) - participants who are resting in the scanner (no task to perform). rsfMRI provides insight into the naturally occurring unprompted activity that is within the brain, which subsequently promotes communication across regions (Douet et al., 2014). For this dissertation chapter only rsfMRI is considered.

5.3.2 fMRI Data Analysis – ARIMA Model

ARIMA modeling is a method used for predicting variables, by using the information obtained from the data itself to forecast its trend by regression on its past values. However, fMRI BOLD time series data typically has some autocorrelation (values that are influenced by previous values) and are considered non-stationary data (i.e. have parameters/ trends such as means, variances and autocovariances that change over time). It is essential that such data be rendered stationary so that statistical parameters of interest do not vary along the time series; otherwise, calculations derived from the time series analysis, can be misleading and lead to spurious results due to the reflection of both the internal properties of the series and any 'true' relation between the two series (Christova et al., 2011). To avoid this mishap, the time series data are pre-whitened using the ARIMA model (see below) to remove such effects.

Pre-whitening for the time series data is typically accomplished by applying the Autoregressive (AR) Integrative (I) Moving Average (MA) model (ARIMA) (Box and Jenkins, 1976). An ARIMA model is concisely described as (*p, d, q*) orders, where *p* denotes the AR orders (the dependence on past values of the series or number of AR lags in the model), *d* denotes the I orders (the number times a variable is differenced to become stationary), and *q* denotes the MA orders (the dependence on the past values of random shocks or the number of MA lags in the model) (Christova et al., 2011).

In ARIMA modeling, the integration (I) component is addressed first, followed by the AR and MA components (i.e. model orders). The raw BOLD time series data (figure 5.3-4 top) shows that the BOLD values vary with time (trends, or autocorrelated). The

integration of the data transforms and renders the non-stationary and autocorrelated data as stationary and non-autocorrelated, i.e. convert it to white noise - hence the term 'pre-whitening'. After the differencing (integration, 'I') of the data, the ARMA model can be applied.

The ARMA model has two steps (Fig 5.3-4):

1) The first step, after the removal of the trends, is to identify and select the model. The main tool for model identification is the autocorrelation (ACF) and partial autocorrelation functions (PACF). Based on the data time series plot and the shape of ACF and PACF, a tentative model is suggested. Typically, the model is started with (p = 0, d = 1, q = 0), which involves first-order differencing. For the HCP fMRI data, differencing was not enough as shown in figure 5.3-4 (middle). The ACF of the (p = 0, d = 1, q = 0) innovations still contain autocorrelations.
2) The second step involves the model parameter estimation by using an estimation function to optimize the values. This stage involves computations that are implemented to yield the coefficients for the AR and MA lags. Typical diagnostic checking of the model involves plotting the residuals, their ACF and PACF, to ensure that the AR and MA coefficients are within bounds of stationarity. The model is evaluated through iterative refining the model until the data has been rendered stationary and non-autocorrelated. After an extensive and iterative investigation yielded an ARIMA model of p = 15, d = 1, q = 1, or (15, 1, 1) figure 5.3-4 (bottom). The aim of the modeling is not to

model the time series perfectly, but rather sufficiently enough to ensure that the series obtained are stationary and non-autocorrelated.

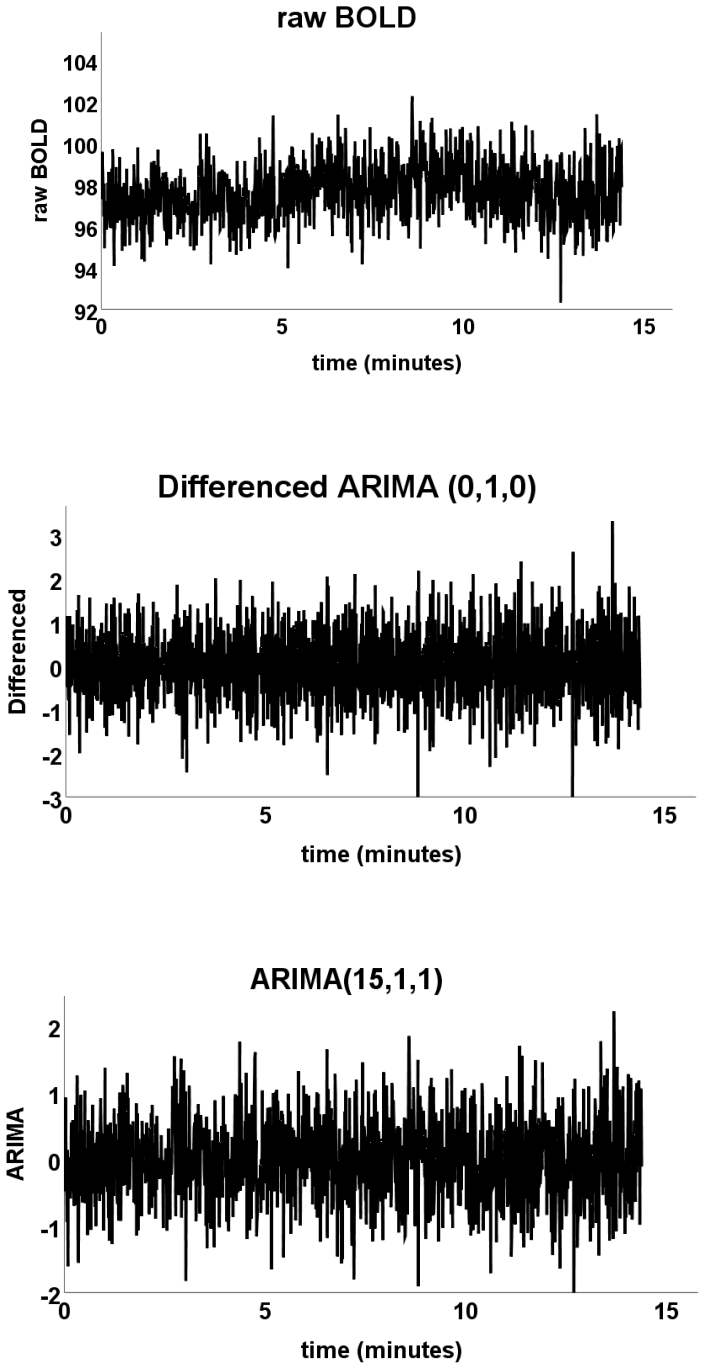

Figure 5.3 Raw, Differenced, ARIMA (15,1,1)

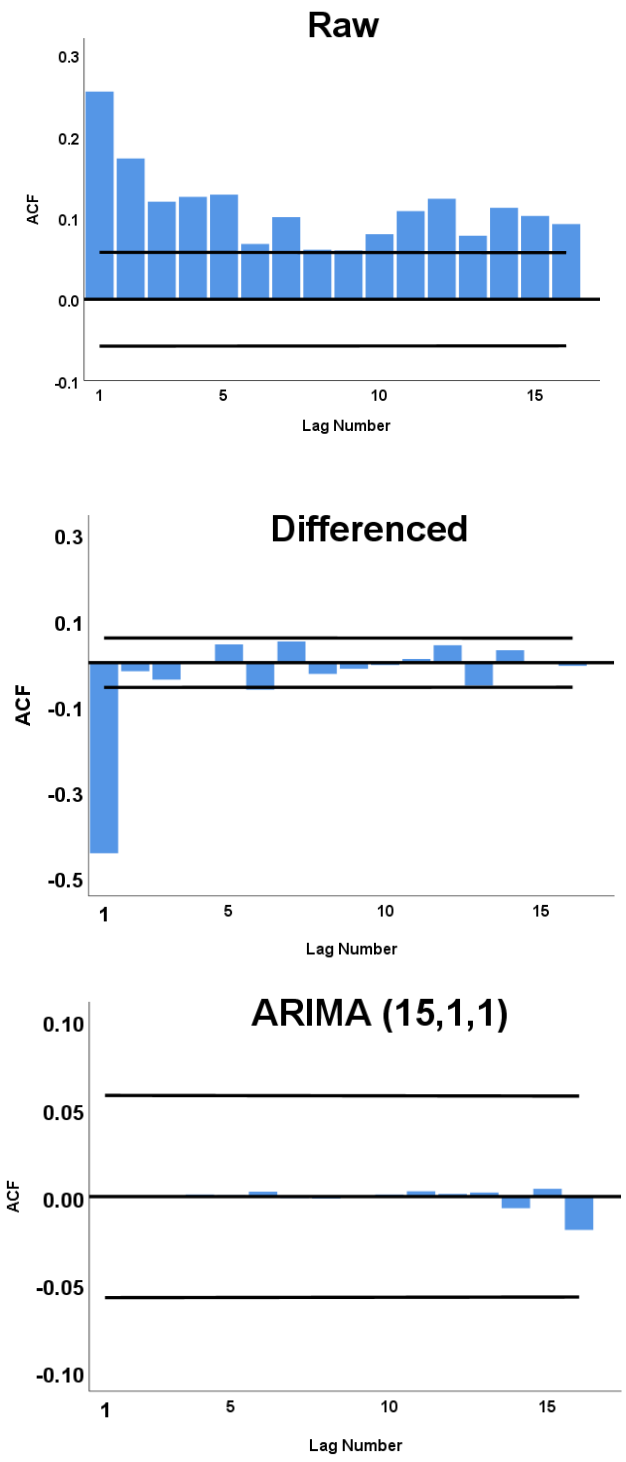

Figure 5.4 Autocorrelations Raw, Differenced, ARIMA (15,1,1)

5.4 Methods

5.4.1 Subjects

The following 4 groups of participants were studied by pairing the individuals with available fMRI data: (1) 246 (123 pairs) MZ twins (MZ); (2) 144 DZ (72 pairs) twins (DZ); (3) 324 (162 pairs) siblings (SB) and (4) 125 (64 pairs) unrelated individuals (NR). See Chapter 1 for more details.

5.4.2 fMRI data collection and preprocessing

fMRI data were collected at Washington University St. Louis using a customized Siemens 3T scanner. The structural scans include T1-weighted and T2-weighted images, acquired at high resolution of 0.7 mm (compared to the standard 1 mm resolution) (Glasser et al., 2013). fMRI data were acquired in approximately 15 minutes. Within each session, oblique axial acquisitions alternated between phase encoding in a right-to-left (RL) direction in one run and phase encoding in a left-to-right (LR) direction in the other run (HCP Ref Manual 1200 Feb 2017). Resting state images were collected using a gradient-echo echo planar imaging (EPI) sequence with the following parameters: TR=720 m/s, TE=33.1 m/s, flip angle=52 degrees, FOV=208×180 mm (RO×PE), matrix=104×90 (RO×PE), 2.0 mm isotropic voxels, 72 axial slices, and multiband factor=8. The HCP's main pipeline, fMRISurface, was implemented on the fMRI datasets for preprocessing. This pipeline removes spatial distortions, realigns volumes to compensate for subject motion, and registers the fMRI data to the structural MRI. The

standard volume-based analyses of the fMRI data can proceed from the output of this pipeline (HCP Ref Manual 1200).

5.4.4 fMRI extracting values

For each subject, 1200 functional images were acquired continuously, yielding a sequence of 1200 BOLD signal values per voxel. The number of voxels in a region of interest (ROI) varies according to the size of an ROI. For example, larger ROIs such as the post central has approximately 1800 voxels, compared to a smaller ROI, such as the frontal pole, with approximately 30 voxels. The BOLD time series data were extracted from fMRI data using Matlab (R2016b, Mathworks, Natick, MA, USA). The ARIMA (15,1,1) model was applied to the data (See section fMRI Data Analysis – ARIMA), thus removing the sixteen images of the 1200 images, leaving 1184 pre-whitened BOLD values per voxel, henceforth referred to as innovations. After removing outlier voxels (coefficient of variation of no more than 5% (Christova et. al, 2001)), all the remaining voxels in the whole brain of each subject, are grouped into different ROIs based on the Desikan atlas (Desikan et al., 2006) parcellation scheme described below.

5.4.5 Desikan-Killiany Atlas

The Desikan-Killiany atlas parcellation scheme, labels the cortical sulci and gyri of the brain into 68 (34 for the left hemisphere and 34 for the right hemisphere) ROIs. These ROIs are automatically calculated and labeled for each subject (as opposed to calculated by group or hand labeled).

5.4.6 Statistical methods

5.4.6.1 General Methods

See Chapter 1 for details on the general statistical methods used in this chapter.

5.4.6.2 Specific to this Chapter

The statistical methods specific to this chapter are: 1) average standard deviation of the standard deviations of all the innovations for a particular ROI (PASD) and 2) correlations between the average of the innovations for each ROI (PAC) for a total of 2278 correlations. Details are described below.

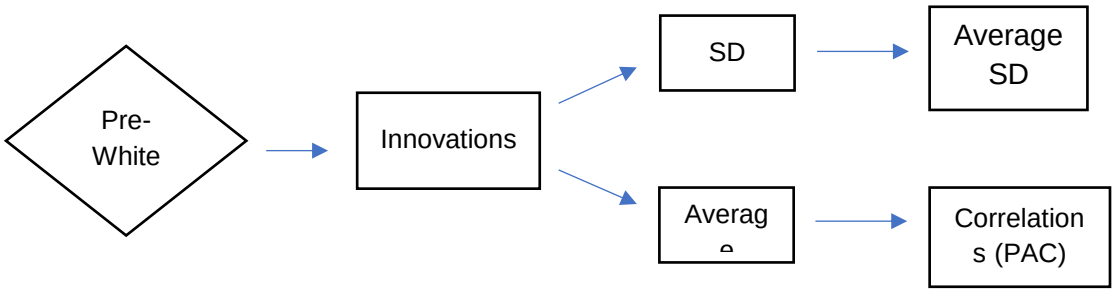

Figure 5.5 Schematic diagram of statistical methods PASD and PAC

The PASD is calculated by taking the standard deviations of the innovations at each voxel (1184 time points). Then all the standard deviations for the voxels were averaged to find the average standard deviation of the innovations for that ROI. The 68 ROIs are then grouped into brain groups based on the four brain lobes (frontal lobe, occipital lobe, parietal lobe and temporal lobe). Then the general statistical methods described in Chapter 1 were implemented.

The PAC is calculated for each ROI by averaging the innovations across the time series, and then calculating correlations between each ROI for a total of 2278 correlations

per subject. The ICC value for the 2278 correlations was calculated (see Chapter 1) and then grouped into one of these 3 brain groups based on anatomy: homotopic, ispsiLR, and heterotopic. In the homotopic brain group, correlations were calculated between the average innovations of the ROIs in the left hemisphere with average innovations of the same ROI in the right hemisphere (ex: precentral gyrus left with precentral gyrus right). In the ipsi lateral (ipsiLR) brain groups correlations were calculated between the average innovations of all possible combinations of ROI pairs that are located in the same hemisphere. For the heterotopic brain group, correlations were calculated between the average innovations of a ROI located in one hemisphere (for example: left) and the average innovations of a ROI located the opposite hemisphere (for example: right), excluding the homotopic pair.

5.5 Results

5.5.1 Results: PASD

First, zICC differed significantly among groups ($p < .05$, F-test in ANOVA) and varied systematically, such that MZ>SB>DZ>NR (Fig. 5.5) for the standard deviations of the innovations. For PASD the ziCC of the SB were slightly higher (zICC = .24) than and DZ (zICC = .21) group. These two groups are very similar since they on average share about 50% of their genetics. This general arrangement is consistent with literature reviews as MZ are the most genetically similar and the NR group is the least similar group.

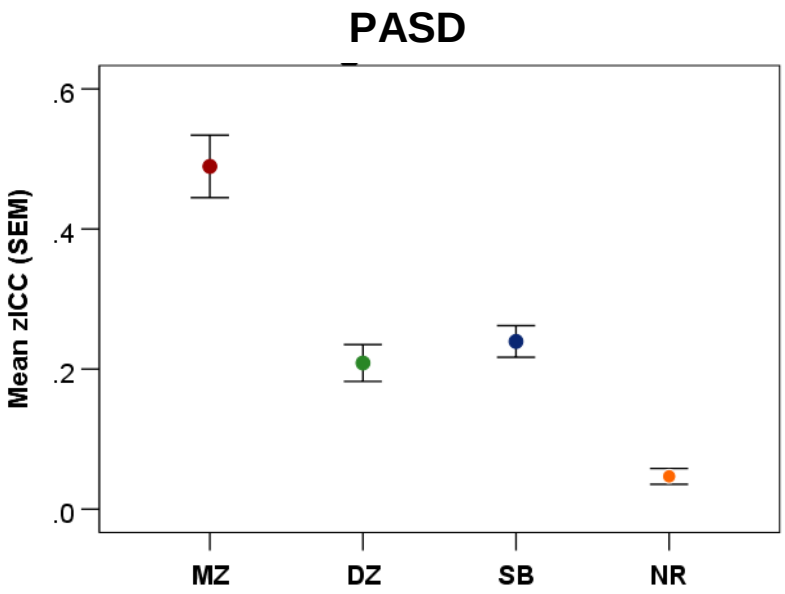

Figure 5.6 PASD zICC ± SEM per genetic group.

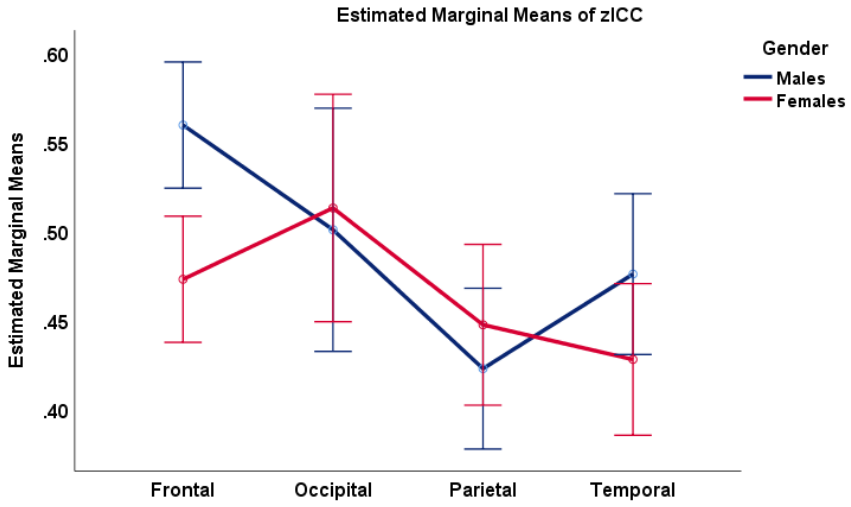

Figure 5.7 zICC by gender and brain group

In order to determine if gender influences mean SD of innovations the zICC was also grouped by gender and by brain lobes but it was not found to be significant ($p < .05$, F-test in ANOVA) (Fig. 5.7).

Second, heritability (See Chapter 1) was calculated for each ROI after averaging the ICC for the left and right hemisphere areas for a total of 34 ROIs. If heritabilities were found to be negative or greater than one they were excluded. In examining the heritability of the Desikan areas, the results show that about half of the Desikan areas have some degree of heritability. A t-test was performed on the Desikan area heritabilities which yielded a significant result (table 5.1) ($p < .05$). For the temporal lobe the entorhinal ($h^2 = .97$) had the highest heritability while the transverse temporal had the lowest heritability ($h^2 = 0.26$). For the parietal lobe the posterior cingulate ($h^2 = 0.72$) highest heritability while the supramarginal had the lowest heritability ($h^2 = 0.22$) value. For the frontal lobe the pars orbitalis ($h^2 = 0.90$) had the highest heritability while medial orbito frontal ($h^2 = 0.62$) had the lowest. And finally, the occipital lobe was excluded from analysis because the heritability values (four ROIs) were negative or greater than one.

Frontal Lobe	h_b^2
medial orbito frontal	0.619
precentral	0.628
lateral orbito frontal	0.684
rostral anterior cingulate	0.688
paracentral	0.793
parsorbitalis	0.903

Parietal Lobe	h_b^2
supramarginal	0.218
postcentral	0.256
inferior parietal	0.481
superior parietal	0.586
precuneus	0.651
posterior cingulate	0.718

Temporal Lobe	h_b^2
transverse temporal	0.264
bankssts	0.356
para hippocampal	0.900
entorhinal	0.968

Table 5.1 Desikan ROIs and heritability (h^2)

The heritability values for ROIs were also averaged and grouped into lobes. In examining the heritability of the lobes, the frontal lobe ($h^2 = 0.72$) was the most heritable, followed by temporal lobe ($h^2 = 0.62$), and parietal lobe ($h^2 = 0.49$) (Fig. 5.7). A t-test was also performed on the three lobes area heritabilities which yielded a significant result (Fig. 5.8) ($p < .05$).

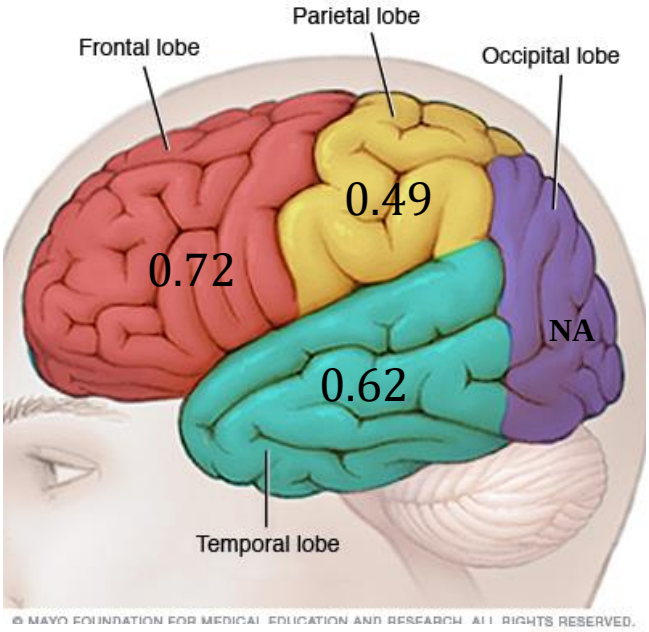

Figure 5.8 Lobes and heritability (h^2)

Third, the MDS analysis of lobular heritabilities (Fig. 5.9) revealed a separation of the heritabilities into 3 quadrants comprising frontal lobe (upper left quadrant), parietal lobe (upper right), and temporal lobe (lower left).

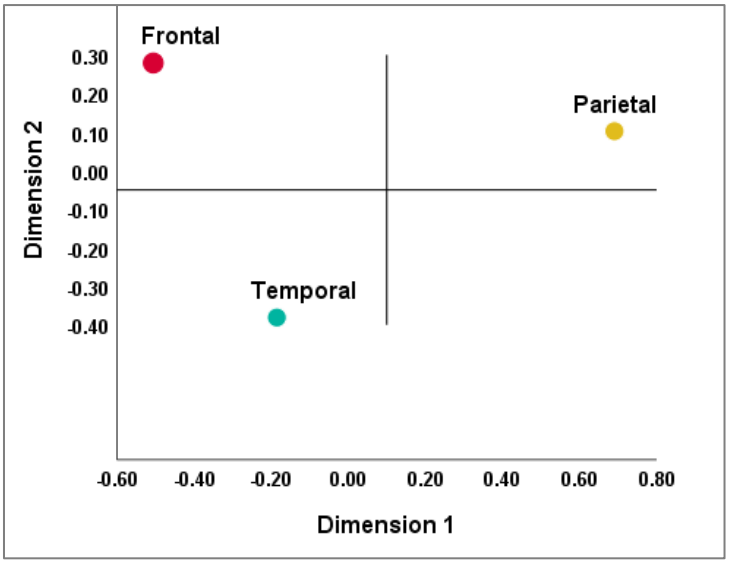

Figure 5.9 MDS of Lobes and heritability (h^2)

Finally, the grouping and gradient for lobes was confirmed in the HTC dendrogram (Fig. 5.10), which comprises 2 branches, one branch containing the temporal and the frontal lobe, and the second branch contained the parietal lobe.

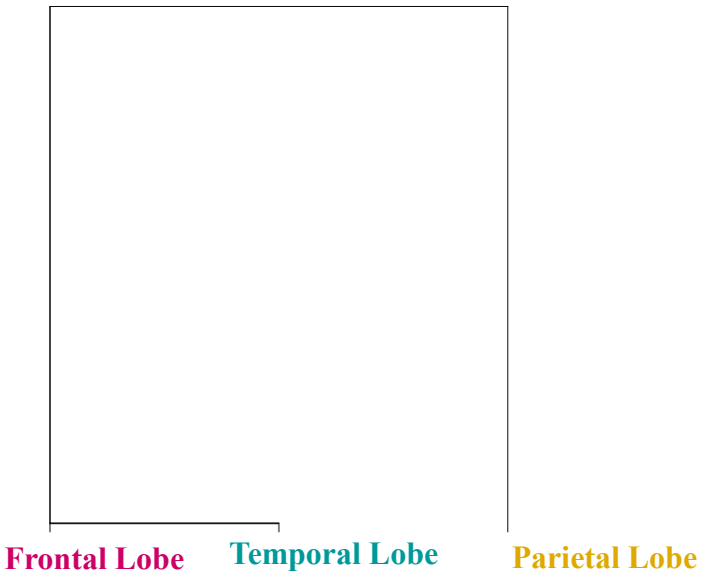

Figure 5.10 HTC of Lobes h^2 values

5.5.2 Results: PAC

The results for the PAC show that the zICC differed significantly among the genetic groups ($p < .05$, F-test in ANOVA) and varied systematically, such that MZ>DZ>SB>NR (Fig. 5.11) for the correlations. A specific comparison was carried out for zICC between DZ and SBs groups, since those pairs on average share the same amount (50%) of genetic material; the zICC was found to be significantly different ($p < .05$) between DZ and SBs groups.

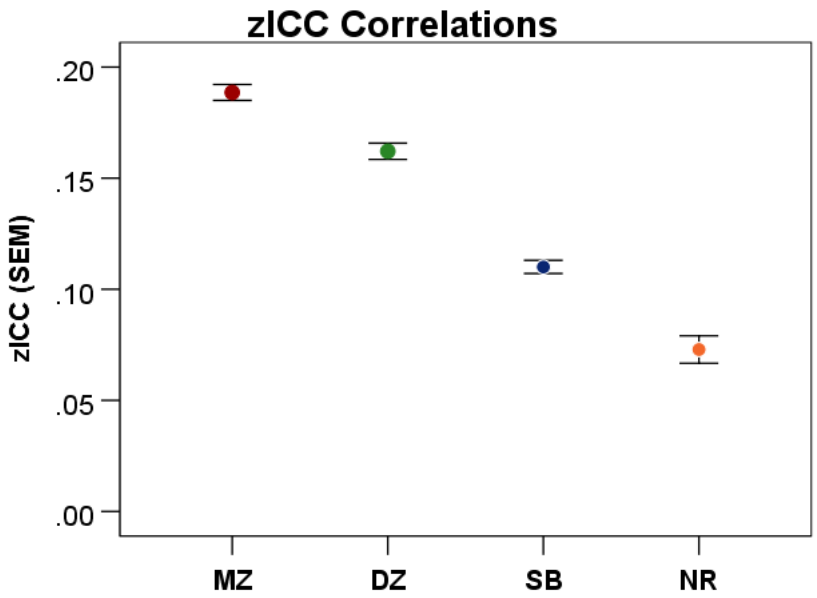

Figure 5.11 zICC of PAC per genetic group

zICC correlation values were also distinguished for each genetic group and the three brain groups (Figure 5.12). The values varied systematically, such that MZ>DZ>SB>NR for the grouping of the correlations for each brain group, except for the homotopic brain group in the DZ group which was lower than the SB group.

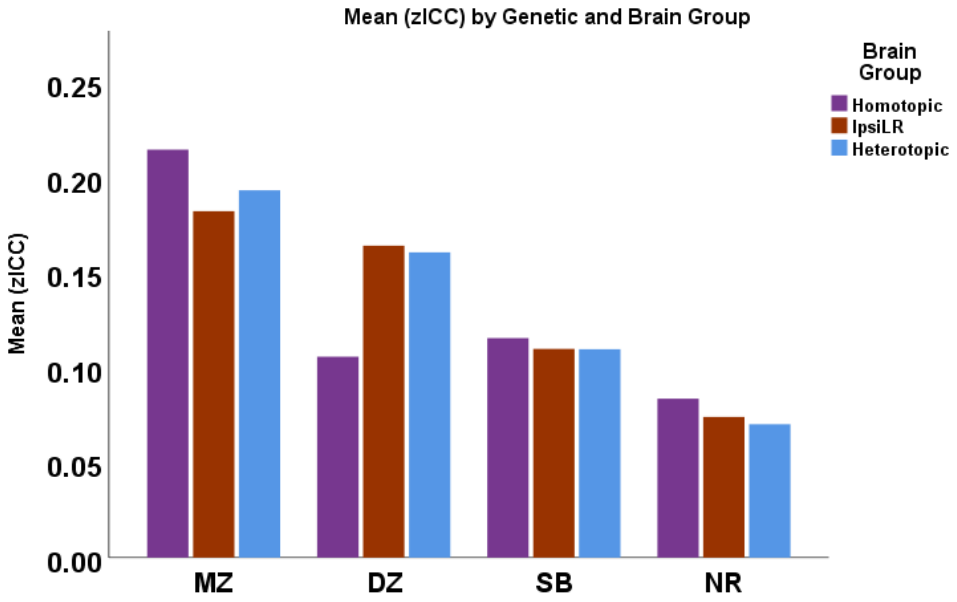

Figure 5.12 zICC of PAC by homotopic brain per genetic group

The gender analysis for the PAC was analyzed by using MZ twins and found to be significant ($p < .05$) (Figure 5.13).When gender and the three brain groups were analyzed for the MZ twins, the homotopic brain group was found not to be significant ($p > .05$), while the ipsiLR and heterotopic brain group were found to be significant ($p < .05$) (Figure 5.14).

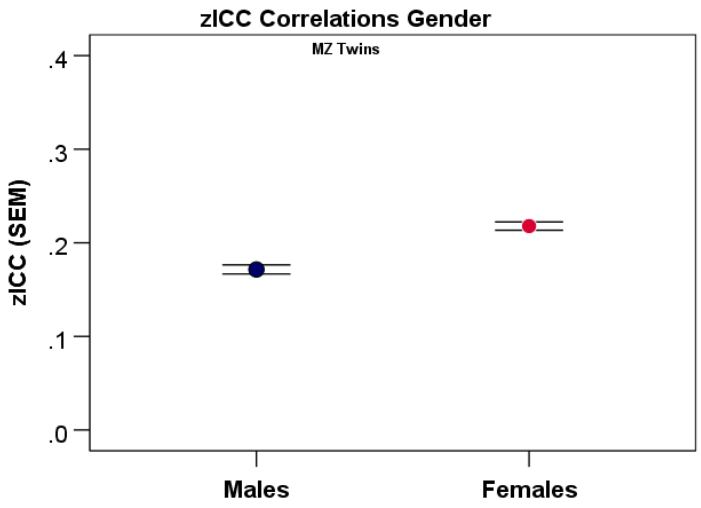

Figure 5.13 zICC of the 2278 PAC by gender

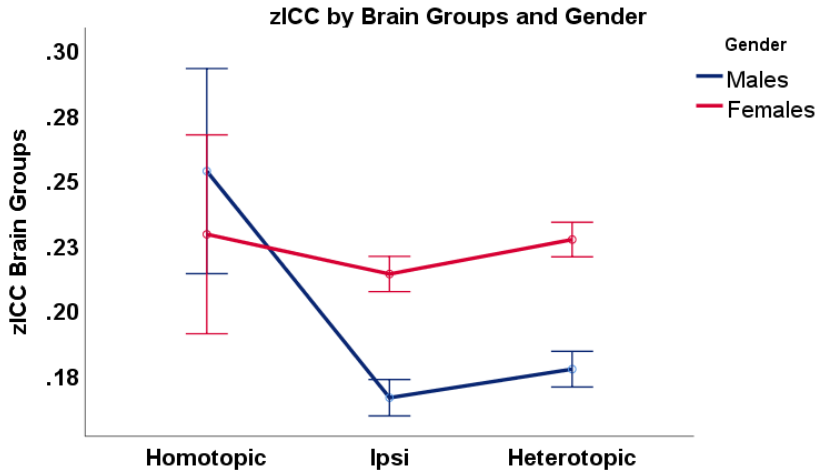

Figure 5.14 zICC of PAC by homotopic brain group and gender

Heritability was calculated (Figure 5.15) using the ICC of PAC as a measurement. Heritability was highest in the homotopic group (h^2 = .209), followed by the heterotopic group (h^2 = .065), and then by the ipsiLR group (h^2 = .0355).

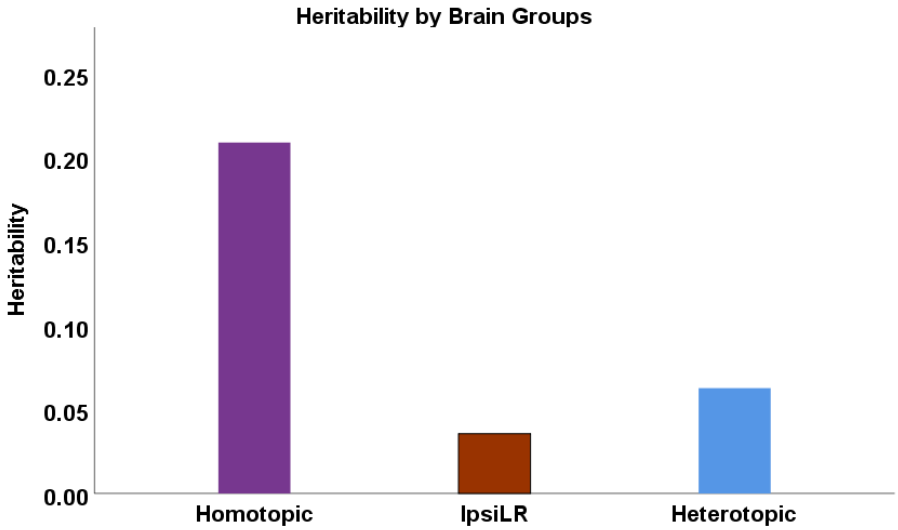

Figure 5.15 Heritability of brain groups

Third, the MDS analysis of brain group heritabilities (Fig. 5.16) revealed a separation of the heritabilities into 3 quadrants comprising ipsiLR (upper left quadrant), homotopic (upper right), and heterotopic (lower left).

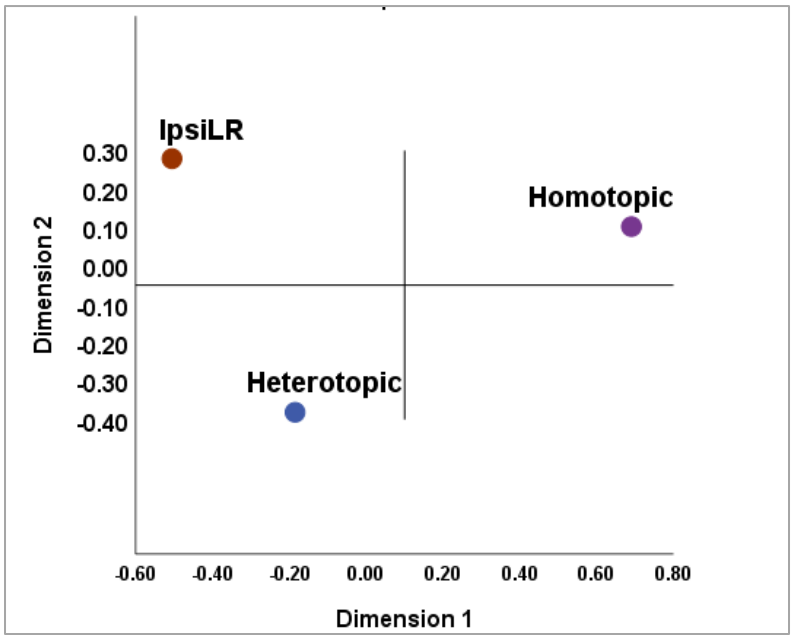

Figure 5.16 MDS of Brain Groups h_b^2 values

Finally, the grouping and gradient for lobes was confirmed in the HTC dendrogram (Fig. 5.17), which comprises 2 branches, one branch containing the heterotopic and ipsiLR group, and the second branch contained the homotopic group.

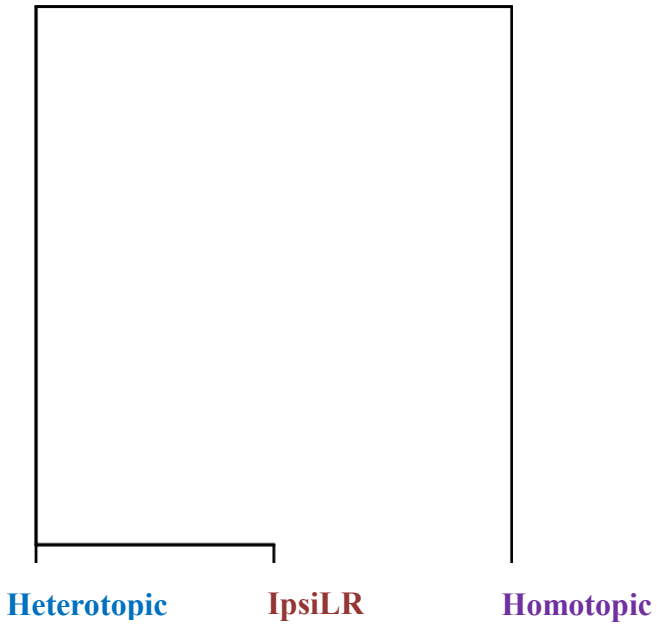

Figure 5.17 HTC of Brain Groups h_b^2 values

5.6 Discussion

The goal of Chapter 5 is to determine the heritability of healthy brain regions using the BOLD signal innovations and known genetic relationships. This was accomplished by pre-whitening the BOLD time series data for each participant by using the ARIMA (15,1,1) model, computing the PASD and PAC, and then grouping the calculations into their respective brain and genetic groups.

The results provide evidence that pre-whitening the fMRI data using the ARIMA (15,1,1) model is an important step to determine the true association between time series

because fMRI BOLD time series data is typically considered as autocorrelated and non-stationary data. Without correcting for this, the true association between the time series is undetermined and might lead to spurious results due to the reflection of the internal properties of the series. To avoid this, the time series data are pre-whitened using the ARIMA (15,1,1) model to remove such effects. In addition to the pre-whitened BOLD signal, this chapter uses the results of the pre-whiten BOLD signal, the innovations (variations), to calculate two measurements, PASD and PAC, to determine heritability. Several studies of neuroscience have examined the properties and unique functions of variance to understand and predict several important phenomena (Faisal et al., 2008; Garrett et al., 2010; Grady and Garrett, 2014). This research takes advantage of the true associations of the pre-whiten BOLD signal and the innovations of the BOLD signal to calculate heritability may reveal novel brain-related effects not previously considered in fMRI research.

The finding provide evidence that the zICC for both PASD and PAC measurements varied systematically, such that MZ>DZ>SB>NR. This pattern of genetic influence for a heritable trait is expected, since MZ twins share all genetic effects, while DZ twins share on average 50 % genetic effects. Siblings also share on average 50 % of their genetics; however, it is expected that they would have lower zICC (and heritability values) because their environmental variation is higher compared to twins. The non-related participants are expected to be last in terms of similarity since they are not expected to have any genetic effects.

When zICC of PASD for monozygotic twins were grouped by gender it was found not to be significant; the measurements were also grouped by gender and brain lobes, but it was also found not to be significant. Using the zICC of PASD to calculate heritability, show that about half of the Desikan areas have some degree of heritability (table 5.1). The parsorbitalis ($h^2 = 0.903$) in the frontal lobe was the most heritable while by supramarginal ($h^2 = .218$) in the parietal lobe was the lowest (Table 5.1, Fig. 5.4). The heritability findings for the lobes in this dissertation are the following: frontal lobe (72%), temporal lobe (62%), and parietal lobe (49%). This suggests out of the lobes the frontal lobe is under the most genetic influence. The grouping of the heritabilities (MDS) of the lobes into three separate quadrants show a similar pattern to their anatomical position in the brain.

The zICC values of PAC were grouped into three different brain groups and varied systematically for each genetic group, except for the homotopic brain group in the DZ group which was lower than the SB group. The homotopic group has the highest zICC value among the three brain groups, for all genetic groups, expect the DZ group which the ipsi and heterotopic group was higher than the homotopic group. The zICC correlations for the NR group were very similar and didn't have much variation compared to the other genetic groups.

The zICC of PAC for MZ twins were grouped by gender for the 2278 zICC correlations and found to be significant. When gender and the three brain groups were analyzed for the MZ twins, the homotopic brain group was found not to be significant, while the ipsiLR and heterotopic brain group were found to be significant.

Using the zICC of PAC as a measurement to calculate heritability, showed heritability highest in the homotopic group (h^2 = 21%), followed by the heterotopic group (h^2 = 6.5 %), and then in the ipsiLR group (h^2 = 3.6%). The grouping of the brain heritabilities using HTC found the heterotopic and ipsiLR grouping together and the homotopic grouped separately. These findings show an overall trend of heritability that reflect the varying density of anatomical connectivity; extensive across the homotopic areas and sparse across heterotopic areas.

The research presents evidence that using the ARIMA (15,1,1) model to pre-whiten the BOLD time series data and using the innovations of the BOLD signal to calculate two measurements, PASD and PAC, has a genetic component due to the systematic variation for MZ, DZ, SB and NR, genetic groups. Using innovation-based measures to calculate heritability may reveal novel brain-related effects not previously considered in fMRI research.

Chapter 6 Summary

MRI allows for a multifaceted, noninvasive study of the brain structure and function. The advances and availability of data from the high-quality Human Connectome Project (HCP) provides a unique and unprecedented opportunity to evaluate genetic effects on a multitude of neural and behavioral measures and thus allowing researchers to systematically explore the human connectome. This research analyzes three neuroimaging modalities (sMRI, rfMRI, dMRI) as well as the large amount of behavioral data, to estimate the genetic contribution of each, by looking at 4 genetic groups in MZ twins, DZ twins, siblings (SB) and unrelated participants (NR).

6.1 Behavior Summary

The relationship between genetics, behavior and heritability is a topic of interest across many different disciplines (Toga & Thompson, 2005). The goal of Chapter 2 is to determine the heritability of behavioral traits in five domains (motor, cognition, emotion, personality and sensory) in a young, healthy population using known genetic relationships (twins, siblings).

The grouping of participants into genetic groups resulted in the zICC differing significantly and varying systematically among the groups, such that MZ>DZ>SIB>NR for behavioral measurements overall.

The heritability results are in agreement with the literature: most human behavioral traits have some degree of heritability across different domains (W. Johnson, 2011; Turkheimer, 2000). The heritabilities did not differ significantly among domains.

MDS and HTC were used to decipher grouping of the heritabilities based on domain. A reasonable interpretation of the MDS findings can be achieved by splitting the graph by the 2nd dimension. This would position motor-sensory on the right side of the graph and cognition-personality on the left side of the graph with emotion in the middle. This grouping of the MDS is further confirmed in the HTC results.

6.2 dMRI Summary

The goal of Chapter 3 is to determine the heritability of white matter (WM) regions of the healthy brain using known genetic relationships and key measurements, fractional anisotropy (FA) and mean diffusivity (MD).

The results show that grouping of participants into genetic groups resulted in the zICC differing significantly and systematically among the groups, such that MZ>DZ>SB>NR for both FA and MD measurements.

Heritability was calculated by grouping the WM areas of the brain into 4 groups based on (Mori et al., 2008) atlas and are as follows (from most heritable to lowest): for FA, association fibers, tracts in brain stem, projection fibers, and commissural fibers and for MD, the tracts in the brainstem, projections fibers, association fibers and finally commissural fibers. For both FA and MD, results show the commissural fibers had the lowest heritability of the four areas; however, their heritability value of .60 and 0.79 respectively is considered a high heritability value.

HTC and MDS were used to decipher grouping of the heritabilities based on areas. For FA, results showed commissural fibers and projection fibers in the same quadrant, association fibers in another quadrant, and tracts of the brain stem as a separate quadrant.

The MDS analysis of the MD heritabilities revealed a separation of the areas into 4 quadrants. For both the measurements the association fibers and the tracts of the brain stem were in opposite quadrants, while for FA commissural fibers and projection fibers in the same quadrant but in the MD, they were in opposite quadrants.

6.3 sMRI Summary

The goal of Chapter 4 is to determine the heritability of structural brain volumes of the healthy brain using known genetic relationships in 35 different regions of the brain using the Desikan atlas and the four major lobes.

The grouping of participants into genetic groups resulted in the zICC differing significantly and systematically varying among the groups, such that MZ>DZ>SB>NR for the lobes and Desikan areas. All participant groups, except for the NR groups, showed a pattern of decreasing ICC with overall decreasing volume of brain regions from the larger lobe volumes to the smaller cortical ROIs.

The heritability results show that most Desikan areas have some degree of heritability. The heritability findings for the four lobes in this dissertation are the following: frontal lobe (50%), temporal lobe (73%), parietal lobe (46%) and occipital lobe (44%).

The HTC results can give insight on how to split the MDS graph; splitting the graph by the second-dimension results in the frontal, parietal and occipital lobes to be in a single dimension. One possible explanation for this result is that the heritability of the lobes follows the anatomical and spatial positioning of the lobes. The actual extent of genetic influence on brain structures and volumes is likely to vary spatially across the

brain. A plausible developmental hypothesis could be that the earliest-maturing brain regions have structural volumes that are more genetically influenced.

6.4 fMRI Summary

The goal of Chapter 5 is to determine the heritability of healthy brain regions using the BOLD signal innovations and known genetic relationships. This was accomplished by pre-whitening the BOLD time series data for each participant by using the ARIMA (15,1,1) model, computing the pre-whiten average standard deviation (PASD) and pre-whiten average correlation (PAC), and then grouping the calculations into their respective brain and genetic groups.

The finding provide evidence that the zICC for both PASD and PAC measurements varied systematically, such that MZ>DZ>SB>NR. When zICC of PASD for monozygotic twins were grouped by gender it was found not to be significant; the measurements were also grouped by gender and brain lobes, but it was also found not to be significant.

Using the zICC of PASD to calculate heritability reveals that about half of the Desikan areas have some degree of heritability. The heritability findings for the lobes in this dissertation are the following: frontal lobe (72%), temporal lobe (62%), and parietal lobe (49%). This suggests out of the lobes the frontal lobe is under the most genetic influence. The grouping of the heritabilities (MDS) of the lobes into three separate quadrants show a similar pattern to their anatomical position in the brain.

The zICC values of PAC were grouped into three different brain groups and varied systematically for each genetic group, except for the homotopic brain group in the DZ group which was lower than the SB group. The zICC correlations for the NR group were

very similar and didn't have much variation compared to the other genetic groups, since they are expected to be zero or close to zero.

Using the zICC of PAC as a measurement to calculate heritability, showed heritability highest in the homotopic group (h^2 = 21%), followed by the heterotopic group (h^2 = 6.5 %), and then in the ipsiLR group (h^2 = 3.6%). These findings show an overall trend of heritability that reflect the varying density of anatomical connectivity; extensive across the homotopic areas and sparse across heterotopic areas.

6.5 Gender Summary

Analyses were carried out in each chapter to assess possible differences between males and females. In the behavior data (chapter 2), the zICC varied systemically for men and women and, when grouped by domain, there was nearly no difference between the genders. In chapter 3 (dMRI) zICC of MZ twins were grouped by gender for FA and MD; the zICCs of these groups did differed significantly. In chapter 4 (sMRI) the zICCs of MZ twins were grouped by gender and differed significantly. However, when the zICCs were grouped by gender and lobes, these did not differ significantly. In Chapter 5 (fMRI) the zICC of PASD were grouped by gender and found to be significant; however, when grouped by gender and by brain lobes, it was not found to be significant. Also, from chapter 5, when using the zICC of the PAC of MZ twins grouped by gender, was found to be significant. However, when gender and the three brain groups were analyzed, the homotopic brain group was found not to be significant, while the ipsiLR and heterotopic brain group were found to be significant.

ICC describes how strongly the units in the same group resemble each other. If the MZ female ICC is higher than the MZ male that means higher similarities between female MZ twins in comparison with MZ male twins.

It is interesting to note that for the brain measures (sMRI, dMRI, fMRI), even though there is a difference between men and women overall, the difference is not significant when grouped into brain areas or lobes. Also, the overall zICC values, across behavioral domains, for men and women are very similar. It is interesting to note, that even though there is a significant difference between men and women for the brain measures across the domains, it does not reflect a difference in the behavior domain.

6.6 Main contributions and findings

This dissertation includes three MRI modalities, sMRI, dMRI and fMRI. This is a significant contribution since most studies evaluate only one modality, such as sMRI or fMRI. In order to compare the heritability measures of different characteristics of brain structure and function, it is important to contrast heritability measures across imaging modalities within the same twin populations (Jansen, 2015). The insights from heritability studies aid the understanding of individual differences in brain structure and function.

The zICC across all domains and measures varied systematically such that MZ>DZ>SB>NR. This general arrangement is as anticipated since MZ twins are genetically identical compared to DZ, which are on average 50 percent similar. A specific comparison concerns the difference of zICC between DZ and SB groups, since those pairs share the same amount (50%) of genetic material. Overall across most

measures and domains this difference was not significant. ICC for non-related participants is zero or close to zero since they do not share any genetic material.

The heritability for the behavioral domains in chapter 2 ranged from (from highest to lowest): personality, cognition, emotion, sensory, motor. The heritability measures from chapter 3 in FA and MD overall had very high heritability, suggesting a high consistency of additive genetic contribution to FA values in WM regions of the brain. The sMRI heritability results show that most Desikan areas have some degree of heritability. The heritability findings for the four lobes in this dissertation are the found (highest to lowest): temporal, frontal, parietal lobe and occipital lobe. The results from this dissertation found that the occipital lobe had the weakest genetic contribution of the four lobes. In chapter 5 residuals, of pre-whitened fMRI BOLD signal with ARIMA (15,1,1), called innovations are used to calculate their SD (PASD) and correlations between them (PAC). The heritability of these parameters were calculated.

A significant advantage of this dissertation is the state-of-the-art high-resolution dataset provided by the HCP. For sMRI the high-resolution MRI T1-weighted scans with voxel dimensions of 0.7 x 0.7 x 0.7 mm compared to e standard T1- weighted acquisition dimensions of 1 x 1 x 1 mm. fMRI resting-state activity of the same areas extracted from long-duration (1200 volumes), fast-acquisition (every 0.72 s), high-resolution (2 mm isotropic). dMRI white matter integrity measures at 1.25 mm spatial resolution and very strong magnetic field gradients at (100 mT/m).

Another major advantage of this study is that it involved a young healthy adult population with an age range of 22- 37. Currently, most studies using MRI to study

heritability have been used to study diseased brains with few studies covering the healthy brain. This age range was specifically chosen because it's an age range that is considered a fully developed adult brain, but not an aging brain or a developing brain.

6.7 Conclusion

Multimodal neuroimaging is becoming more common in neuroscientific research and in clinical applications. Through the combined efforts of the community, many technical limitations have been overcome and solved; however, with the overwhelming amount of complex and heterogeneous neuroimaging data, there needs to be clear examination and analysis of the data. This research analyzes a large amount of behavioral data and three neuroimaging modalities: sMRI, rfMRI, and dMRI. In order to estimate the genetic contribution of each modality, the participants were divided into 4 genetic groups in monozygotic twins, dizygotic twins, siblings and unrelated participants. This research study uses the neuroimaging and behavioral data of young, healthy, adult population with a narrow age range. This is a valuable study for identification of an overall blue print of the young healthy adult brain. The insights from heritability studies aid the understanding of differences in brain structure and function. Thus, providing an overall excellent blue print for heritability values in a young healthy population across multimodal neuroimaging techniques.

Bibliography

Adhikari, B. M., Jahanshad, N., Shukla, D., Glahn, D. C., Blangero, J., Reynolds, R. C., … Kochunov, P. (2018). Heritability estimates on resting state fMRI data using ENIGMA analysis pipeline. *Pacific Symposium on Biocomputing. Pacific Symposium on Biocomputing*, *23*, 307–318. Retrieved from http://www.ncbi.nlm.nih.gov/pubmed/29218892

Alexander, A. L., Lee, J. E., Lazar, M., & Field, A. S. (2007a). Diffusion tensor imaging of the brain. *Neurotherapeutics : The Journal of the American Society for Experimental NeuroTherapeutics*, *4*(3), 316–29. http://doi.org/10.1016/j.nurt.2007.05.011

Alexander, A. L., Lee, J. E., Lazar, M., & Field, A. S. (2007b). Diffusion tensor imaging of the brain. *Neurotherapeutics : The Journal of the American Society for Experimental NeuroTherapeutics*, *4*(3), 316–29. http://doi.org/10.1016/j.nurt.2007.05.011

American Roentgen Ray Society., & American Society of Neuroradiology. (2005). *American journal of neuroradiology : AJNR. American Journal of Neuroradiology* (Vol. 26). [Williams & Wilkins Co.]. Retrieved from http://www.ajnr.org/content/26/10/2703

Amir, S., Batouli, H., Trollor, J. N., Wen, W., & Sachdev, P. S. (2014). The heritability of volumes of brain structures and its relationship to age: A review of twin and family studies. *Ageing Research Reviews*, *13*, 1–9. http://doi.org/10.1016/j.arr.2013.10.003

Bandettini, P. A., Wong, E. C., Hinks, R. S., Tikofsky, R. S., & Hyde, J. S. (1992). Time course EPI of human brain function during task activation. *Magnetic Resonance in Medicine*, *25*(2), 390–397. http://doi.org/10.1002/mrm.1910250220

Basser, P. J., Mattiello, J., & LeBihan, D. (1994). MR diffusion tensor spectroscopy and imaging. *Biophysical Journal*, *66*(1), 259–267. http://doi.org/10.1016/S0006-3495(94)80775-1

Bevilacqua, L., & Goldman, D. (2011). Genetics of emotion. *Trends in Cognitive Sciences*, *15*(9), 401–8. http://doi.org/10.1016/j.tics.2011.07.009

Blokland, G. A. M., de Zubicaray, G. I., McMahon, K. L., & Wright, M. J. (2012). Genetic and environmental influences on neuroimaging phenotypes: a meta-analytical perspective on twin imaging studies. *Twin Research and Human Genetics : The Official Journal of the International Society for Twin Studies*, *15*(3), 351–71. http://doi.org/10.1017/thg.2012.11

Bouchard, T. J., & Loehlin, J. C. (2001). Genes, evolution, and personality. *Behavior Genetics*, *31*(3), 243–73. Retrieved from http://www.ncbi.nlm.nih.gov/pubmed/11699599

Bouchard, T. J., & McGue, M. (1990). Genetic and Rearing Environmental Influences on Adult Personality: An Analysis of Adopted Twins Reared Apart. *Journal of Personality*, *58*(1), 263–292. http://doi.org/10.1111/j.1467-6494.1990.tb00916.x

Box GEP, Jenkins GM (1976) Time series analysis: forecasting and control. Holden-Day, San Francisco, CA

Briley, D. A., & Tucker-Drob, E. M. (2013). Explaining the Increasing Heritability of Cognitive Ability Across Development. *Psychological Science*. http://doi.org/10.1177/0956797613478618

Brun, C. C., Leporé, N., Pennec, X., Lee, A. D., Barysheva, M., Madsen, S. K., … Thompson, P. M. (2009). Mapping the regional influence of genetics on brain structure variability — A Tensor-Based Morphometry study. *NeuroImage*, *48*(1), 37–49. http://doi.org/10.1016/J.NEUROIMAGE.2009.05.022

Buckner, R. L., Andrews-Hanna, J. R., & Schacter, D. L. (2008). *The Brain's Default Network. Annals of the New York Academy of Sciences*, *1124*(1), 1–38. http://doi.org/10.1196/annals.1440.011

Carey. (n.d.). Heritability: Introduction. Retrieved February 6, 2019, from http://psych.colorado.edu/~carey/hgss/hgssapplets/heritability/heritability.intro.html

Chiang, M.-C., McMahon, K. L., de Zubicaray, G. I., Martin, N. G., Hickie, I., Toga, A. W., … Thompson, P. M. (2011). Genetics of white matter development: A DTI study of 705 twins and their siblings aged 12 to 29. *NeuroImage*, *54*(3), 2308–2317. http://doi.org/10.1016/J.NEUROIMAGE.2010.10.015

Christova, P., & Georgopoulos, A. P. (2018). RAPID REPORT Neural Circuits Invariant and heritable local cortical organization as revealed by fMRI. *J Neurophysiol*, *120*, 760–764. http://doi.org/10.1152/jn.00137.2018.-Neural

Christova, P., Lewis, S. M., Jerde, T. A., Lynch, J. K., & Georgopoulos, A. P. (2011a). True associations between resting fMRI time series based on innovations. *J. Neural Eng*, *8*, 46025–46045. http://doi.org/10.1088/1741-2560/8/4/046025

Christova, P., Lewis, S. M., Jerde, T. A., Lynch, J. K., & Georgopoulos, A. P. (2011b). True associations between resting fMRI time series based on innovations. *Journal of Neural Engineering*, *8*(4), 46025. http://doi.org/10.1088/1741-2560/8/4/046025

Dale, A. M., Fischl, B., & Sereno, M. I. (1999). Cortical Surface-Based Analysis: I. Segmentation and Surface Reconstruction. *NeuroImage*, *9*(2), 179–194.

http://doi.org/10.1006/NIMG.1998.0395

Desikan, R. S., Se, F., Fischl, B., Quinn, B. T., Dickerson, B. C., Blacker, D., … Killiany, R. J. (2006). An automated labeling system for subdividing the human cerebral cortex on MRI scans into gyral based regions of interest, *31*, 968–980. http://doi.org/10.1016/j.neuroimage.2006.01.021

Dolan, R. J. (2002). Emotion, cognition, and behavior. *Science (New York, N.Y.)*, *298*(5596), 1191–4. http://doi.org/10.1126/science.1076358

Douet, V., Chang, L., Cloak, C., & Ernst, T. (2014). Genetic influences on brain developmental trajectories on neuroimaging studies: from infancy to young adulthood. *Brain Imaging and Behavior*, *8*(2), 234–50. http://doi.org/10.1007/s11682-013-9260-1

Elster, A. (n.d.). Diffusion tensor - Questions and Answers in MRI. Retrieved March 29, 2018, from http://www.mriquestions.com/diffusion-tensor.html

Faisal, A. A., Selen, L. P. J., & Wolpert, D. M. (2008). Noise in the nervous system. *Nature Reviews Neuroscience*, *9*(4), 292–303. http://doi.org/10.1038/nrn2258

Falconer, D. S. (1965). The inheritance of liability to certain diseases, estimated from the incidence among relatives. *Annals of Human Genetics*, *29*(1), 51–76. http://doi.org/10.1111/j.1469-1809.1965.tb00500.x

Fischl, B., & Dale, A. M. (2000). Measuring the thickness of the human cerebral cortex from magnetic resonance images. *Proceedings of the National Academy of Sciences of the United States of America*, *97*(20), 11050–5. http://doi.org/10.1073/pnas.200033797

Fischl, B., van der Kouwe, A., Destrieux, C., Halgren, E., Ségonne, F., Salat, D. H., … Dale, A. M. (2004). Automatically parcellating the human cerebral cortex. *Cerebral Cortex (New York, N.Y. : 1991)*, *14*(1), 11–22. Retrieved from http://www.ncbi.nlm.nih.gov/pubmed/14654453

Fornito, A., Yoon, J., Zalesky, A., Bullmore, E. T., & Carter, C. S. (2011). General and specific functional connectivity disturbances in first-episode schizophrenia during cognitive control performance. *Biological Psychiatry*, *70*(1), 64–72. http://doi.org/10.1016/j.biopsych.2011.02.019

Fritsch, V., Da Mota, B., Loth, E., Varoquaux, G., Banaschewski, T., Barker, G. J., … Thirion, B. (2015). Robust regression for large-scale neuroimaging studies. *NeuroImage*, *111*, 431–441. http://doi.org/10.1016/J.NEUROIMAGE.2015.02.048

Garrett, D. D., Kovacevic, N., McIntosh, A. R., & Grady, C. L. (2010). Blood oxygen level-dependent signal variability is more than just noise. *The Journal of*

Neuroscience : The Official Journal of the Society for Neuroscience, *30*(14), 4914–21. http://doi.org/10.1523/JNEUROSCI.5166-09.2010

Gazes, Y., Bowman, F. D., Razlighi, Q. R., O'Shea, D., Stern, Y., & Habeck, C. (2016). White matter tract covariance patterns predict age-declining cognitive abilities. *NeuroImage*, *125*, 53–60. http://doi.org/10.1016/J.NEUROIMAGE.2015.10.016

Geschwind, D. H., Miller, B. L., DeCarli, C., & Carmelli, D. (2002). Heritability of lobar brain volumes in twins supports genetic models of cerebral laterality and handedness. *Proceedings of the National Academy of Sciences of the United States of America*, *99*(5), 3176–81. http://doi.org/10.1073/pnas.052494999

Glahn, D. C., Winkler, A. M., Kochunov, P., Almasy, L., Duggirala, R., Carless, M. A., … Blangero, J. (2010). Genetic control over the resting brain. *Proceedings of the National Academy of Sciences of the United States of America*, *107*(3), 1223–8. http://doi.org/10.1073/pnas.0909969107

Glasser, M. F., Sotiropoulos, S. N., Wilson, J. A., Coalson, T. S., Fischl, B., Andersson, J. L., … Jenkinson, M. (2013). The minimal preprocessing pipelines for the Human Connectome Project. *NeuroImage*, *80*, 105–24. http://doi.org/10.1016/j.neuroimage.2013.04.127

Gogtay, N., Giedd, J. N., Lusk, L., Hayashi, K. M., Greenstein, D., Vaituzis, A. C., … Thompson, P. M. (2004). *Dynamic mapping of human cortical development during childhood through early adulthood* (Vol. 101). PNAS. Retrieved from www.pnas.orgcgidoi10.1073pnas.0402680101

Grady, C. L., & Garrett, D. D. (2014). Understanding variability in the BOLD signal and why it matters for aging. *Brain Imaging and Behavior*, *8*(2), 274–83. http://doi.org/10.1007/s11682-013-9253-0

Hart, B., Cribben, I., & Fiecas, M. (n.d.). A Longitudinal Model for Functional Connectivity Networks Using Resting-State fMRI. http://doi.org/10.1101/152538

Haworth, C. M. A., Wright, M. J., Luciano, M., Martin, N. G., de Geus, E. J. C., van Beijsterveldt, C. E. M., … Plomin, R. (2010). The heritability of general cognitive ability increases linearly from childhood to young adulthood. *Molecular Psychiatry*, *15*(11), 1112–20. http://doi.org/10.1038/mp.2009.55

Jang, K. L., Livesley, W. J., & Vemon, P. A. (1996). Heritability of the Big Five Personality Dimensions and Their Facets: A Twin Study. *Journal of Personality*, *64*(3), 577–592. http://doi.org/10.1111/j.1467-6494.1996.tb00522.x

Jansen, A. G., Mous, S. E., White, T., Posthuma, D., & Polderman, T. J. C. (2015). What Twin Studies Tell Us About the Heritability of Brain Development, Morphology, and Function: A Review. *Neuropsychology Review*, *25*(1), 27–46.

http://doi.org/10.1007/s11065-015-9278-9

Jellison, B. J., Field, A. S., Medow, J., Lazar, M., Salamat, M. S., & Alexander, and A. L. (2002). High-resolution line scan diffusion tensor MR imaging of white matter fiber tract anatomy. *AJNR. American Journal of Neuroradiology*, *23*(1), 67–75. Retrieved from http://www.ncbi.nlm.nih.gov/pubmed/11827877

Jenkinson, M., Beckmann, C. F., Behrens, T. E. J., Woolrich, M. W., & Smith, S. M. (2012). FSL. *NeuroImage*, *62*(2), 782–790. http://doi.org/10.1016/J.NEUROIMAGE.2011.09.015

Johnson, S. B., Blum, R. W., & Giedd, J. N. (2009). Adolescent maturity and the brain: the promise and pitfalls of neuroscience research in adolescent health policy. *The Journal of Adolescent Health : Official Publication of the Society for Adolescent Medicine*, *45*(3), 216–21. http://doi.org/10.1016/j.jadohealth.2009.05.016

Johnson, W. (2011). Beyond Heritability: Twin Studies in Behavioral Research, *18*(4), 217–220. http://doi.org/10.1111/j.1467-8721.2009.01639.x.Beyond

Keller, S. S., & Roberts, N. (2009). Measurement of brain volume using MRI: software, techniques, choices and prerequisites. *JASs Invited Reviews Journal of Anthropological Sciences*, *87*, 127–151. Retrieved from http://www.isita-org.com/jass/Contents/2009 vol87/PDF/On-Line_bassa/JASs2009_05_Keller.pdf

Koay, C. G., Chang, L.-C., Carew, J. D., Pierpaoli, C., & Basser, P. J. (2006). A unifying theoretical and algorithmic framework for least squares methods of estimation in diffusion tensor imaging. *Journal of Magnetic Resonance (San Diego, Calif. : 1997)*, *182*(1), 115–25. http://doi.org/10.1016/j.jmr.2006.06.020

Kochunov, P., Glahn, D. C., Lancaster, J. L., Winkler, A. M., Smith, S., Thompson, P. M., … Blangero, J. (2010). Genetics of microstructure of cerebral white matter using diffusion tensor imaging. *NeuroImage*, *53*(3), 1109–1116. http://doi.org/10.1016/J.NEUROIMAGE.2010.01.078

Kochunov, P., Jahanshad, N., Marcus, D., Winkler, A., Sprooten, E., Nichols, T. E., … Van Essen, D. C. (2015). Heritability of fractional anisotropy in human white matter: a comparison of Human Connectome Project and ENIGMA-DTI data. *NeuroImage*, *111*, 300–11. http://doi.org/10.1016/j.neuroimage.2015.02.050

Kochunov, P., Thompson, P. M., Winkler, A., Morrissey, M., Fu, M., Coyle, T. R., … Hong, L. E. (2016). The common genetic influence over processing speed and white matter microstructure: Evidence from the Old Order Amish and Human Connectome Projects. *NeuroImage*, *125*, 189–197. http://doi.org/10.1016/j.neuroimage.2015.10.050

Kwong, K. K., Belliveau, J. W., Chesler, D. A., Goldberg, I. E., Weisskoff, R. M.,

Poncelet, B. P., … Turner, R. (1992). Dynamic magnetic resonance imaging of human brain activity during primary sensory stimulation. *Proceedings of the National Academy of Sciences of the United States of America*, *89*(12), 5675–9. http://doi.org/10.1073/pnas.89.12.5675

Langfelder, P., Zhang, B., & Horvath, S. (2008). Defining clusters from a hierarchical cluster tree: The Dynamic Tree Cut package for R. *Bioinformatics*, *24*(5), 719–720. http://doi.org/10.1093/bioinformatics/btm563

Le Bihan, D., & Breton, E. (1986). *MR Imaging of Intravoxel Incoherent Motions: Application to Diffusion and Perfusion in Neurologic Disorders'*. Retrieved from https://mriquestions.com/uploads/3/4/5/7/34572113/dlbihanradiology1986.pdf

Le Bihan, D., & Iima, M. (2015). Diffusion Magnetic Resonance Imaging: What Water Tells Us about Biological Tissues. *PLOS Biology*, *13*(7), e1002203. http://doi.org/10.1371/journal.pbio.1002203

Le Bihan, D., Mangin, J.-F., Poupon, C., Clark, C. A., Pappata, S., Molko, N., & Chabriat, H. (2001). Diffusion tensor imaging: Concepts and applications. *Journal of Magnetic Resonance Imaging*, *13*(4), 534–546. http://doi.org/10.1002/jmri.1076

Luis C. Maas, MD, PhD and Pratik Mukherjee, MD, P. (2005.). Diffusion MRI: Overview and clinical applications in neuroradiology. Retrieved June 3, 2017, from http://appliedradiology.com/articles/diffusion-mri-overview-and-clinical-applications-in-neuroradiology

Lukies, M. W., Watanabe, Y., Tanaka, H., Takahashi, H., Ogata, S., Omura, K., … Osaka University Twin Research Group, the O. U. T. R. (2017). Heritability of brain volume on MRI in middle to advanced age: A twin study of Japanese adults. *PloS One*, *12*(4), e0175800. http://doi.org/10.1371/journal.pone.0175800

Madden, D. J., Bennett, I. J., Burzynska, A., Potter, G. G., Chen, N.-K., & Song, A. W. (2012). Diffusion tensor imaging of cerebral white matter integrity in cognitive aging. *Biochimica et Biophysica Acta*, *1822*(3), 386–400. http://doi.org/10.1016/j.bbadis.2011.08.003

Manual, R., Release, S., Consortium, W., Human, N. I. H., & Project, C. (2017). WU-Minn HCP 1200 Subjects Data Release : Reference Manual, (June), 1–169. Retrieved from http://www.humanconnectome.org/documentation/S1200/HCP_S1200_Release_Reference_Manual.pdf

Marcus, D. S., Harms, M. P., Snyder, A. Z., Jenkinson, M., Anthony, J., Glasser, M. F., … Essen, D. C. Van. (2014). Human Connectome Project Informatics: quality control, database services, and visualization. *NeuroImage*, (314). http://doi.org/10.1016/j.neuroimage.2013.05.077.Human

Mayfield, (2018). Functional MRI and Diffusion Tensor Imaging Mayfield Brain & Spine Cincinnati, Ohio. Retrieved March 20, 2019, from https://www.mayfieldclinic.com/PE-fMRI_DTI.HTM

McKinstry, R. C., Miller, J. H., Snyder, a. Z., Mathur, a., Schefft, G. L., Almli, C. R., … Neil, J. J. (2002). A prospective, longitudinal diffusion tensor imaging study of brain injury in newborns. *Neurology*, *59*(6), 824–833. http://doi.org/10.1212/WNL.59.6.824

Michelon, P. (2006). What are Cognitive Skills and Abilities? | SharpBrains. Retrieved October 7, 2019, from https://sharpbrains.com/blog/2006/12/18/what-are-cognitive-abilities/

Missitzi, J., Gentner, R., Misitzi, A., Geladas, N., Politis, P., Klissouras, V., & Classen, J. (2013). Heritability of motor control and motor learning. *Physiological Reports*, *1*(7), e00188. http://doi.org/10.1002/phy2.188

Mohamed;, S. H. F. F. B. (2010). *A guide to functional imaging for neruoscientists*. SpringerLink (Online service).

Mori, S., Oishi, K., Jiang, H., Jiang, L., Li, X., Akhter, K., … Mazziotta, J. (2008). Stereotaxic white matter atlas based on diffusion tensor imaging in an ICBM template. *NeuroImage*, *40*(2), 570–582. http://doi.org/10.1016/J.NEUROIMAGE.2007.12.035

Moseley, M. (2002). Diffusion tensor imaging and aging - A review. *NMR in Biomedicine*, *15*(7–8), 553–560. http://doi.org/10.1002/nbm.785

Mukherjee, P., Berman, J. I., Chung, S. W., Hess, C. P., & Henry, R. G. (2008). Diffusion tensor MR imaging and fiber tractography: theoretic underpinnings. *AJNR. American Journal of Neuroradiology*, *29*(4), 632–41. http://doi.org/10.3174/ajnr.A1051

Neil, J., Miller, J., Mukherjee, P., & Hüppi, P. S. (2002). Diffusion tensor imaging of normal and injured developing human brain - A technical review. *NMR in Biomedicine*, *15*(7–8), 543–552. http://doi.org/10.1002/nbm.784

Ogawa, S., Lee, T. M., Kay, A. R., & Tank, D. W. (1990). *Brain magnetic resonance imaging with contrast dependent on blood oxygenation (cerebral blood flow/brain metabolism/oxygenation)*. *Proc. NatI. Acad. Sci. USA* (Vol. 87). Retrieved from https://www.ncbi.nlm.nih.gov/pmc/articles/PMC55275/pdf/pnas01049-0370.pdf

Ogawa, S., Tank, D. W., Menon, R., Ellermann, J. M., Kim, S. G., Merkle, H., & Ugurbil, K. (1992). Intrinsic signal changes accompanying sensory stimulation: functional brain mapping with magnetic resonance imaging. *Proceedings of the National Academy of Sciences of the United States of America*, *89*(13), 5951–5.

http://doi.org/10.1073/pnas.89.13.5951

Panizzon, M. S., Fennema-Notestine, C., Eyler, L. T., Jernigan, T. L., Prom-Wormley, E., Neale, M., … Kremen, W. S. (2009). Distinct Genetic Influences on Cortical Surface Area and Cortical Thickness. *Cerebral Cortex*, *19*(11), 2728–2735. http://doi.org/10.1093/cercor/bhp026

Pauling and CD Coryell (1936). "The Magnetic Properties and Structure of Hemoglobin, Oxyhemoglobin and Carbonmonoxyhemoglobin". *PNAS* 22: 210–6. doi:10.1073/pnas.22.4.210.

Park, H., Kennedy, K. M., Rodrigue, K. M., Hebrank, A., & Park, D. C. (2013). An fMRI study of episodic encoding across the lifespan: changes in subsequent memory effects are evident by middle-age. *Neuropsychologia*, *51*(3), 448–56.

Pederson, D. G. (1971). The Estimation Of Heritability And Degree Of, (1961), 247–264. Retrieved from https://www.nature.com/hdy/journal/v27/n2/pdf/hdy197188a.pdf

Peper, J. S., Schnack, H. G., Brouwer, R. M., Van Baal, G. C. M., Pjetri, E., Székely, E., … Hulshoff Pol, H. E. (2009). Heritability of regional and global brain structure at the onset of puberty: A magnetic resonance imaging study in 9-year-old twin pairs. *Human Brain Mapping*, *30*(7), 2184–2196. http://doi.org/10.1002/hbm.20660

Peter B. Kingsley. (2010). Introduction to Diffusion Tensor Imaging Mathematics: Part I. Tensors, Rotations, and Eigenvectors, *88*(12), 17–25. http://doi.org/10.1002/cmr.a

Pfefferbaum, A., Sullivan, E. V, Hedehus, M., Lim, K. O., Adalsteinsson, E., & Moseley, M. (2000). *Age-Related Decline in Brain White Matter Anisotropy Measured With Spatially Corrected Echo-Planar Diffusion Tensor Imaging*. *Magn Reson Med* (Vol. 44). Retrieved from https://pdfs.semanticscholar.org/01ba/a03eb8ba03d61e3dcc7a3deb1e40bf8a5b47.pdf

Plomin, R. (1994). The genetic basis of complex human behaviors. Retrieved from http://personal.psc.isr.umich.edu/yuxie-web/files/pubs/Articles/Plomin1994.pdf

Polderman, T. J. C., Benyamin, B., de Leeuw, C. A., Sullivan, P. F., van Bochoven, A., Visscher, P. M., & Posthuma, D. (2015). Meta-analysis of the heritability of human traits based on fifty years of twin studies. *Nature Genetics*, *47*(7), 702–709. http://doi.org/10.1038/ng.3285

Poldrack, R. A., Mumford, J. A., & Nichols, T. E. (1996). 1.1 A brief overview of fMRI, 1–12.

Ponzoni, R. W., & James, J. W. (1978). Possible Biases in Heritability Estimates from Intraclass Correlation, *27*, 25–27.

Power, R. A., & Pluess, M. (2015). Heritability estimates of the Big Five personality traits based on common genetic variants. *Translational Psychiatry*, *5*(7), e604. http://doi.org/10.1038/tp.2015.96

Ribas, G. C. (2010). The cerebral sulci and gyri. *Neurosurgical Focus*, *28*(2), E2. http://doi.org/10.3171/2009.11.focus09245

Roy CS, Sherrington CS (January 1890). "On the Regulation of the Blood-supply of the Brain". *Journal of Physiology* 11 (1-2): 85–158.17.

Sedgwick, P. (2013). Intraclass correlation coefficient. *Bmj*, *346*(mar22 1), f1816–f1816.

Shen, K.-K., Rose, S., Fripp, J., McMahon, K. L., de Zubicaray, G. I., Martin, N. G., … Salvado, O. (2014). Investigating brain connectivity heritability in a twin study using diffusion imaging data. *NeuroImage*, *100*, 628–41. http://doi.org/10.1016/j.neuroimage.2014.06.041

Shi, Y., & Toga, A. W. (2017). Connectome imaging for mapping human brain pathways. *Molecular Psychiatry*, *22*(9), 1230–1240. http://doi.org/10.1038/mp.2017.92

Snook, L., Paulson, L.-A., Roy, D., Phillips, L., & Beaulieu, C. (2005). Diffusion tensor imaging of neurodevelopment in children and young adults. *NeuroImage*, *26*(4), 1164–1173. http://doi.org/10.1016/J.NEUROIMAGE.2005.03.016

Soares, J. M., Marques, P., Alves, V., & Sousa, N. (2013). A hitchhiker's guide to diffusion tensor imaging. *Frontiers in Neuroscience*, *7*, 31. http://doi.org/10.3389/fnins.2013.00031

Sotiropoulos, S. N., Jbabdi, S., Xu, J., Andersson, J. L., Moeller, S., Auerbach, E. J., … Behrens, T. E. J. (2013). Advances in diffusion MRI acquisition and processing in the Human Connectome Project. *NeuroImage*, *80*, 125–43. http://doi.org/10.1016/j.neuroimage.2013.05.057

Sowell, E. R. (2004). Longitudinal Mapping of Cortical Thickness and Brain Growth in Normal Children. *Journal of Neuroscience*, *24*(38), 8223–8231. http://doi.org/10.1109/CDC.2017.8264670

Symms, M. (2004). A review of structural magnetic resonance neuroimaging. *Journal of Neurology, Neurosurgery & Psychiatry*, *75*(9), 1235–1244. http://doi.org/10.1136/jnnp.2003.032714

Thompson, P. M., Ge, T., Glahn, D. C., Jahanshad, N., & Nichols, T. E. (2013). Genetics of the connectome ☆. *NeuroImage*, *80*, 475–488. http://doi.org/10.1016/j.neuroimage.2013.05.013

Toga, A. W., & Thompson, P. M. (2005). Genetics of Brain Structure and Intelligence. http://doi.org/10.1146/

Tromp, D. (2015). DTI Tutorial 1 - From Scanner to Tensor, 1–7. http://doi.org/10.15200/winn.145653.31559

Trost, Z., Strachan, E., Sullivan, M., Vervoort, T., Avery, A. R., & Afari, N. (n.d.). Heritability of pain catastrophizing and associations with experimental pain outcomes: a twin study. http://doi.org/10.1097/01.j.pain.0000460326.02891.fc

Tuch, D. S., Wisco, J. J., Khachaturian, M. H., Ekstrom, L. B., Kötter, R., & Vanduffel, W. (2005). Q-ball imaging of macaque white matter architecture. *Philosophical Transactions of the Royal Society of London. Series B, Biological Sciences*, *360*(1457), 869–79. http://doi.org/10.1098/rstb.2005.1651

Turkheimer, E. (2000). Three Laws of Behavior Genetics and What They Mean. *Current Directions in Psychological Science*, *9*(5), 160–164. http://doi.org/10.1111/1467-8721.00084

Uğurbil, K., Xu, J., Auerbach, E. J., Moeller, S., Vu, A. T., Duarte-Carvajalino, J. M., … Yacoub, E. (2013). Pushing spatial and temporal resolution for functional and diffusion MRI in the Human Connectome Project. *NeuroImage*, *80*, 80–104. http://doi.org/10.1016/j.neuroimage.2013.05.012

van den Heuvel, M. P., van Soelen, I. L., Stam, C. J., Kahn, R. S., Boomsma, D. I., & Hulshoff Pol, H. E. (2013). Genetic control of functional brain network efficiency in children. http://doi.org/10.1016/j.euroneuro.2012.06.007

Van Essen, D. C., Smith, S. M., Barch, D. M., Behrens, T. E. J., Yacoub, E., & Ugurbil, K. (2013). The WU-Minn Human Connectome Project: an overview. *NeuroImage*, *80*, 62–79. http://doi.org/10.1016/j.neuroimage.2013.05.041

Visscher, P. M., Hill, W. G., & Wray, N. R. (2008). Heritability in the genomics era — concepts and misconceptions. *Nature Reviews Genetics*, *9*(4), 255–266. http://doi.org/10.1038/nrg2322

Voevodskaya, O., Simmons, A., Nordenskjöld, R., Kullberg, J., Ahlström, H., Lind, L., … Alzheimer's Disease Neuroimaging Initiative, A. D. N. (2014). The effects of intracranial volume adjustment approaches on multiple regional MRI volumes in healthy aging and Alzheimer's disease. *Frontiers in Aging Neuroscience*, *6*, 264. http://doi.org/10.3389/fnagi.2014.00264

Wager, T. D., & Lindquist, M. A. (2015). Principles of fMRI.

Wen, W., Thalamuthu, A., Mather, K. A., Zhu, W., Jiang, J., de Micheaux, P. L., … Sachdev, P. S. (2016). Distinct Genetic Influences on Cortical and Subcortical Brain

Structures. *Scientific Reports*, *6*(1), 32760. http://doi.org/10.1038/srep32760

Whitwell, J. L. (2009). Voxel-based morphometry: an automated technique for assessing structural changes in the brain. *The Journal of Neuroscience : The Official Journal of the Society for Neuroscience*, *29*(31), 9661–4. http://doi.org/10.1523/JNEUROSCI.2160-09.2009

Winterer, G., Hariri, A. R., Goldman, D., & Weinberger, D. R. (2005). Neuroimaging and Human Genetics. *International Review of Neurobiology*, *67*, 325–383. http://doi.org/10.1016/S0074-7742(05)67010-9